REPORT DOCUMENTATION PAGE

Form Approved
OMB No. 0704-0188

1. AGENCY USE ONLY (Leave blank)	2. REPORT DATE 31 May 1995	3. REPORT TYPE AND DATES COVERED Final Report 29 Sept 94 – 29 Mar 95

4. TITLE AND SUBTITLE
Individual Blade Control for Helicopter Rotor Blade One/Rev Vibration Reduction

6. AUTHOR(S)
Robert M. McKillip, Jr.

5. FUNDING NUMBERS
NAS2-14071

7. PERFORMING ORGANIZATION NAME(S) AND ADDRESS(ES)
Continuum Dynamics, Inc.
P.O. Box 3073
Princeton, New Jersey 08543-3073

8. PERFORMING ORGANIZATION REPORT NUMBER
C.D.I. Report No. 95-06

9. SPONSORING/MONITORING AGENCY NAME(S) AND ADDRESS(ES)
National Aeronautics and Space Administration
Ames Research Center
Moffett Field, California 94035-1000

10. SPONSORING/MONITORING AGENCY REPORT NUMBER

11. SUPPLEMENTARY NOTES
Brent Wellman, Contracting Officer's Technical Representative
Code YR, M/S:215-1, U. S. Army Aeroflightdynamics Directorate

12a. DISTRIBUTION/AVAILABILITY STATEMENT

Unclassified – Unlimited

This document has been approved for public release and sale; its distribution is unlimited.

12b. DISTRIBUTION CODE

DTIC SELECTED
JUN 08 1995
F

13. ABSTRACT (Maximum 200 words)

Results of a Phase-I SBIR study directed at the use of Individual Blade Control (IBC) for 1/rev helicopter rotor vibration reduction are described. Past approaches, analytical studies, and current technology for 1/rev vibration reduction are surveyed, and then a notional scheme for implementing an IBC-based control device using shape memory alloys (SMA) is introduced. In order to quantify the required performance from this scheme, investigations into the sources of 1/rev vibration, and possible methods for its control are simulated using an aeroelastic analysis. Actuation concepts using SMA wires are analyzed, with engineering support from limited benchtop conceptual test models. Finally, implementation issues are discussed, and a plan for continued work leading to prototype development for this system is outlined. The results from this Phase-I study indicate that the proposed innovative scheme for providing active 1/rev vibration control for helicopter rotors should lead to a practical system, that would be developed and prototyped under a follow-on Phase-II program.

14. SUBJECT TERMS
Individual Blade Control (IBC); 1/Rev Vibration; Automatic Blade Tracking; Helicopter Vibration; Smart Materials

15. NUMBER OF PAGES 69

16. PRICE CODE

17. SECURITY CLASSIFICATION OF REPORT	18. SECURITY CLASSIFICATION OF THIS PAGE	19. SECURITY CLASSIFICATION OF ABSTRACT	20. LIMITATION OF ABSTRACT
UNCLASSIFIED	UNCLASSIFIED	UNCLASSIFIED	UL

NSN 7540-01-280-5500

Standard Form 298 (Rev 2-89)
Prescribed by ANSI Std 239-18
298-102

1950607 076

PROJECT SUMMARY

ARMY SBIR 93.2 PHASE I FINAL REPORT

Project Topic No.: A93-153   Contract No.: NAS2-14071   ARC

PROJECT TITLE: Individual Blade Control for Helicopter Rotor Blade One/Rev Vibration Reduction

COMPANY: Continuum Dynamics, Inc.

ADDRESS: P.O. Box 3073
Princeton, NJ 08543-3073

SUMMARY:

    Results of a Phase-I SBIR study directed at the use of Individual Blade Control (IBC) for 1/rev helicopter rotor vibration reduction are described. Past approaches, analytical studies, and current technology for 1/rev vibration reduction are surveyed, and then a notional scheme for implementing an IBC-based control device using shape memory alloys (SMA) is introduced. The method investigated in this report constitutes a novel combination of on-blade sensing and control, using blade-mounted accelerometer sensors with SMA-based actuators. In order to quantify the required performance from this scheme, investigations into the sources of 1/rev vibration, and possible methods for its mitigation are simulated using an aeroelastic analysis. Actuation concepts using SMA wires are analyzed, with engineering support from limited benchtop conceptual test models. A notional device, consisting of SMA-controlled "smart" blade trailing edge deformable tab, is proposed for further development, due to its promising capability for 1/rev vibration suppression and its ease of retro-fit installation on Army aircraft. Finally, implementation issues are discussed, and a plan for continued work leading to prototype development for this system is outlined. The promising results from this Phase-I study indicate that the proposed innovative scheme for providing active 1/rev vibration control for helicopter rotors should lead to a practical system, that would be developed and prototyped under a follow-on Phase-II program. It is anticipated that such a device for providing *in-flight* helicopter 1/rev vibration control would have wide interest in both the military and the commercial aviation sectors.

Accesion For		
NTIS CRA&I	N	
DTIC TAB	☐	
Unannou :ced	☐	
Justification		
By		
Distribution /		
Availability Codes		
Dist	Avail and / or Special	
A-1		

INDIVIDUAL BLADE CONTROL FOR

HELICOPTER ROTOR BLADE

ONE / REV VIBRATION REDUCTION
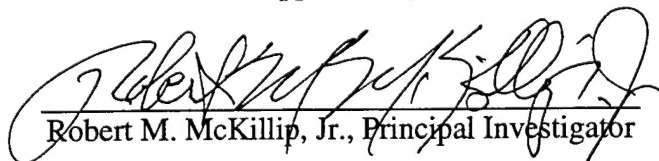
Final Report Prepared by

Robert M. McKillip, Jr.

CONTINUUM DYNAMICS, INC.
P. O. BOX 3073
PRINCETON, NEW JERSEY 08543

Prepared Under Contract No. NAS2-14071 for Phase I
of the Small Business Innovation Research Project Entitled:
"Individual Blade Control for Helicopter Rotor
Blade One/Rev Vibration Reduction"

Prepared for

U.S. ARMY AEROFLIGHTDYNAMICS DIRECTORATE
MR. BRENT WELLMAN, TECHNICAL MONITOR
CODE YR, MS 215-1
AMES RESEARCH CENTER
MOFFETT FIELD, CALIFORNIA 94035-1000

Approved by

Robert M. McKillip, Jr., Principal Investigator

May 1995

SBIR RIGHTS NOTICE (JUN 1987), NASA Deviation

INDIVIDUAL BLADE CONTROL FOR HELICOPTER
ONE / REV VIBRATION REDUCTION

Robert M. McKillip, Jr.
Continuum Dynamics, Inc., Princeton, New Jersey 08543

SUMMARY

Results of a Phase-I SBIR study directed at the use of Individual Blade Control (IBC) for 1/rev helicopter rotor vibration reduction are described. Past approaches, analytical studies, and current technology for 1/rev vibration reduction are surveyed, and then a notional scheme for implementing an IBC-based control device using shape memory alloys (SMA) is introduced. In order to quantify the required performance from this scheme, investigations into the sources of 1/rev vibration, and possible methods for its control are simulated using an aeroelastic analysis. Actuation concepts using SMA wires are analyzed, with engineering support from limited benchtop conceptual test models. A notional device, consisting of SMA-controlled "smart" blade trailing edge deformable tab, is proposed for further development, due to its promising capability for 1/rev vibration suppression and its ease of retro-fit installation on Army aircraft. Finally, implementation issues are discussed, and a plan for continued work leading to prototype development for this system is outlined. The results from this Phase-I study indicate that the proposed innovative scheme for providing active 1/rev vibration control for helicopter rotors should lead to a practical system, that would be developed and prototyped under a follow-on Phase-II program.

TABLE OF CONTENTS

1.0 INTRODUCTION AND BACKGROUND

Excessive vibration is perhaps the most fundamental and elusive problem affecting helicopter operating costs for both military and commercial aircraft (Reichert, 1981; Loewy, 1984). Vibratory motion usually means oscillatory strain, which reduces the fatigue life of components, leading to increased weight of the total aircraft. Since fatigue life dictates the service life of a helicopter part, and life-limited components comprise the majority of parts on a helicopter, life-cycle costs grow with increased vibration as well. This vibration is largely due to oscillatory airloads, which are an undesired but unavoidable consequence of flying a rotor edgewise through the air. Design of helicopter components and systems to avoid vibratory motion is difficult, due to the complex aeroelastic interactions present in the rotor and helicopter fuselage structure. As a result, most production helicopters incorporate some form of vibration treatment that was often added after the first prototype aircraft was built (with a resultant reduction in payload capability). While most of these vibration absorbers or isolators are designed to eliminate harmonics of blade passing frequency (or, N/rev, where N is the number of blades), vibration may also be present at rotor rotation frequency, if all of the rotor blades are not producing the same forces and moments at the hub during each revolution. The innovation proposed here is to provide an automatic system incorporating Individual Blade Control (IBC) for elimination of the vibration caused by this nonuniform loading between rotor blades. This system will comprise a unique combination of on-blade aerodynamic control using "smart" materials-based actuators and a novel instrumentation scheme for sensing differences in blade motion.

1.1 Mechanisms for 1/Rev Vibration

One-per-revolution (1/rev, or 1P) vibration arises from dissimilarities in rotor blade mass properties, aerodynamic contours, and to a lesser degree, structural stiffness. Mass nonuniformities between rotor blades produce classical dynamic imbalance problems due to the rotor center of gravity being located away from the shaft centerline. This problem is typically referred to as a "balance" problem for a rotor system. Aerodynamic contour mismatch results in differing airloads between blades, which is aggravated by high thrust and high forward speed conditions. Differences in airloads typically manifest themselves as the blades flying "out of track" as they spin about the shaft, best observed by the difference in the location of the blade tips at the same rotor azimuth location.

Elimination of the 1/rev vibration on Army helicopters would substantially reduce the costs required for maintenance and support. These costs include maintenance personnel hours, faulty rejection of functional parts, and defective parts replacement. It is estimated that a resulting 10% savings in the spare parts budget alone would net over $100M per year (Crews, 1987).

Vibration at 1/rev is currently addressed by the helicopter manufacturer by imposing strict quality standards on the production of helicopter rotor blades. Blades are often whirl-tower tested and matched to each other, and then shipped as sets to be flown together. Several manufacturers maintain the use of a master blade to which other blades are compared during whirl tower testing, and even have a master-master blade for balancing new master blades when a previous one has expended its useful life.

Maintaining blade-to-blade similarity is becoming particularly important with the use of composite materials as primary structure in rotor blades. Quality control is

1

especially difficult in composite blade construction, since tooling is often not as mature as that for metal manufacturing. Locations for added tip weights and trailing edge tabs for aerodynamic adjustments are typically included in blade design to allow for whirl tower and field adjustments to improve blade track and balance (T/B).

Even if all blades were identical, repair procedures for damaged rotor blades are typically done by hand, resulting in an inevitable change of a blade's mass, stiffness, and aerodynamic properties to some degree. The capability to continue to use a previously damaged blade is important to both military and commercial helicopter operators, and thus, some means of accommodating these blade variations is important.

Finally, increased performance requirements in hover have led helicopter manufacturers to incorporate blades with airfoils having increased camber. Such sections generate a higher steady torsional moment on the pitch links, which can often be tolerated using hydraulically boosted swashplate controls. However, any variation between blades in these steady moments will produce a noticeable 1/rev vibration on both the airframe and in the pilot's controls.

1.2 Past and Current Approaches for Rotor Smoothing

Vibration at 1/rev on in-service helicopters is typically measured using specialized tracking and balancing instrumentation (Clay, 1987; Trigg, 1984; Crews, 1993), and controlled through modifications on individual blades. Track is achieved through adjustment of aerodynamic properties so that all blades fly in the same position as they rotate about the shaft. These adjustments involve changing the pitch link lengths or deflecting a built-in spanwise trailing edge tab. Rotor balance is performed by maintaining inertial symmetry both radially and chordwise, through the addition of root or tip weights or adjustments in a "drag brace" to alter the steady lead-lag orientation of the blade's hub connection.

Early track and balance measurement procedures used a flag system and blade tip markers. Different colored chalk or crayon was rubbed onto the rotor blade tips, and a flag was brought within contact of the rotating blades during ground spin-up. Variations in position of the marks on the flag indicated which blade was out of track, and adjustments were made on that blade until it matched the tip displacements of the others. Variations on this approach used optical detectors to replace the flag system, which improved operator safety but was still limited in that tracking could only be accomplished on the ground.

Later efforts incorporated a strobe light and reflective tape and/or symbology on each blade so that the blades could be viewed in flight. Observation from the cockpit was typically hampered due to the obliqueness of the viewing angle, so more recent systems incorporated a video camera mounted in a better viewing position near the nose of the aircraft. In-flight tracking became possible, but some systems required night operation in order to properly resolve blade positions. Balance charts were developed for each type of aircraft to indicate the modifications required to achieve a smoother rotor.

The most recent systems use fuselage-mounted accelerometers to sense vibrations, and may include graphical print-outs or computer displays of imbalance and suggested fixes for a particular rotor system (Chadwick Helmuth, 1992; Scientific Atlanta, 1993). The accelerometers are positioned in predetermined locations for each particular helicopter, so that known relationships between sensed vibration and rotor adjustments may be used to suggest the proper smoothing action to be taken. These systems have now incorporated capabilities to record vibration readings onto magnetic media, allowing post-flight

2

monitoring of trends in vibration level as a function of flight hour. Such added health monitoring has provided the ability to perform maintenance on an on-demand schedule, helping to reduce operating costs. For that reason, track and balance instrumentation was incorporated as a dedicated feature of the V-22's health monitoring system (Augustin, 1989), due to the added complexity inherent in tiltrotor aircraft.

Despite the increasing sophistication and added features of the available instrumentation, track and balance operations still vex both civilian and government maintenance personnel alike. Recent flight tests to expand the envelope of a highly instrumented UH-60A aircraft by the NASA were continually hampered by track and balance difficulties, in part due to their use of special highly instrumented rotor blades. The 1/rev problem was not solved until the president of the track and balance instrumentation company personally flew out to aid the NASA test engineers (TRENDS, 1993). Army maintenance personnel still struggle with track and balance problems due to a combination of aging aircraft, high operator turnover rate and training difficulties, and less than optimum test instrumentation (Crews, 1993).

The innovation investigated here in this Phase I effort was the use of a combination of Individual Blade Control (IBC) and onboard signal processing to provide <u>automatic tracking and balancing of helicopter rotors in flight</u>. Such capability would eliminate 1/rev maintenance downtime and loss of productive flight hours dedicated solely to track and balance operations. Reduction in 1/rev vibrations would improve fatigue life of dynamic components, with reduced costs required for spares and ultimately lower weight designs for these parts. Fly-away unit cost savings may be realized as well, since the innovation proposed here may allow some relaxation of the tight tolerances on rotor blade manufacturing, leading to a less expensive rotor system. These track and balance adjustments would be performed on each blade either automatically, or on-demand by the pilot during flight.

Some past efforts have been made in automatic track and balance equipment, but were deemed impractical due to the added complexity of the system (Wilson, 1974). Certain aircraft, notably the Kaman H-2, has an automatic tracking system that can adjust the mean level of the blade's outboard servoflap in flight. This system, while convenient, is also necessary, as the servoflap rotor is even more sensitive to blade-to-blade variations due to its low torsional stiffness.

1.3 Scope of the Present Investigation

The Phase-I effort described in this report was an investigation into the use of IBC and "smart" materials-based actuation concepts to design an automatic vibration reduction system that: (1) may be used on a wide variety of rotor blades; (2) provides maximal tracking benefit with minimal power requirements and performance penalties on the aircraft; and (3) is robust to failures, so as not to replace one maintenance problem with another. The work described here addresses these issues by identifying the most promising possibilities for automatic on-blade track and balance using IBC, while imposing practical limitations on required power, support electronics, and general system sophistication in order to design equipment that will have a high probability of success during prototype development as part of a Phase-II effort.

In order to provide for a useful and innovative system for elimination of helicopter 1/rev vibration, several approaches were combined to address the shortcomings of the hardware representing current technology:

3

> First, despite gains in computer processing capability, current vibration devices require a significant amount of user interaction and training to perform successful tracking and balancing of a rotor system. Automation and on-blade automatic control, in the form of IBC, can be used to reduce these requirements for maintenance personnel training, such that the "loop closure" may be made electronically instead of through the T/B specialist.

> Second, since all track and balance procedures involve adjustment of the blade properties through either aerodynamic or mass changes on each individual blade, these adjustments will be automated as best as is practicable. While addition of mass would be virtually impossible with an automated system, deflection of trailing edge tabs and adjustment of pitch link lengths are certainly candidates ripe for active control. In addition, dynamic components in the rotor hub that influence 1/rev vibration, such as lag dampers, may be provided with automatic tuning capabilities as well.

> And third, in order to eliminate the requirement for "pre-calibration" of a helicopter's track and balance procedures (as is done in the generation of track and balance charts for a particular helicopter), on-blade vibration sensing would be incorporated in the system design. Use of blade accelerometer sensors will guarantee that the 1/rev loads are sensed at their source, and hence the vibration control equipment need not rely on assumed linearity relationships between various fuselage locations and forces in the rotor system that may or may not change over time.

The improved capability of the proposed investigation to automate the above track and balance adjustments comes from a unique combination of (1) on-blade control provided by the IBC concept; (2) recent advances in the application of "smart materials"; (3) decreasing costs and size of electronic components and sensors; and (4) innovative advances in the use of accelerometer-based instrumentation for rotor system measurement and control applications. How each of these factors contributes to provide a conceptual overall system design comprises the bulk of this report.

1.4 Outline of the Report

In order to provide some understanding of the sources of 1/rev vibration, and the effectiveness of various on-blade mechanical and aerodynamic changes on its mitigation, simulations of the aeroelastic response of a rotor blade with postulated blade perturbations were performed. The details of the simulation, and the results and assessment of vibration suppression schemes, are given in Section 2. This section also addresses what the most appropriate sensors would be for this task. Issues related to actuation concepts that incorporate SMA materials are described in Section 3, along with some results from limited benchtop testing on proof-of-concept actuator models. A notional actuation concept is presented as the leading candidate for further study. Conclusions from the research are cited in Section 4, and Phase-I Option tasks to be performed, and Phase-II continuation work are given in Sections 5 and 6 respectively. Finally, references cited in the discussion are in Section 7.

2.0 SIMULATION RESULTS

Since no model rotor testing was performed as part of this Phase-I effort, assessment of schemes for 1/rev vibration reduction was done using results from computer simulation studies. These calculations were directed at three fundamental investigations to determine: (1) how blade variations influence 1/rev vibratory loads transmitted to the fuselage; (2) what means exist to control 1/rev vibrations, their effectiveness, and the additional effects the control inputs produce while attacking the 1/rev vibration problem; and (3) the most appropriate control logic and sensing scheme for identifying and mitigating the 1/rev vibration source. Each of these topics is addressed in this section, following a general description of the analytical model used for these studies.

2.1 Computational Model and Previous Validation

The analytical model used in this Phase I effort was the primary analysis tool for assessing the feasibility of the proposed 1/rev vibration reduction scheme. As discussed in the proposal, this model consisted of a modified form of Continuum Dynamics, Inc.'s RotorCRAFT (Computation of Rotor Aerodynamics in Forward FlighT) aeroelastic rotor code (Quackenbush, et. al. 1991) for helicopter performance prediction, with modifications to allow for the aeroelastic and aerodynamic effects of the candidate actuation and control schemes of interest here.

The ability to predict both the performance and unsteady loads that appear on rotors in hover and forward flight is clearly critical to the success of any design of a vibration control system of the type discussed above; lacking such a capability, extensive cut-and-try testing would be required to formulate a successful system configuration. For this reason the capabilities available for the prediction of rotor performance and unsteady airloads at Continuum Dynamics, Inc. were of considerable importance in the present effort.

The original RotorCRAFT code was described in detail in Quackenbush, et al. (1991a, 1991b), and features an advanced wake model that captures many features of rotor loading missed by earlier, more simplified models. This Constant Vorticity Contour (CVC) wake approach permits generation of an exceptionally accurate prediction of wake upwash at the rotor which is particularly important in cases with strong wake/rotor interaction (Figure 2-1). The CVC model is used in conjunction with a vortex lattice aerodynamic model and a full flap/lag/torsion aeroelastic model based on a finite element description of the blade structure. The code is presently in use in industry (Torok and Berezin 1992) and in support of NASA tests on unsteady hub loading (Quackenbush et al. 1992). The CVC wake model is also used by Boeing Helicopters in its comprehensive Tech 01 code (Dadone et. al 1993).

The airload calculation model in RotorCRAFT computes the local sectional lift based on the bound circulation from the vortex lattice model. This treatment automatically incorporates finite planform and linear compressibility effects, but does not directly allow for the computation of sectional drag and pitching moment. This is accomplished through the use of the inclusion of table look-ups of 2D aerodynamic coefficients. Tabulations of 2D lift, drag, and moment coefficients are read into the analysis as a function of angle of attack and Mach number.

In normal operation, at each blade section the lift coefficient computed from the vortex lattice is used in conjunction with tabulated lift values to find an effective angle of

attack for the section. This angle is then used to enter the tables of drag and moment coefficients to find the 2D values of these coefficients. Unsteady flow effects are captured both through the time-varying downwash imposed by the trailing vorticity field of the wake and through corrections to the induced downwash that account for near wake unsteady effects (Quackenbush, et al. 1992). Another feature important to the prediction of vibratory hub loading in response to blade design perturbations or tab deflection is blade flexibility. The RotorCRAFT code incorporates a full flap/lag/torsion elastic blade model that has successfully correlated airloads on dynamically scaled models, such as the UH-60 model rotor whose testing was described by Lorber (1991).

RotorCRAFT has produced good correlation of both integrated performance and sectional loads for rotors in forward flight, as well as vibratory hub loads (Quackenbush, et al. 1991b, 1992). Figure 2-2 shows that for time-averaged performance calculations for a four-bladed rotor in a wind tunnel yields good correlation. Correlation studies with respect to internal blade stresses have also been undertaken, and representative results of comparisons with the flight test data of Scheiman (1962) are shown in Figure 2-3.

A particularly important capability for the present application is the prediction of hub loads. Quackenbush, et al. (1992) discusses the application of RotorCRAFT to the prediction of vibratory vertical hub shears. A data base for this correlation was generated by the wind tunnel tests of a model scale four-bladed rotor by Brooks, et al. (1990); this rotor had no twist, constant chord, and operated at full scale tip speed. These tests included both measurements of baseline vibratory force levels as well as increments due to the application of higher harmonic root pitch at 4P. Figure 2-4 shows the predicted and measured magnitudes of 4/rev hub loads for a case with no higher harmonic pitch inputs; the good accuracy evident in these results provides encouraging evidence of the fidelity of the model for the prediction of hub loads. Finally, studies of distributed rotor blade loading have also been made, as is described in Quackenbush (1991b, 1994). Figure 2-5 shows several comparisons to predicted sectional loading on a model scale UH-60 at moderate advance ratio; again, generally good correlation is observed.

2.2 Model Modifications to Support Studies of 1/Rev Load Control

The suite of correlation results discussed above indicated that RotorCRAFT was an appropriate tool for undertaking the type of sensitivity studies of hub loading to perturbations in tab deflection, root pitch control, or alterations in blade properties of interest in this effort. With respect to trailing edge tab deflection, several modifications were required to adapt the baseline RotorCRAFT code to this application. Most of these were carried over from previous work on the analysis of the performance of flapped rotors in forward flight, as described in Quackenbush and McKillip (1993).

These changes included modifications to the zero lift angle, the maximum lift coefficient, and the sectional drag and moment coefficients to account for tab deflection. For the purposes of the present study, the tab deflection was modeled via the deflection of a plain trailing edge "flap" with a maximum chord fraction c_f/c of 0.07; as will be seen below, only very modest angular deflections (typically no more that 5 deg.) are required for applications of interest here.

6
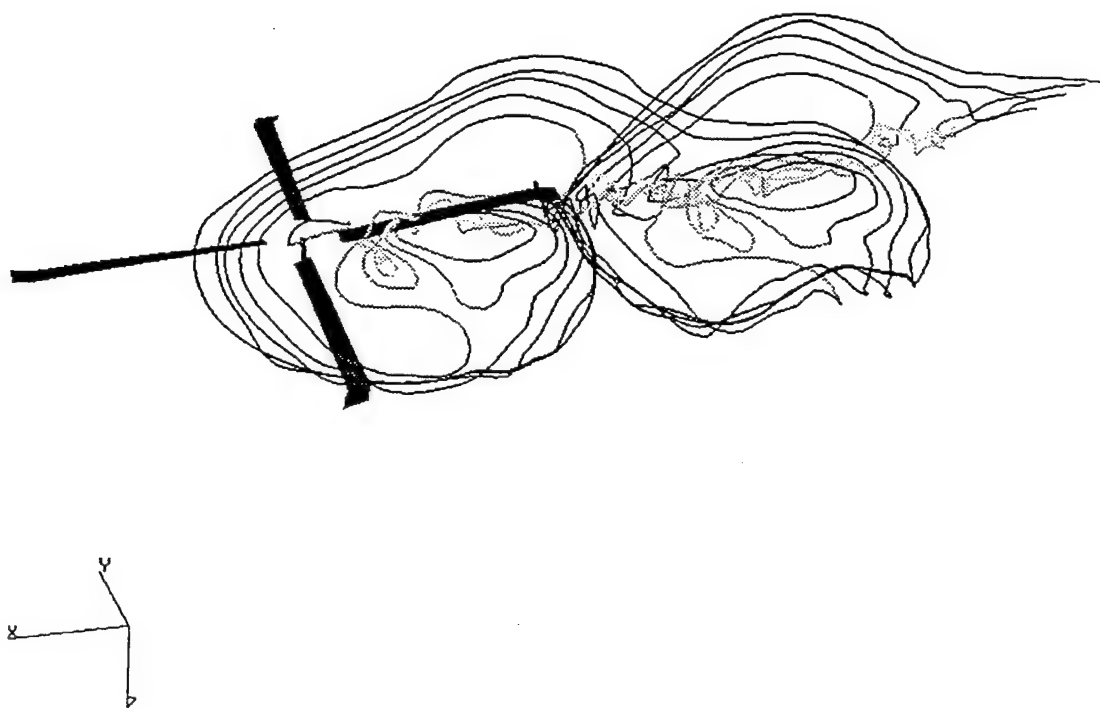
a) Reference blade at $\Psi = 0°$
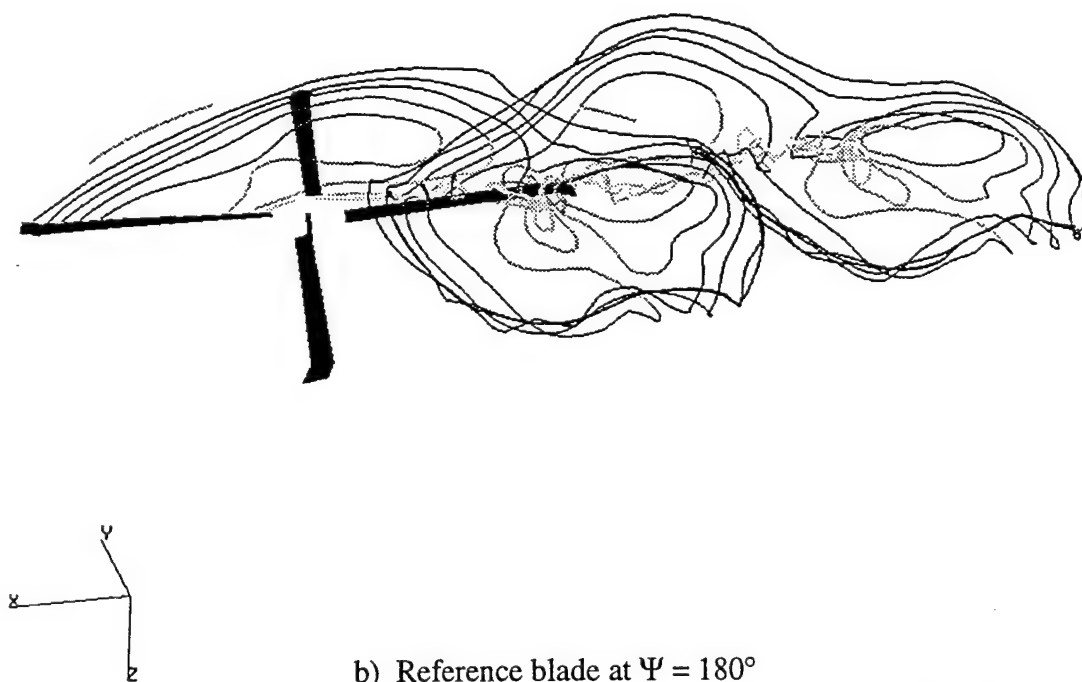
b) Reference blade at $\Psi = 180°$

Figure 2-1. Oblique view of CVC rotor wake geometry for a UH-60A rotor, advance ratio 0.2, $C_T/\sigma = .07$, $\alpha_s = +4.0$ deg.; only the wake of one blade is shown.
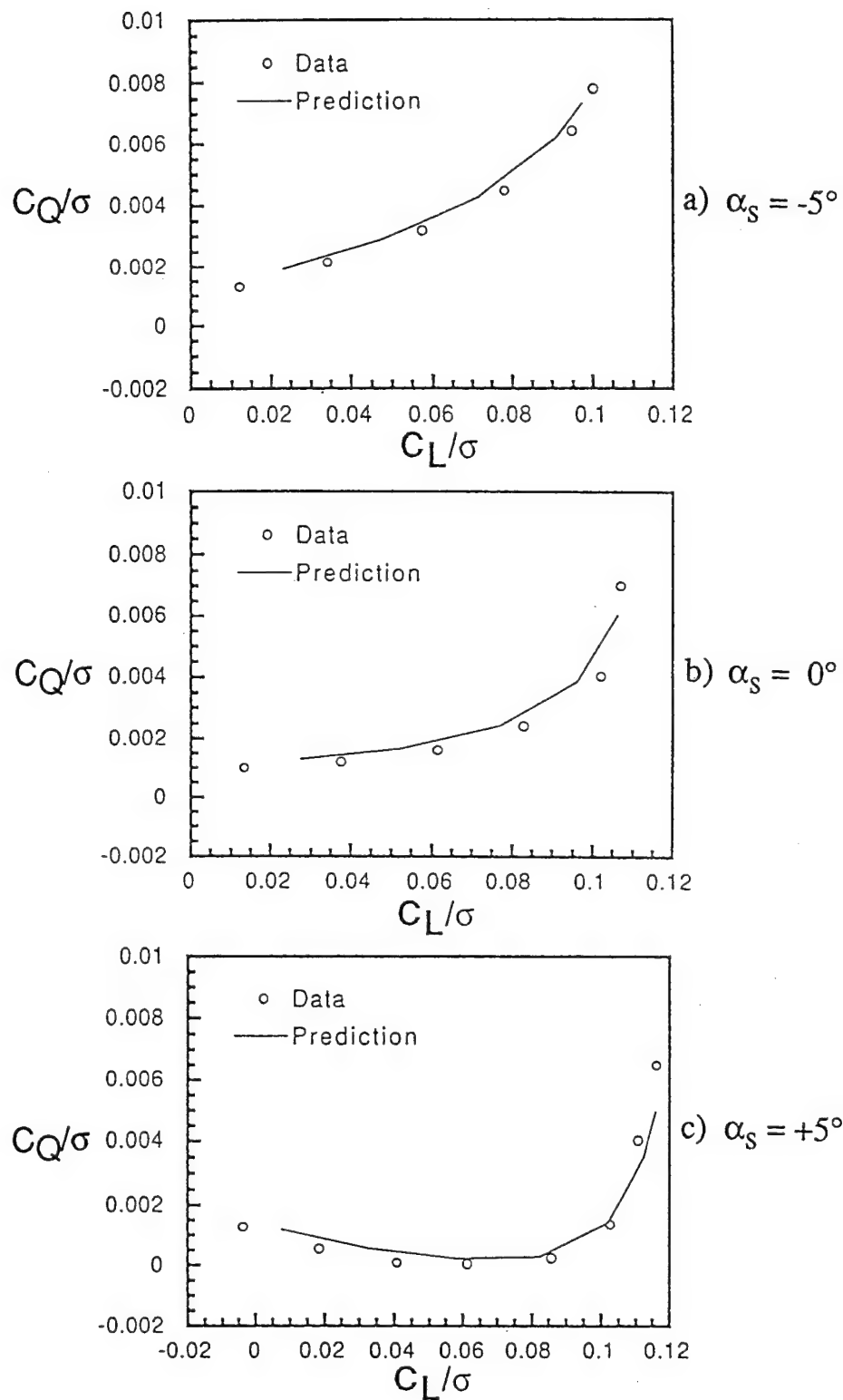
Figure 2-2. Predicted and measured performance for an H-34 main rotor at advance ratio 0.3 (data from McCloud, et al. 1965).
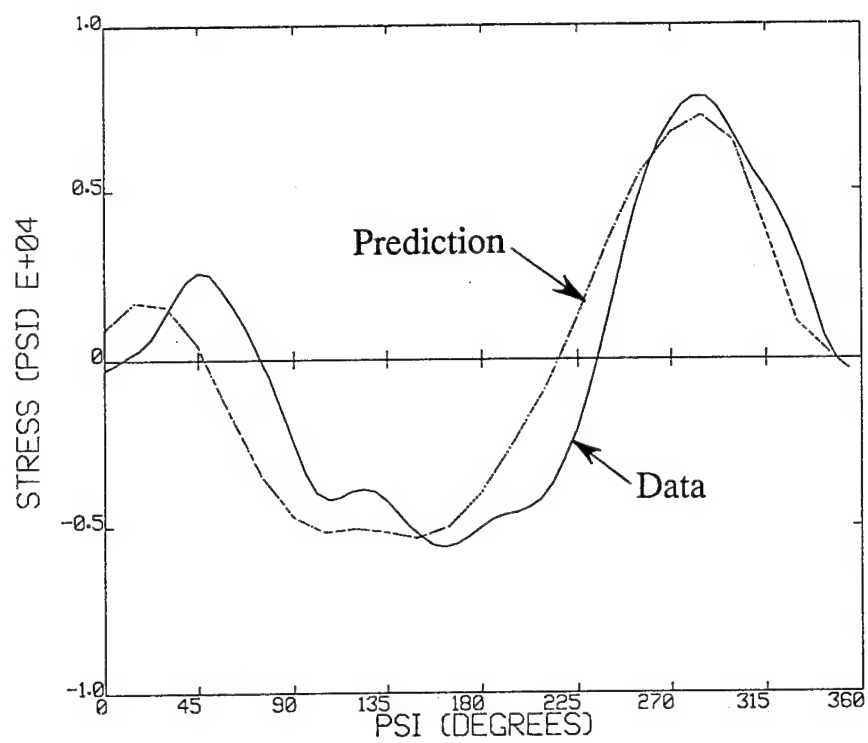
a) Harmonics 1-10
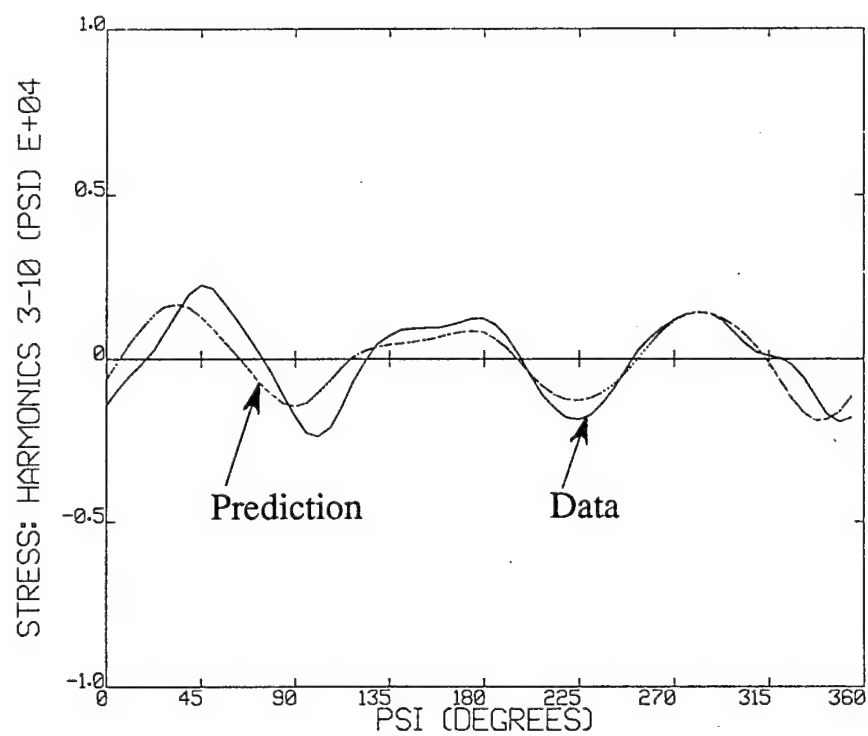
b) Harmonics 3-10

Figure 2-3. Predicted and measured unsteady blade stress at r/R = 0.65 for an H-34 rotor at advance ratio 0.29 (flight test data from Scheiman 1962).
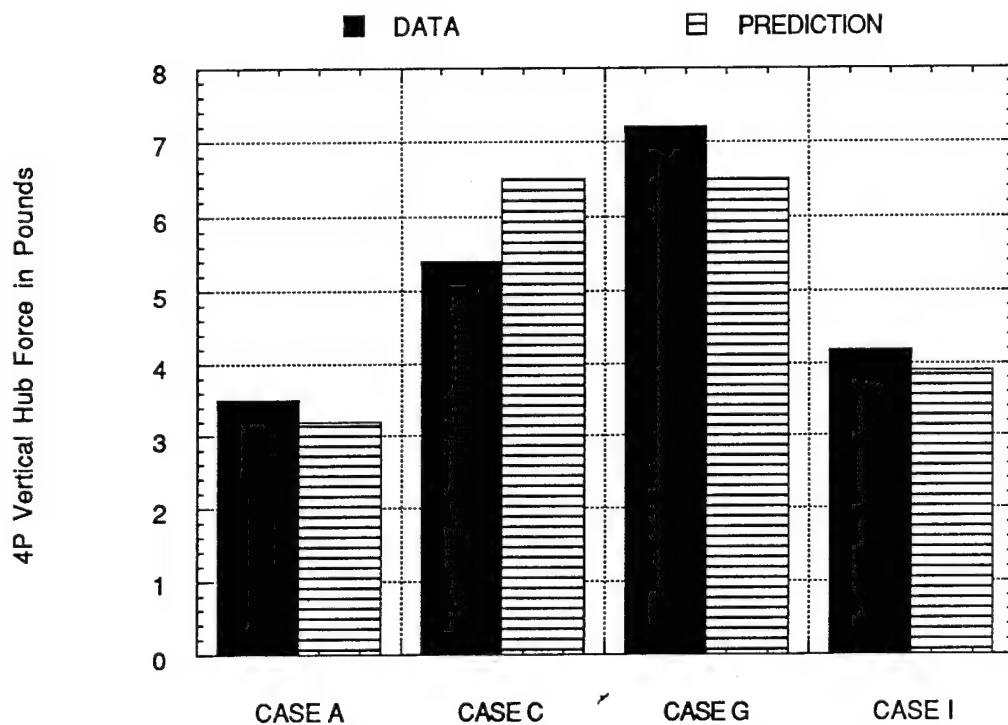
Figure 2-4. Comparison of predicted and measured 4P vertical hub force amplitude for a four-bladed model rotor in four flight conditions: CASE A ($\mu = 0.166$, $\alpha_s = 6.0$ deg.), CASE C ($\mu = 0.300$, $\alpha_s = 2.0$ deg.), CASE G ($\mu = 0.166$, $\alpha_s = 0.0$ deg.), CASE I ($\mu = 0.300$, $\alpha_s = -4.0$ deg.) (wind tunnel data from Brooks, et al. 1990).
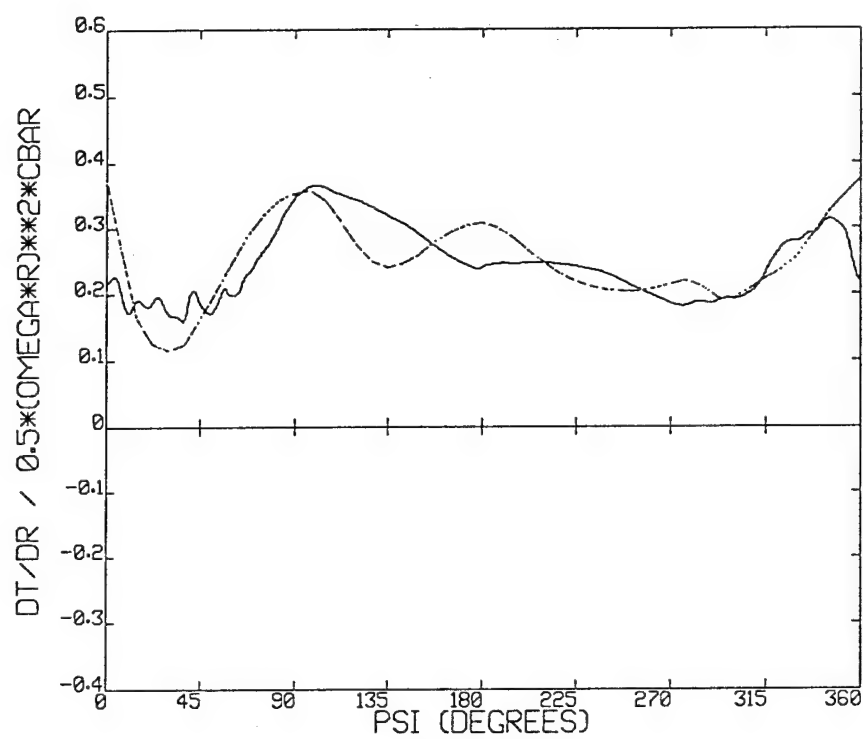
a) r/R = 0.675
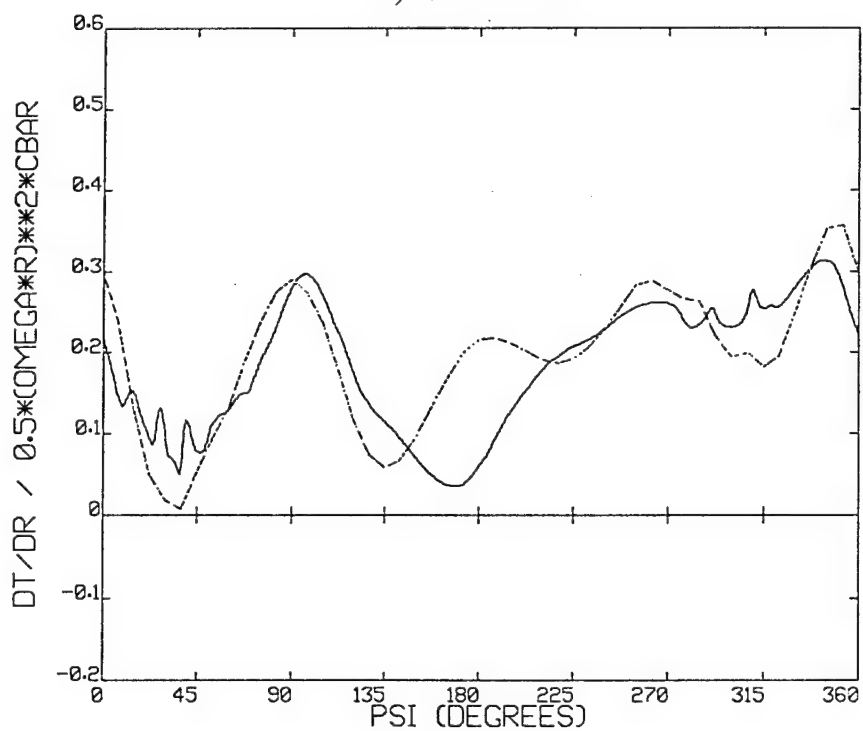
b) r/R = 0.865

Figure 2-5. UH-60A model rotor nondimensional thrust coefficient dC_T/dx at advance ratio 0.2, $C_T/\sigma = 0.07$ (solid = measured, dotted = predicted) (wind tunnel data from Lorber 1991).

11
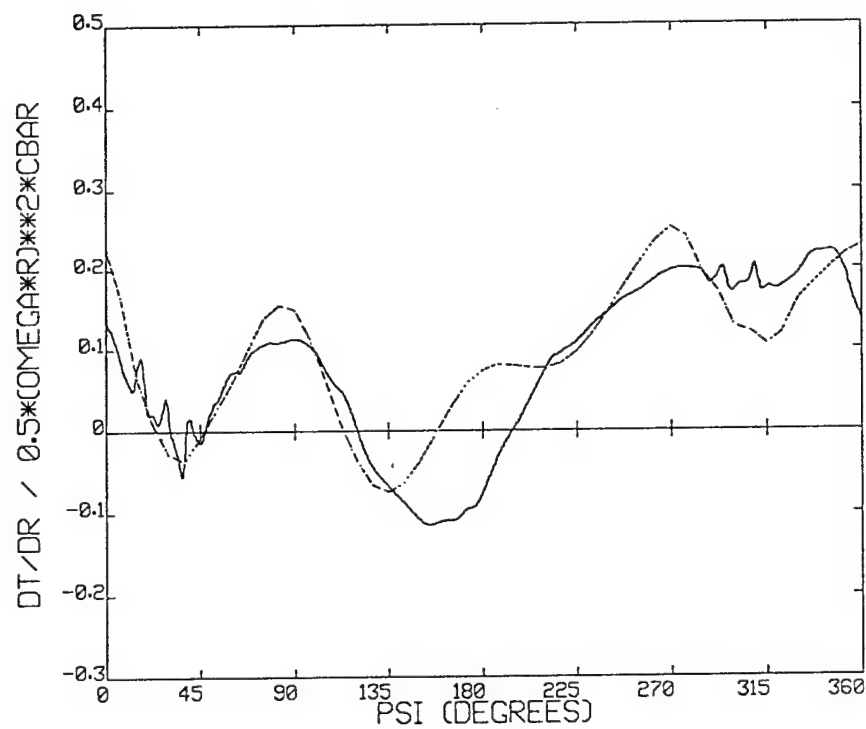
c) r/R = 0.965

Figure 2-5 (Cont'd). UH-60A model rotor nondimensional thrust coefficient dC_T/dx at advance ratio 0.2, $C_T/\sigma = 0.07$ (solid = measured, dotted = predicted) (wind tunnel data from Lorber 1991).

One important effect of the deflection of a trailing edge surface on an airfoil section is to shift its zero lift angle of attack, or equivalently, to shift the lift coefficient at zero alpha. A theoretical formula (from Torenbeek 1988, p 529) for the change in lift coefficient at zero alpha was applied here:

$$\Delta c_{l_o} = -\frac{\partial c_l}{\partial \delta_f} \delta_f, \text{ where } \frac{\partial c_l}{\partial \delta_f} = \frac{4}{\pi}\sqrt{\frac{c_f}{c}} \tag{2-1}$$

assuming the action of the tab to be adequately approximated by a trailing edge flap.

Increments in the sectional drag coefficient were also applied for nonzero tab deflection. For airfoils with plain flaps, Torenbeek indicates that an increment in the minimum sectional drag coefficient may be added consisting of two terms dependent on the chord fraction and the deflection angle:

$$\Delta c_d = \Delta c_{d_{min}} + c_{d_{min}} \left(1 + k_l \left(c_l - (c_{l_o} + 0.5\Delta c_{l_o})\right)^2\right) \tag{2-2}$$

and

$$\Delta c_{d_{min}} \cong k_d \frac{\partial c_l}{\partial \delta_f} \frac{c_f}{c} \delta_f^2 \text{ for small } \delta_f \tag{2-3}$$

Here, $k_l \cong 1.0$ for this case, and the semi-empirical constant k_d may be approximated as 0.25. In addition, the value of the lift coefficient for the minimum drag location is shifted to account for the change in zero-lift angle of attack. Of these two effects, the increment in profile drag represents a clear penalty, though it is generally small for the small angles of deflection and chord fractions considered here. Potentially somewhat more important is the shift in the lift coefficient corresponding to minimum drag. This shift can lead to significant reductions in c_d for a given c_l particularly when blade sections operate at high angles of attack.

Finally, increments in pitching moment are introduced, also based on relationships given in Torenbeek 1988. Given that the change in effective chord length of the tabbed section will be negligible for modest deflections, the appropriate change in pitching moment coefficient may be expressed as:

$$\Delta c_m = -\mu_1 \Delta c_l, \text{ where } -\mu_1 \cong 0,25 - 0.3\left(c_f / c\right) \tag{2-4}$$

Also, output modifications were implemented to accommodate the particular requirements of these calculations. Since the baseline RotorCRAFT code addressed the computation of rotor unsteady loading during steady cruise flight conditions, the rotor motion and wake structure are periodic, and thus, an iterative relaxation technique is used to arrive at a converged solution for the blade response, wake structure, and hub loads. Typical output in these cases focuses on fixed frame hub loads. However, since the rotor shaft is assumed to have an infinite impedance, the only direct coupling between blades is via the wake aerodynamics. Numerical experimentation indicated that though cancellation in fixed frame loads would still take place, changes in vibratory 1/rev loading could be adequately approximated by modifying the blade properties of the rotor blade and extracting rotating frame hub loads from a single blade of a new four-blade set, with these blades incorporating the desired aerodynamic, structural or control modifications. By

13

using the same rotor wake for the two cases, the difference between the baseline single blade hub loads and the modified blade hub loads would constitute an approximation for the effect of blade perturbations. This approach was deemed adequate, since the lower frequency content of the wake structure would dominate the effects seen at 1/rev in the fixed frame, and it was seen not to vary significantly in the numerical experimentation conducted to support these calculations. However, effects on higher harmonic loading (e.g., at N/rev) would not be approximated as well using this approach, and would most likely require an alternate approach using a fully anisotropic rotor set.

This approach of computing a difference between a baseline and modified rotor set was judged appropriate for the present Phase I feasibility study, but it would be desirable in follow-on work to directly address the tasks required to bypass this approximation: the alteration of the computation logic to provide *time-accurate* updates on rotor response and wake movement, and the incorporation of features to represent non-identical blade properties, as would be characteristic of rotor systems with significant 1/rev vibratory response. The steps to be taken in this endeavor are described in the discussion of Phase II tasking below.

2.3 1/Rev Vibration Sources

While a large body of literature exists on rotor parametric effects on rotor system vibrations (see, e.g. Young, 1991 for a good reference list), most of this work addresses techniques for reducing N/rev vibrations, where N represents the number of blades on the aircraft. A considerably smaller number of papers address the 1/rev vibration problem directly. Part of the reason for this is that the Army has only until recently published a meaningful 1/rev vibration specification (Crews, 1987): ADS-27 (U.S. Army, 1993). Hammond (1974), in one of the earlier analyses on non-isentropic rotor systems, addressed the ground resonance stability of a rotor when one lag damper became inoperative. While his study showed the potential for destabilizing the rotor, it was not directly concerned with vibration prediction. McNulty (1988) showed that differences in non-rotating lag frequencies could produce additional peaks in the frequency spectrum recorded from rotor-body testing, making measurement of damping using transient decay techniques difficult. Wang (1991) also addressed aeromechanical stability effects of dissimilar rotor blades on a hingeless rotor system, and was not concerned with forced response in his paper. Viswanathan (1977) described a computer code for predicting unsymmetric rotor forced response, but only provided limited results and no trending information. Fries (1990) studied structural dynamic effects of ballistic damage on rotor blades, and provided only qualitative discussion on the resulting vibratory loads. Bauchau (1993) computed sensitivity information on an H-34 rotor, but provided information in terms of percentage changes instead of magnitude and phase relationships. His primary concern was the effect movable weights would have on vibration reduction. Kloppel (1984) discussed techniques for balancing tail rotors to eliminate 1/rev thrust shears, but neglected 2/rev in-plane forces that would generate 1/rev in fixed system components. Anthoine (1993) presented sensitivity information in both phase and magnitude, and showed that various effects add linearly for small perturbations in each parameter.

The approach taken here is similar to Anthoine (1993), in that variations in magnitude and phase relationships of 1/rev vibration at two flight speeds were determined for a range of parametric blade perturbations. In addition, effects on higher frequency vibrations will also be produced from the simulations. This information will be seen, in subsequent paragraphs, to aid the determination of the best means of mitigating this 1/rev vibration through applications of IBC.

A first step in the investigation of 1P vibratory loads was to quantify the nature of such loading to be expected on typical U.S. Army rotorcraft. For these the purpose of the Phase I study, a single rotor system was examined. Both because of its importance in the Army inventory and the extensive previous analytical work undertaken on its rotor system, the UH-60A Blackhawk was selected as the baseline blade set. The Blackhawk blade features a highly nonlinear twist distribution (Figure 2-6) as well as a swept tip planform (Figure 2-7).

The computations undertaken here were based a 1:5.73 model of the UH-60A rotor whose use in wind tunnel testing was described by Lorber 1991 and that was used for previous simulations (Quackenbush, et al. 1994). As noted by Lorber, the instrumented blades of this model rotor were some 30% heavier than would be called for by dynamic scaling to the full scale UH-60A rotor; this will reduce blade coning in hover and also serves to decrease blade natural frequencies by roughly 10%. To reduce the complexity of interpreting various projected changes to blade properties and aerodynamics, this model rotor geometry was simplified for the calculations discussed below by deleting the tip sweep and assuming a constant blade chord. In all other respects, the geometry and structural properties of the model blade were identical to that used in previous correlation studies such as Quackenbush, et al. (1994) and Torok and Berezin (1992).

As discussed above, nonuniformities in a blade set will be reflected in blade-out-of-track behavior (unequal coning) in hover and in imperfect load cancellation for rotors in forward flight. The first computations discussed here summarize studies of the likely deviations in blade tracking and the appearance of 1/rev vibratory loads in response to representative nonuniformities in blade structure or behavior. Based on a survey of the available literature as well as discussions with cognizant industry and Government personnel, several scenarios were developed to simulate the effect of blade-to-blade nonuniformities. The three broad types of nonuniformities considered are: mass/stiffness defects due to ballistic damage; stiffness deviations due to manufacturing variances; and aerodynamic surface (airfoil section) imperfections. Other classes of such nonuniformities are of potential interest (e.g., unequal blade mass distributions, deviations in lag damper performance, etc.), but those selected were judged to span a reasonable range of behavior to test the vibration alleviation methods of interest here.

The particular scenarios defined for this study are:

A. Structural defects attributable to ballistic damage extending over 6% of rotor radius (20 in. at full scale for the UH-60A); Viswanthan et al. (1977) suggests that defects of 50% in distributed mass, 30% in in-plane bending stiffness and 70% in out-of-plane bending stiffness are representative of ballistic damage. Within this scenario, two cases were considered: one with this postulated damage centered at 30% of rotor radius (A1), the other at 50% of radius (A2).

B. A stiffness variation of 4.6%, assumed to be distributed across the entire blade span. This scenario was derived from the observation of up to 2.4% variations in predicted blade natural frequencies derived from shake tests of the UH-60A rotor blades used in the UH-60 Airloads program at NASA Ames (Hamade, et. al., 1992).

C. Aerodynamic imperfections leading to sectional deviations of 0.1% in sectional lift curve slope and 1% in moment coefficient. Bauchau (1993) use these levels in assessments of the effects of blade dissimilarities. For estimation purposes, these have been extended to the full span of one UH-60A blade.
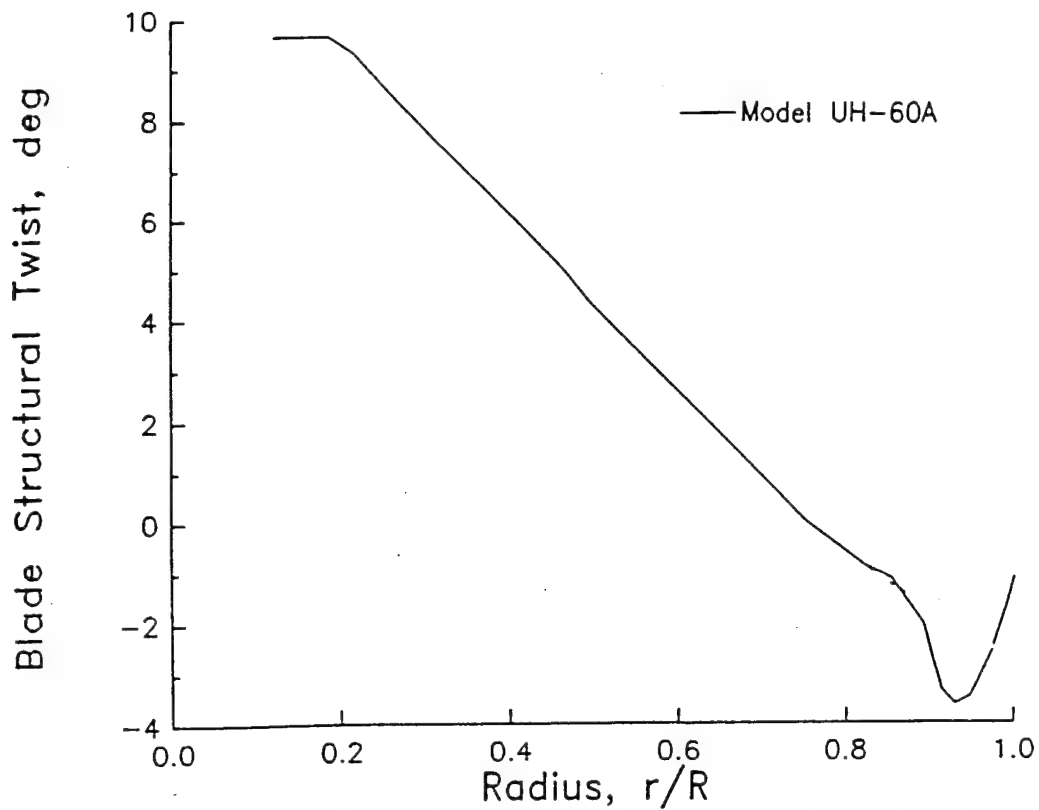
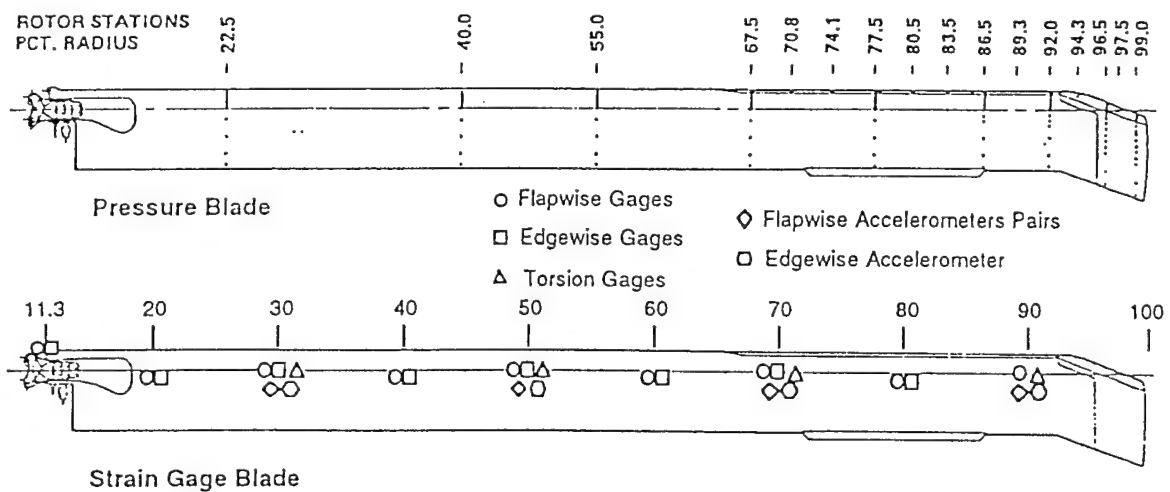Figure 2-6. Geometric twist distribution of the UH-60A model rotor blade (from Lorber 1991).

Figure 2-7. Schematic of the UH-60A planform, showing instrumentation locations from recent flight tests (from Kufeld, et al. 1994).

16

D. Aerodynamic perturbations arising from a 0.5% deviation from the nominal blade twist distribution; this level was also characterized as a representative level by Bauchau and Lee (1993).

2.3.1 Computations in Hover

Though RotorCRAFT was primarily designed to carry out computations of blade loading in steady forward flight using the CVC wake model, it does have the option to bypass the use of the filamentary wake to define a simple inflow downwash model of the following form:

$$w = \Omega R \left(\lambda_0 + \lambda_{1c} \, x \cos \psi \right) \tag{2-5}$$

where

$$\lambda_0 = -\mu \alpha_s + \frac{C_T}{2\mu} \tag{2-6}$$

and

$$\lambda_{1c} = \frac{C_T}{\sqrt{2}\,\mu} \tag{2-7}$$

Moreover, a further option exists to operate the rotor in hover in the presence of a uniform downwash defined by momentum theory (i.e., $w_{unif} = \Omega R (0.5 C_T)^{1/2}$). This option provided the opportunity to explore variations in blade coning that arise from the imposition of one or another of the damage/nonuniformity scenarios just described.

The particular operating condition selected was $C_T/\sigma = 0.08$, corresponding to a thrust coefficient of .0064. A baseline case was run and required a blade root collective pitch of 20.04 deg. With this pitch control set, scenarios A (A1 and A2), B, C, and D above were implemented via a combination of tailored code modifications and altered input files. The nominal coning angle was 2.11 deg. (a smaller value than would be observed on the full-scale rotor owing to the increased mass of the instrumented model blade). The computed coning angles for the reference blade with the defect were: Scenario A1: 2.06 deg.; Scenario A2: 2.21 deg.; Scenario B: 2.01 deg.; Scenario C: 2.06 deg.; and Scenario D 2.01 deg. The maximum coning deviation observed here is an angular change that corresponds to roughly 0.7 in. out-of-track at the blade tip for a full scale UH-60A. This is comparable to the out-of-track predictions made for UH-1 blades by Viswanthan et al. (1977).

Forces and moments transmitted to the fuselage frame as a consequence of these blade perturbations are shown in Figures 2-8 through 2-13. These six figures indicate the sine and cosine component of shear and moment loads perturbations, divided by net rotor thrust, and rotor thrust multiplied by hinge offset distance respectively. This nondimensionalization allows for comparison of these effects across various rotor systems (since the nondimensionalized shear loads would represent "gees" of loading), and also permits relative comparison of these effects with suggested blade IBC control actuation concepts in order to gauge their effectiveness. The sequence for these plots is: longitudinal shears and moments, then lateral shears and moments, and finally vertical shears and moments.

Fixed-frame (fuselage) 1/rev forces and moments are a result of 1/rev modulation of steady and 2/rev loads and moments in the rotating frame for all in-plane components.

Out-of-plane shears and torque or yaw moments are the same in the rotating and fixed frames of reference (Johnson, 1980). Thus, 1/rev overturning moments and inplane shears can be significantly affected through modification of steady changes in blade position, since centrifugal loads would act through different radial arms due to the resultant displacement in blade mass center. It is primarily for this reason that blade tracking is an important component of 1/rev vibration mitigation, although it is not the sole means of smoothing a rotor system.

Figures 2-8 and 2-10, and 2-9 and 2-11, reveal a common trait in the modulation of the blade loads from the rotating frame to the fixed frame: when the steady components dominate over the 2/rev rotating loads, the longitudinal and lateral components of 1/rev inplane loads will only differ through a phase angle of 90°. Phase angle defined here is relative to the damaged (or, control-perturbed) blade, which is referenced to 0° azimuth angle (aft over the aircraft tail). Thus, all blade longitudinal perturbations are shown to have cosine components of load that dominate the response, indicating that the most prevalent mechanism for in-plane shear and moment changes are aligned with the damaged blade. As can be seen in the plots, all of these representative blade perturbations are approximately equal in terms of overturning moment changes, but the ballistic damage scenarios are the principal contributors to in-plane shears. Moment changes are a consequence of a different flapping (coning) angle, whereas in-plane shears would be a result of a significant mass defect in the blade structure, leading to a "classic" balance problem.

2.3.2 Computations in Forward Flight

Similar simulated perturbation studies were conducted on this rotor in forward flight. A representative operating condition was chosen corresponding to advance ratio 0.2 and shaft angle of attack of -4 °, again assuming $C_T/\sigma = 0.08$. A slightly modified set of perturbations were used as compared to Scenarios A-D above. First, since the outboard ballistic damage case was seen to be a larger source of 1/rev loads that the inboard damage case, only the outboard condition was postulated. Secondly, since several references in the literature had dealt with the effects of inoperative lag dampers or changes in their dynamic properties (McNulty, 1988; Anthoine, 1993), a similar scenario was postulated for this rotor as well. These perturbations would include both a change in damping coefficient, which would alter the lag response in both magnitude and phase, as well as an effective change in lag stiffness, for the case of an elastomeric damper, that can provide both damping and stiffness forces due to relative rotation (Smith, 1995). Since the RotorCRAFT code does not currently provide for direct changes in both lag damping and lag stiffness (other than through direct modification of blade properties or lag hinge offset), a compromise perturbation was used. Lag response as it affects 1/rev loads would be due to a static change in the lag angle of the blade (due to a change in stiffness about the lag hinge) or 2/rev rotating-frame motion modifications as a result of lag damper coefficient perturbations. Since 2/rev motion is significantly above typical articulated rigid lag mode frequency (often near .2 or .3 /rev), the 2/rev motion amplitude, and its associated velocity, would be small. As a consequence, mere changes in lag damper viscous damping coefficient was not seen to significantly alter the response of the rotor, and thus a *doubling of the static drag coefficient* for the rotor blade was deemed the easiest approach, short of a major code change, to approximate the effects of a perturbed elastomeric damper in terms of changes in both stiffness and damping coefficient. This comprised the postulated scenario that replaced the inboard ballistic damage case investigated at hover.

Results from the postulated "damage" scenarios are shown in Figures 2-14 through 2-19. While similar trends are seen in 1/rev overturning moments as were noted for the

hover case, both vertical shears and vertical moments (torque effects) are significantly altered for these perturbations under the influence of rotor aerodynamic asymmetry in forward flight. Some differences other than a simple phase shift may also be noted between the longitudinal and lateral in-plane shears and moments, due to the significant 2/rev loading present in forward flight on the rotor blades.

2.4 Potential Actuation Concepts and Effects on 1/Rev Vibration

Actuation concepts considered for this Phase I work included all those means traditionally used in 1P vibration suppression that could conceivably be automated for operation during flight (i.e., the rotor rotating and generating lift). Although this would preclude the addition or removal of blade mass, actuation schemes considered operated on either blade aerodynamic or inertial force-producing mechanisms in order to supply the necessary countering 1/rev inputs to smooth the helicopter rotor system. These included:

> Traditional IBC root pitch control, but of a limited authority. This is equivalent to standard pitch link adjustments made in order to provide a gross change in total blade lift, which aids primarily in tracking the rotor system. This would not include IBC systems that would replace the conventional swashplate with a scheme to provide for full-motion root pitch control (e.g., Guinn, 1982). This latter type of system is much more complicated, since it must include all potential combinations of rotor collective and cyclic motion (and loads!) available from a swashplate as well as perform with equivalent (or better) reliability, since it is a safety-of-flight item.

> Trailing edge tab devices. These devices, when available on the rotor blade, provide a very powerful and effective means of generating favorable blade lift and pitching moment on the blade. They are used as the primary mechanism to achieve a proper track for the OH-6 helicopter in forward flight (McDonnell-Douglas, 1984).

> Chordwise mass balance adjustments. While discrete addition and subtraction of blade mass would be physically impossible, chordwise adjustments of mass at the blade tip or inboard at the root could possibly be automated using a smart-materials actuation device.

Several studies were undertaken using the modified RotorCRAFT code to assess the influence of tab deflections, root pitch adjustments, and tip mass redistribution on blade motion and hub loads. These studies were designed to supply information for subsequent "pre-design" computations to define the requirements for effective 1P vibration control.

The first set of calculations involved the deflection of trailing edge tabs. For simplicity, the tab configuration was assumed to be the same as that for the current UH-60A blade, specifically a 7% chord surface extending from 70% of blade radius to 85%. A series of computations were undertaken to calculate the 1/rev loading for a series of tab deflection levels. Figure 2-20 through 2-25 show the load changes in hover due to trailing edge tab deflections ranging from -3° to 3°. This form of control is seen to provide a very powerful overturning-moment control at 1/rev, with a rather small change to in-plane 1/rev shears. Tab changes generate a rather modest change in spanwise lift, but a significant change in steady torsional response of the blade, thus providing an effect not unlike that of a servo-flap system used on the SH-2 helicopter. Of particular notice is the fact that the 1/rev overturning moment response due to tab deflection is aligned closely with the various postulated blade damage scenarios, indicating that rotor tab deflection would be a significant tool in the alleviation of this vibration source. This same effect is noted in the discussion on the forward flight load analysis below, and was a contributing factor in the design of the candidate actuator that resulted from this Phase I investigation.

Forward flight perturbation calculations included the examination of all three different control effects described above: trailing edge tab deflections, root collective pitch changes, and tip mass chordwise shifts. These control effects were judged to be the most practical for active control implementation using Shape Memory Alloy-based actuation concepts, and represented the type of actual blade track and balance perturbations used in the smoothing of a rotor system (Anthoine, 1993).

Tab deflections at this flight condition were considered over the same range of approximately +/-3°, and the resulting perturbations in forces and moments are shown in Figures 2-26 through 2-31. As was the case for hover, tab changes provide an effective means of controlling 1/rev vibrations for both in-plane and out-of-plane responses, with gradients that approximately match those calculated for the perturbations in the damaged blade (including vertical shears and moments).

Figures 2-32 through 2-37 indicate the perturbations in 1/rev loads possible for changes in root collective pitch on a single blade. The resulting in-plane and out-of-plane loads follow similar trends as for those generated from the tab deflections, with the exception that the resulting yaw moments induced by the collective changes appear to be significantly smaller. While this might appear to be a benefit associated with this type of control, the gradients of yaw moment associated with tab deflection *also* mimic those associated with many of the postulated damage scenarios, and thus, the tab deflection may be more beneficial in the reduction of total 1/rev vibrations. Control effectiveness can be readily seen, in that approximately 0.5 degrees of collective pitch provides the equivalent control as does 1.5 degrees of tab deflection; however, as will be discussed below, the penalty for this improved effectiveness is a substantial boost in system complexity for the actuator designer.

The final proposed perturbations studied for the forward flight case were changes in tap mass chordwise offset. Several rotor blade manufacturers include two locations in the blade tip for installation of blade tip weights, and the concept addressed here was the potential effects of providing an active means of repositioning the tip balance weight chordwise using a small tip-mounted actuator. Rather modest shift ranges of only +/-5% of blade chord were allowed, in order to limit the requirements on both actuator stroke and housing for the moving mass. Figures 2-38 through 2-43 show that this control concept would require significantly improved stroke were it to compete with the previous two aerodynamic control effectors in providing countering 1/rev loadings to achieve a smoothed rotor system.

The overriding conclusion from these studies is that *an active trailing edge tab adjustment for rotor tracking and 1/rev load alleviation would provide a powerful and effective means of helping solve the helicopter 1/rev vibration problem.* The advantages of such an approach would include added safety (since it would not constitute a primary control mechanism for aircraft flight, or interfere with one), limited size requirements, limited power and force requirements (as will be shown), and a potential for use in a retrofit to an existing helicopter rotor system. These features will be further defined in the discussion that follows, along with some additional arguments that support this choice of actuator in the candidate IBC application for 1/rev vibration reduction. Implementation issues and a limited design development for this concept are presented in Section 3 below.
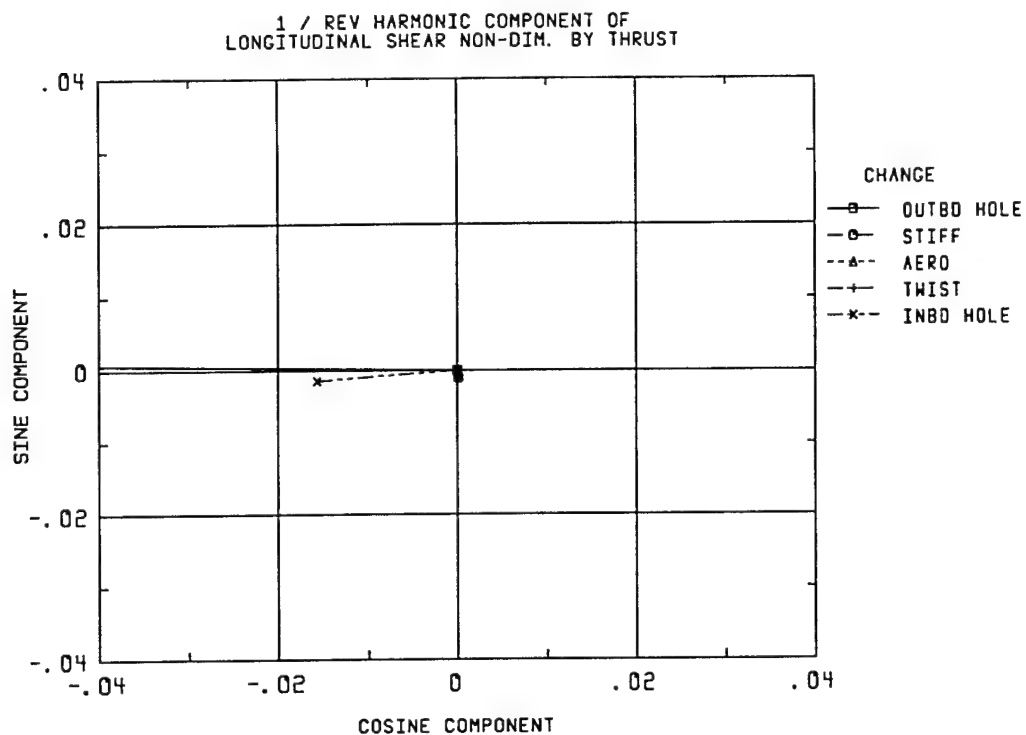
1 / REV HARMONIC COMPONENT OF
LONGITUDINAL SHEAR NON-DIM. BY THRUST

Figure 2-8. Longitudinal shear at 1P for various blade perturbations, hover

1 / REV HARMONIC COMPONENT OF
LONGITUDINAL MOMENT NON-DIM. BY THRUST X OFFSET

Figure 2-9. Longitudinal moment at 1P for various blade perturbations, hover

21

1 / REV HARMONIC COMPONENT OF
LATERAL SHEAR NON-DIM. BY THRUST

Figure 2-10. Lateral shear at 1P for various blade perturbations, hover

1 / REV HARMONIC COMPONENT OF
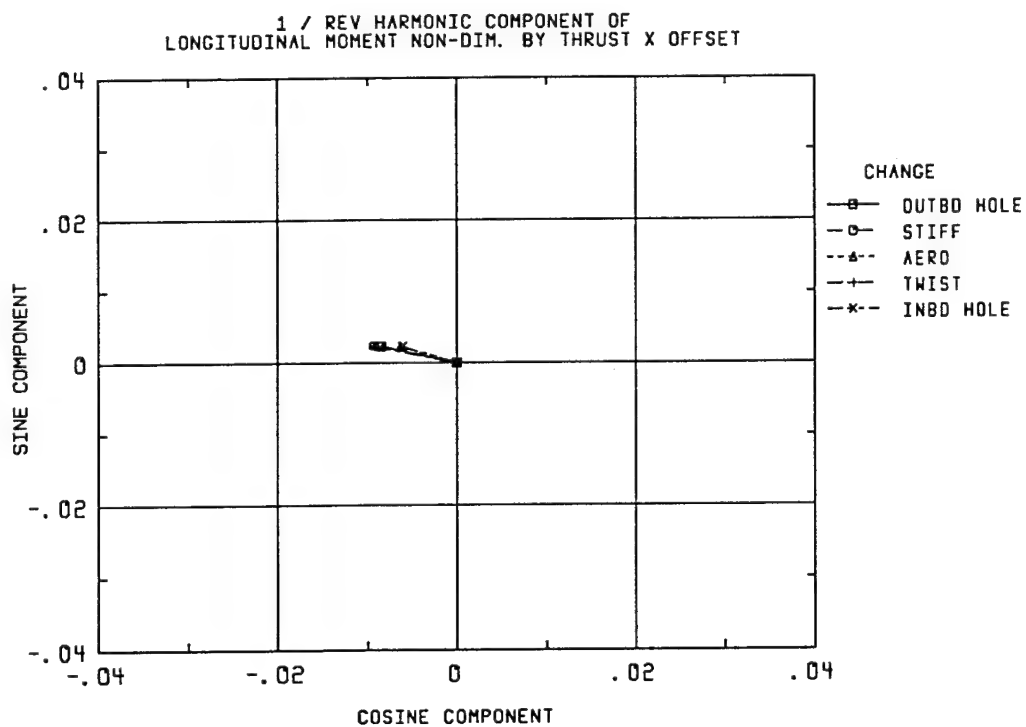LATERAL MOMENT NON-DIM. BY THRUST X OFFSET

Figure 2-11. Lateral moment at 1P for various blade perturbations, hover

22

Figure 2-12. Vertical shear at 1P for various blade perturbations, hover

Figure 2-13. Vertical moment at 1P for various blade perturbations, hover

23

Figure 2-14. Longitudinal shear at 1P for various blade perturbations, mu=0.2

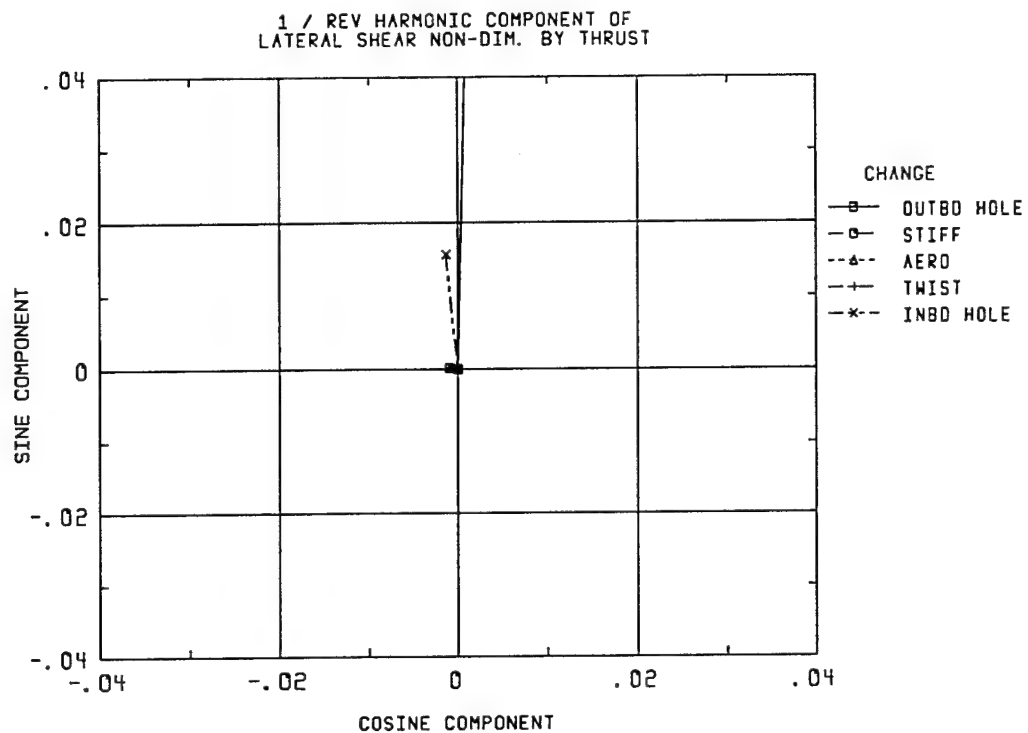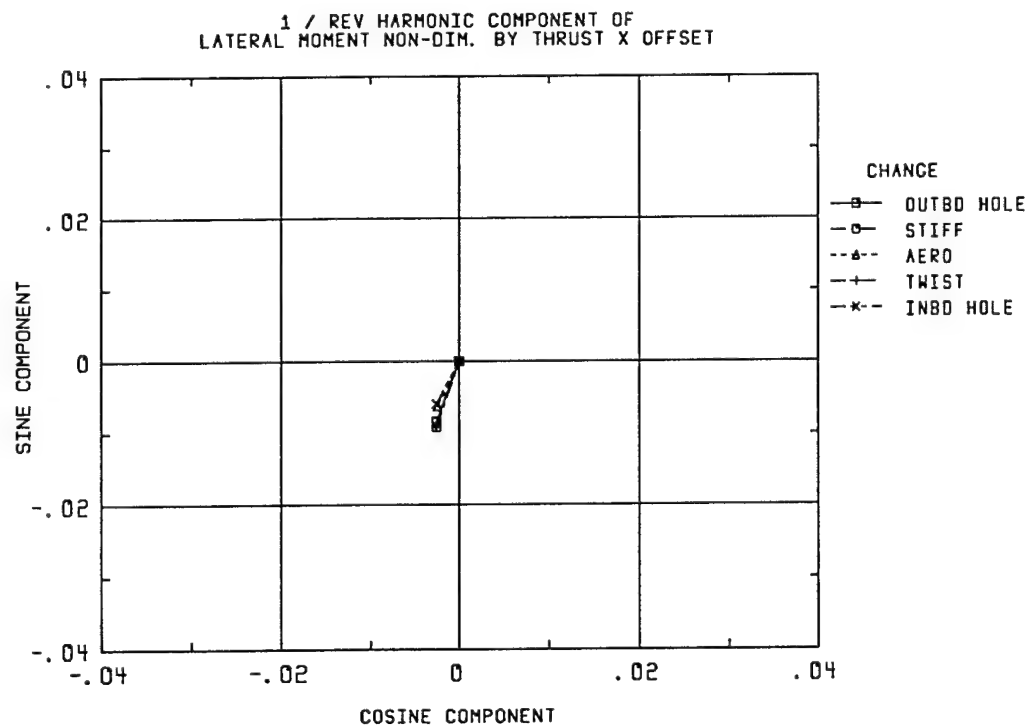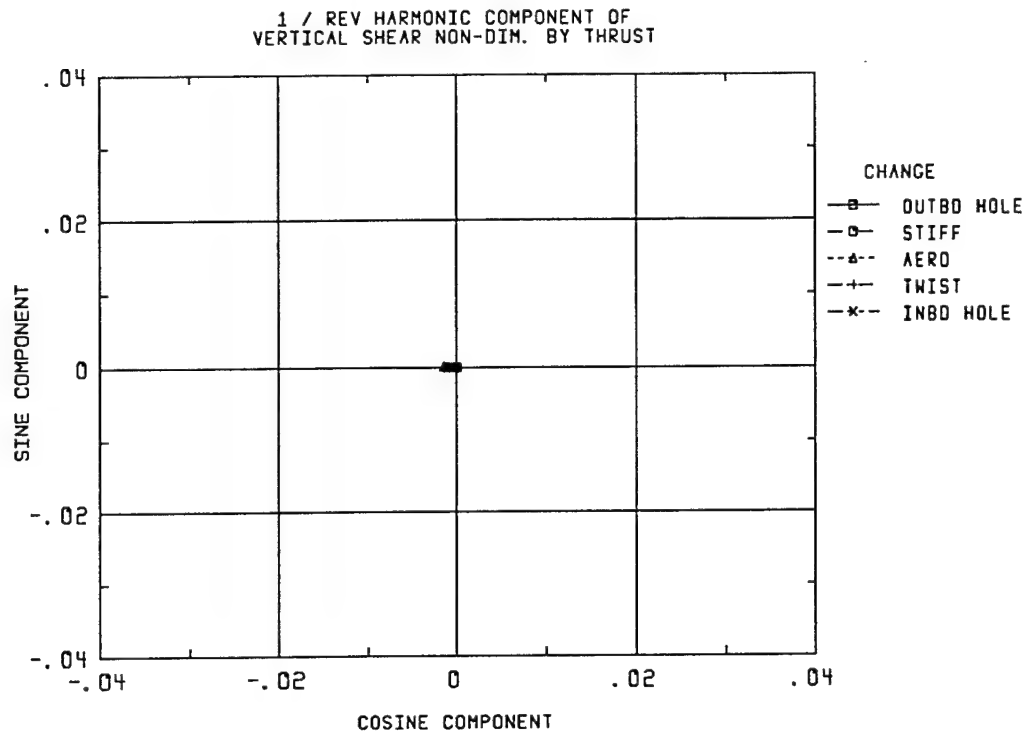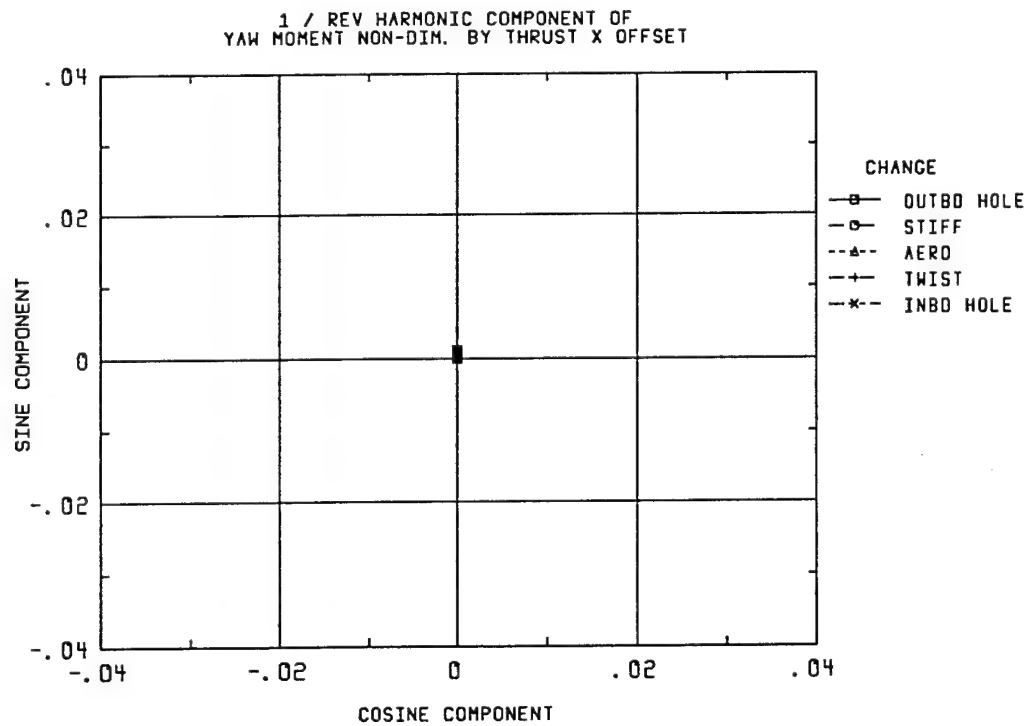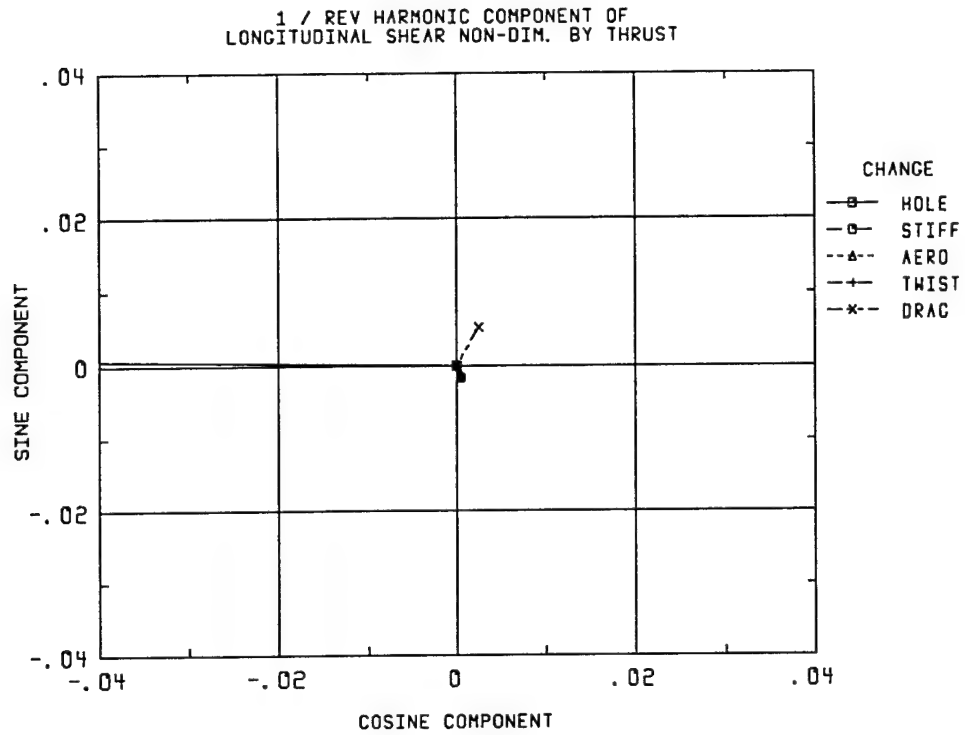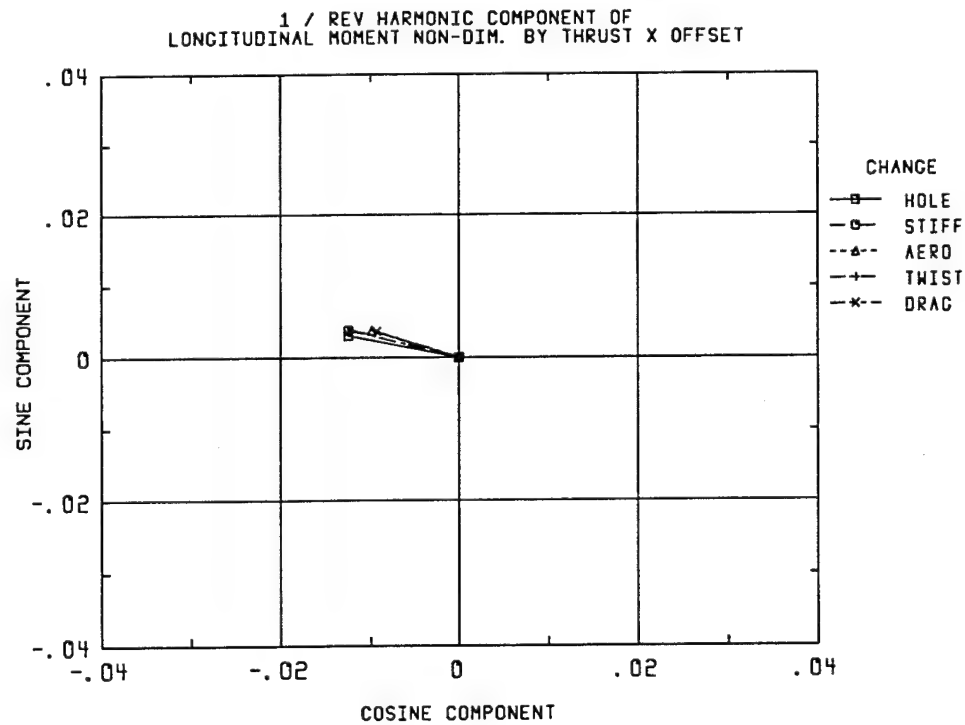Figure 2-15. Longitudinal moment at 1P for various blade perturbations, mu=0.2

24
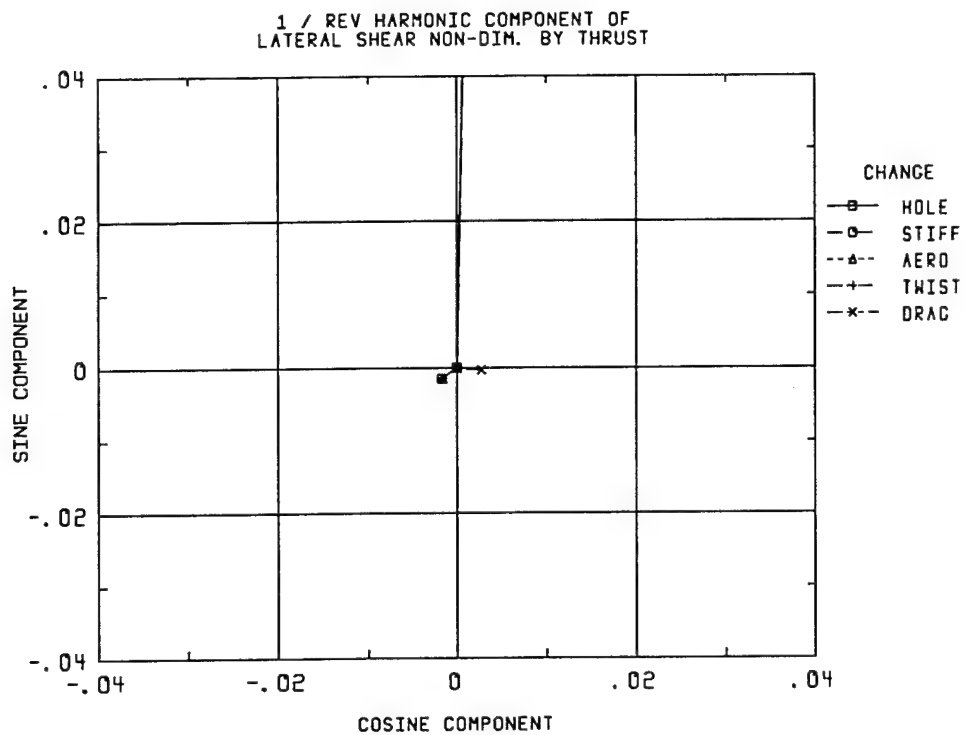
Figure 2-16. Lateral shear at 1P for various blade perturbations, mu=0.2
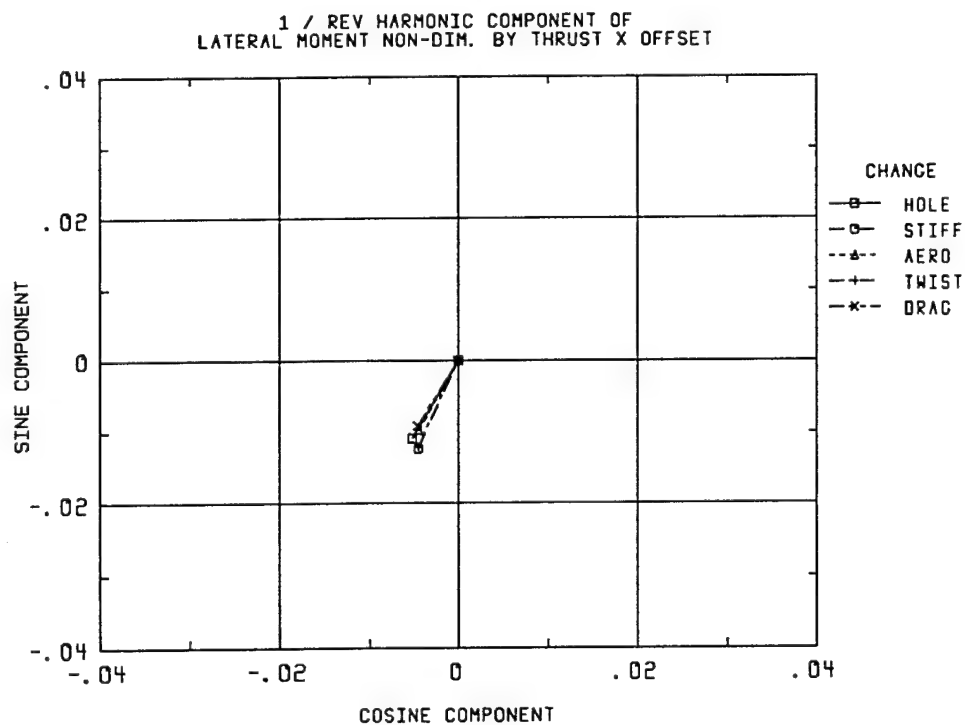
Figure 2-17. Lateral moment at 1P for various blade perturbations, mu=0.2

25

1 / REV HARMONIC COMPONENT OF
VERTICAL SHEAR NON-DIM. BY THRUST
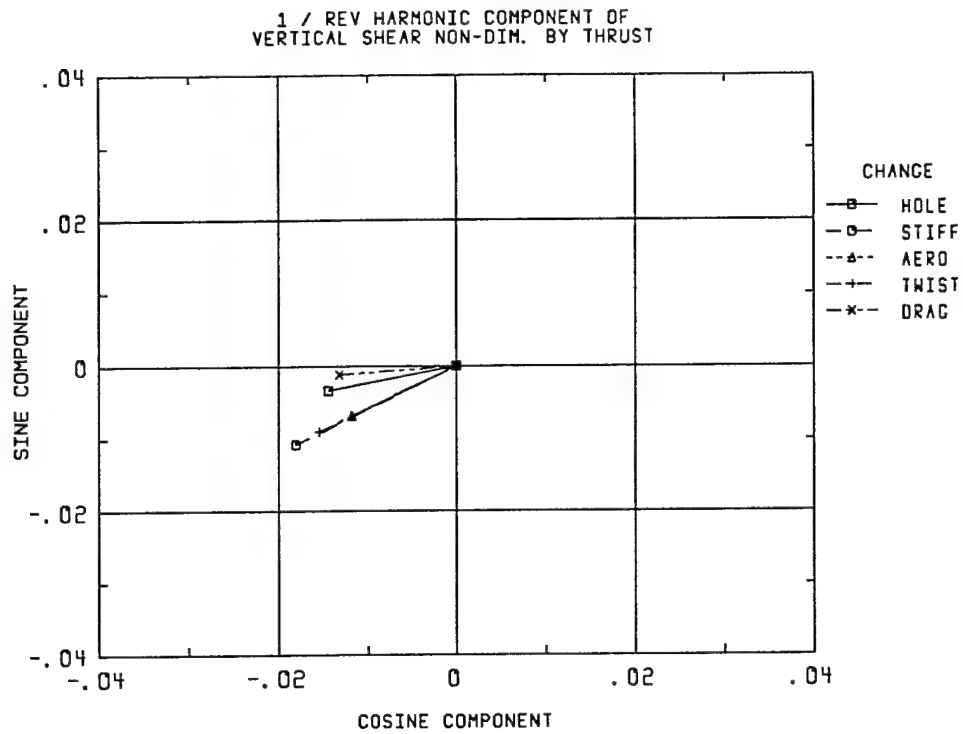
Figure 2-18. Vertical shear at 1P for various blade perturbations, mu=0.2

1 / REV HARMONIC COMPONENT OF
YAW MOMENT NON-DIM. BY THRUST X OFFSET
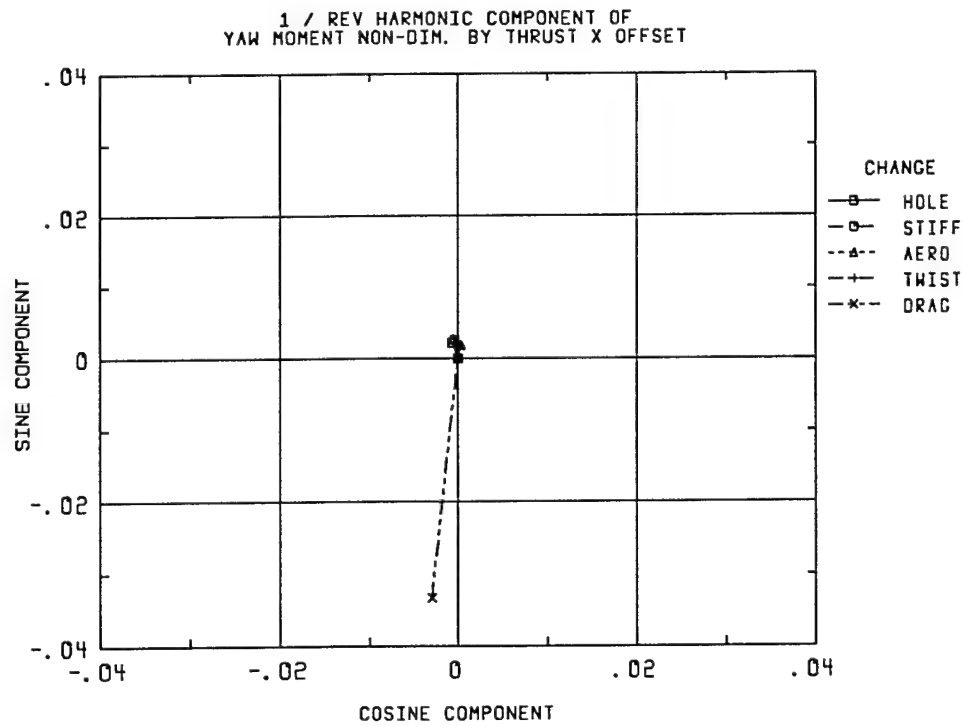
Figure 2-19. Vertical moment at 1P for various blade perturbations, mu=0.2

1 / REV HARMONIC COMPONENT OF
LONGITUDINAL SHEAR NON-DIM. BY THRUST
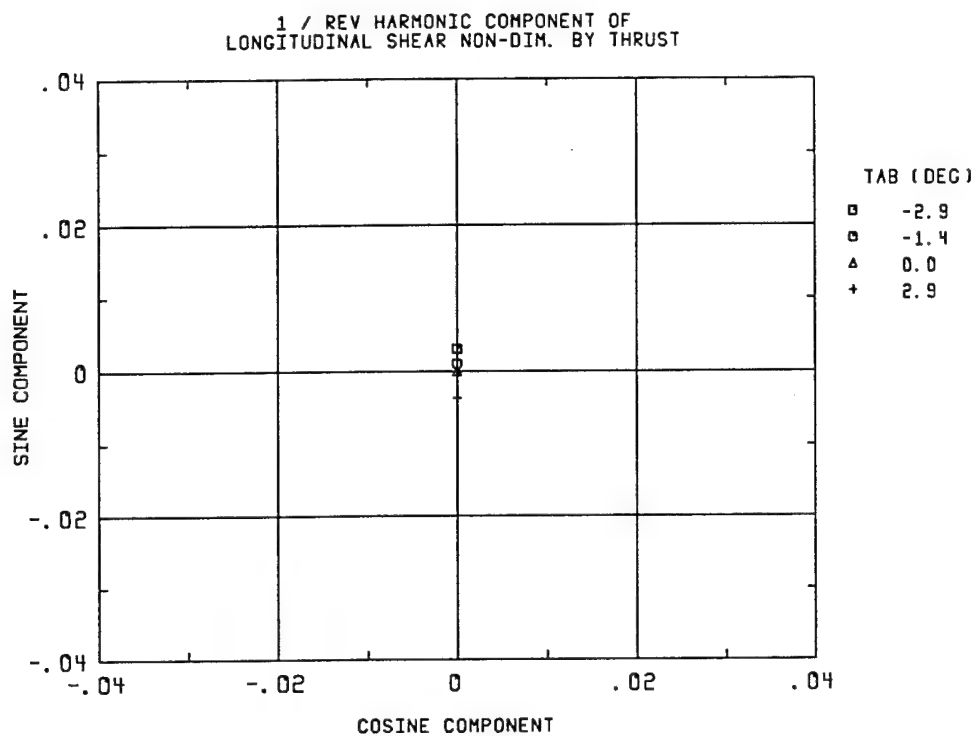
Figure 2-20. Longitudinal shear at 1P for various tab angles, hover

1 / REV HARMONIC COMPONENT OF
LONGITUDINAL MOMENT NON-DIM. BY THRUST X OFFSET
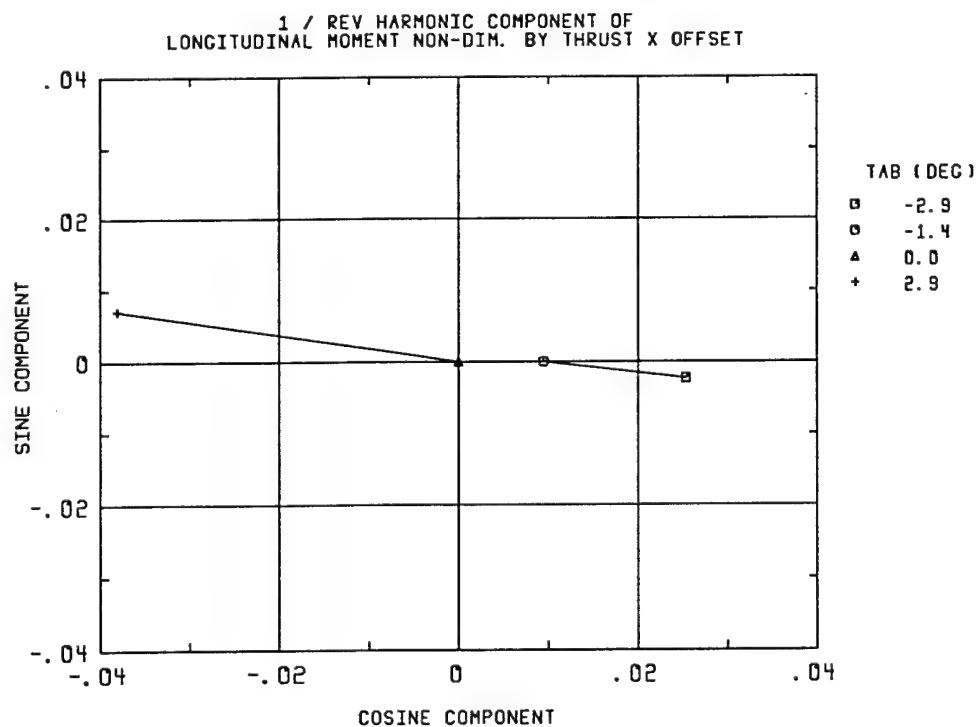
Figure 2-21. Longitudinal moment at 1P for various tab angles, hover

27

1 / REV HARMONIC COMPONENT OF
LATERAL SHEAR NON-DIM. BY THRUST
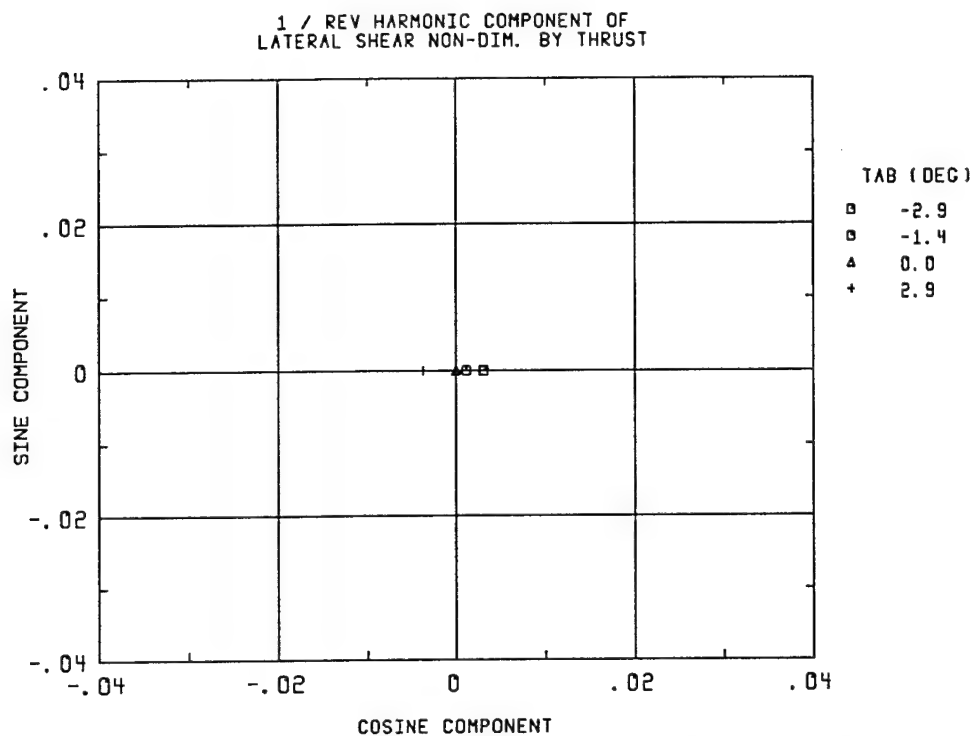
Figure 2-22. Lateral shear at 1P for various tab angles, hover

1 / REV HARMONIC COMPONENT OF
LATERAL MOMENT NON-DIM. BY THRUST X OFFSET
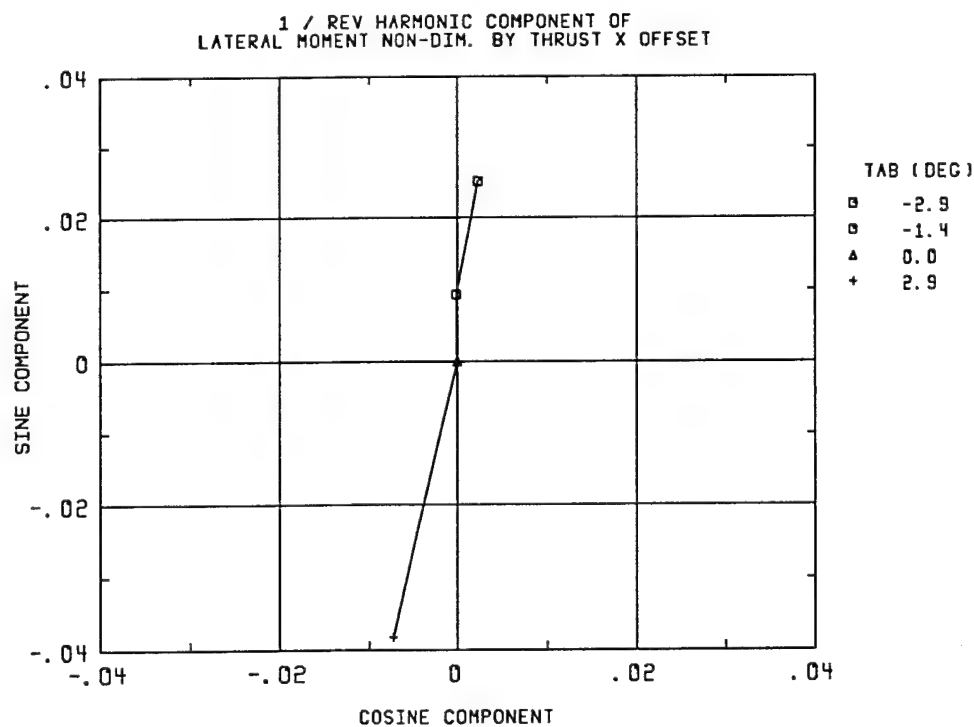
Figure 2-23. Lateral moment at 1P for various tab angles, hover

28
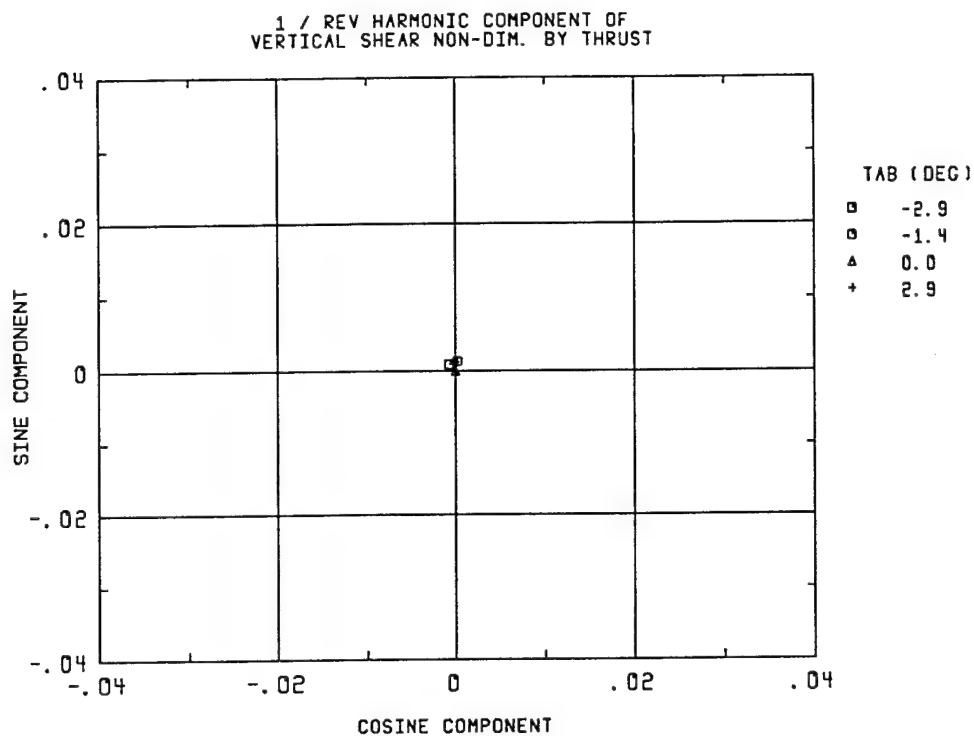
Figure 2-24. Vertical shear at 1P for various tab angles, hover
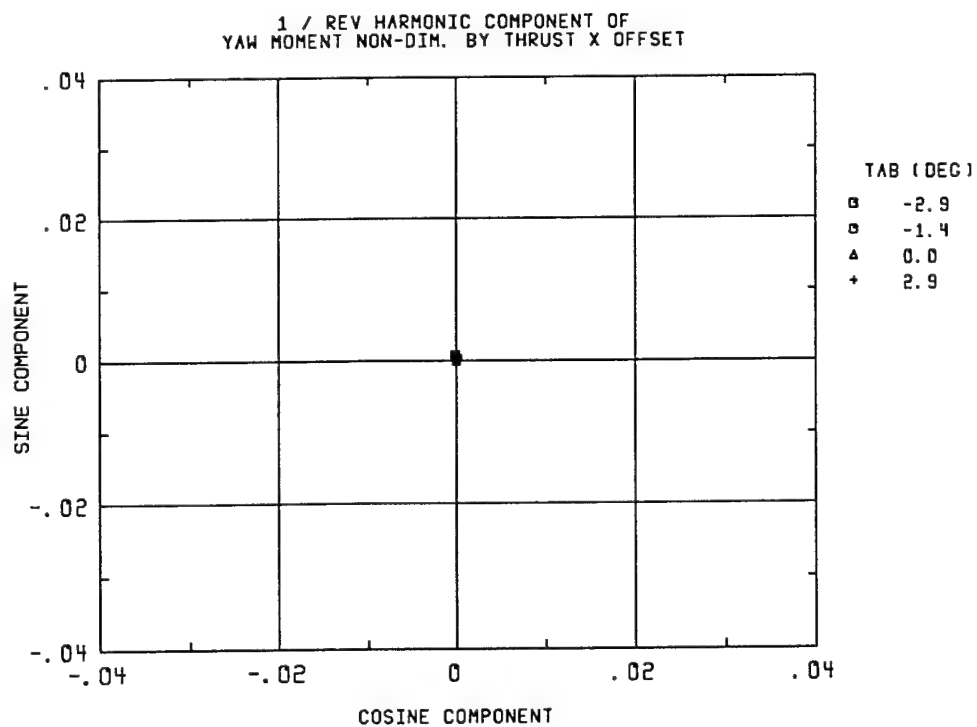
Figure 2-25. Vertical moment at 1P for various tab angles, hover

29
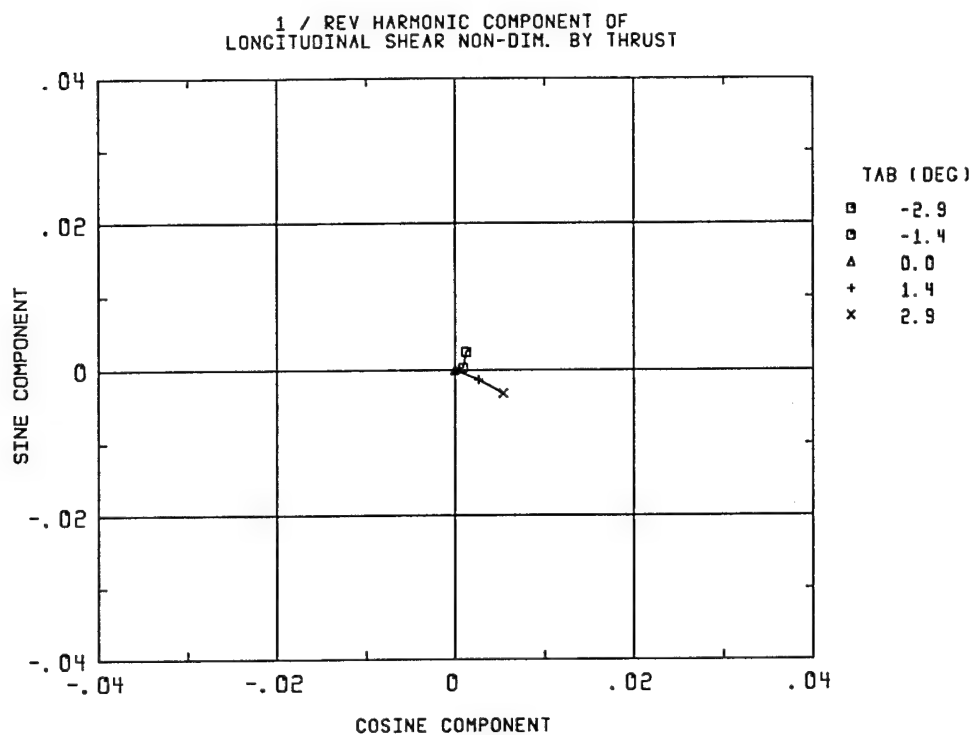
Figure 2-26. Longitudinal shear at 1P for various tab angles, mu=0.2
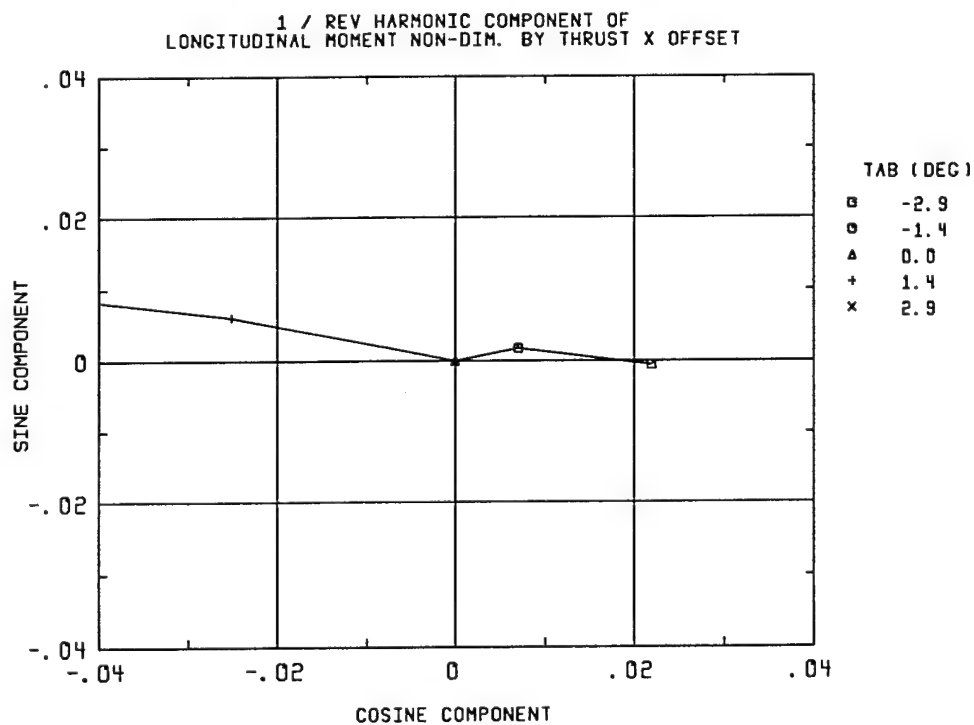
Figure 2-27. Longitudinal moment at 1P for various tab angles, mu=0.2

30

1 / REV HARMONIC COMPONENT OF
LATERAL SHEAR NON-DIM. BY THRUST
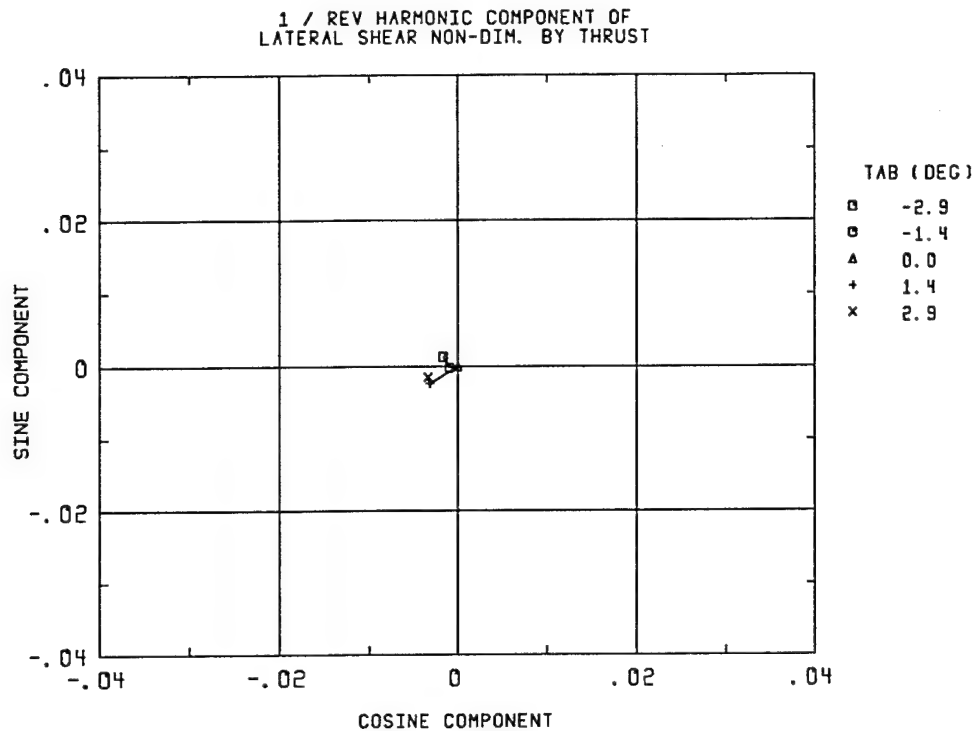
Figure 2-28. Lateral shear at 1P for various tab angles, mu=0.2

1 / REV HARMONIC COMPONENT OF
LATERAL MOMENT NON-DIM. BY THRUST X OFFSET
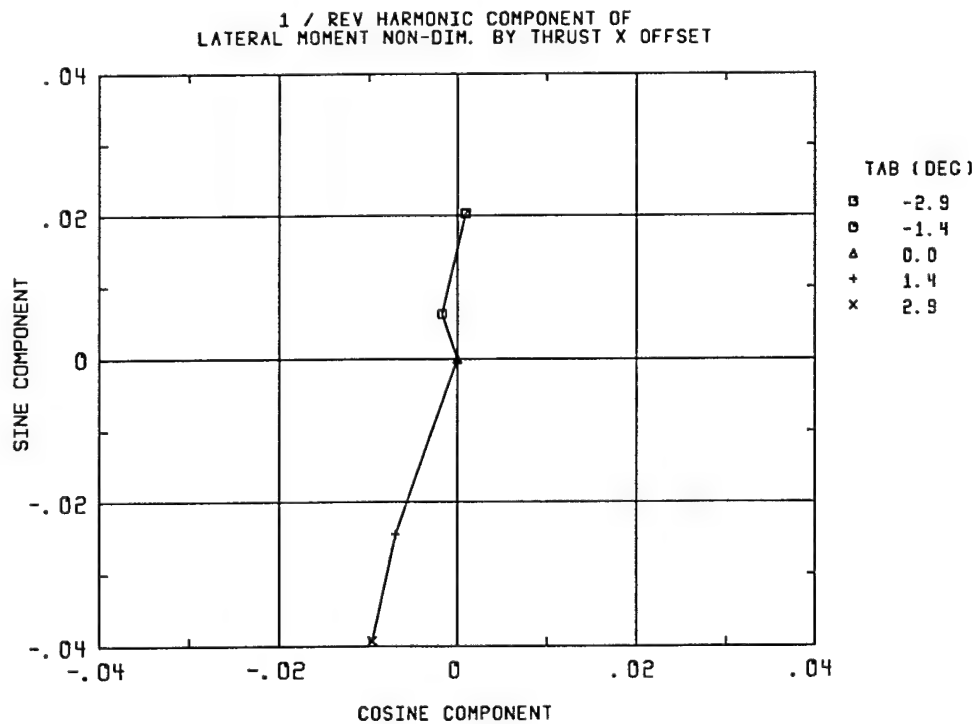
Figure 2-29. Lateral moment at 1P for various tab angles, mu=0.2

31

1 / REV HARMONIC COMPONENT OF
VERTICAL SHEAR NON-DIM. BY THRUST
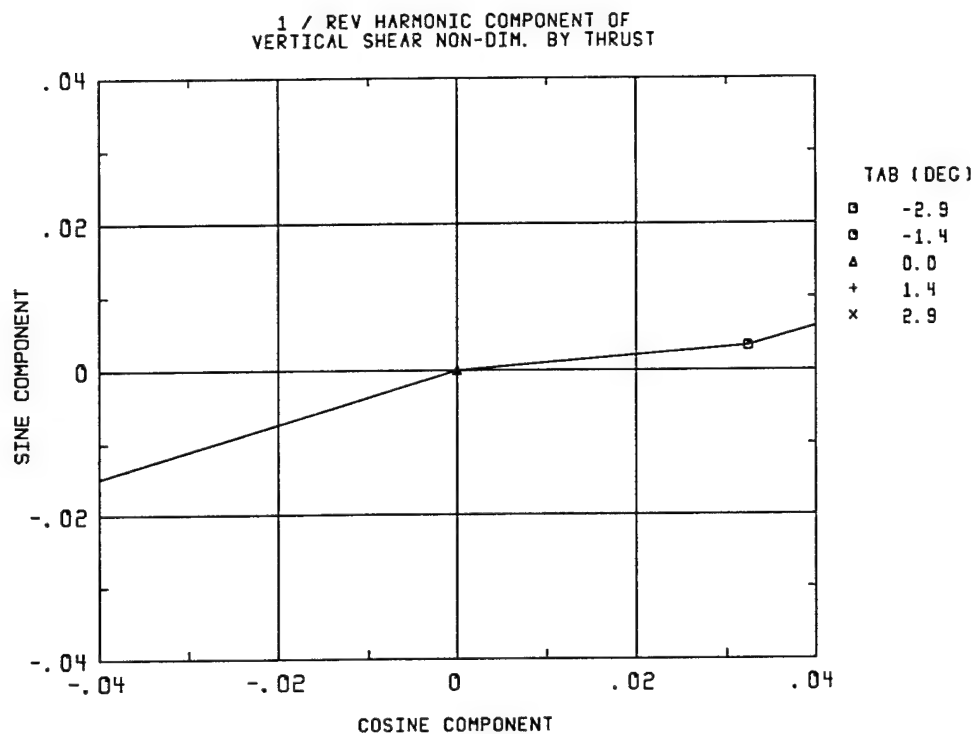
Figure 2-30. Vertical shear at 1P for various tab angles, mu=0.2

1 / REV HARMONIC COMPONENT OF
YAW MOMENT NON-DIM. BY THRUST X OFFSET
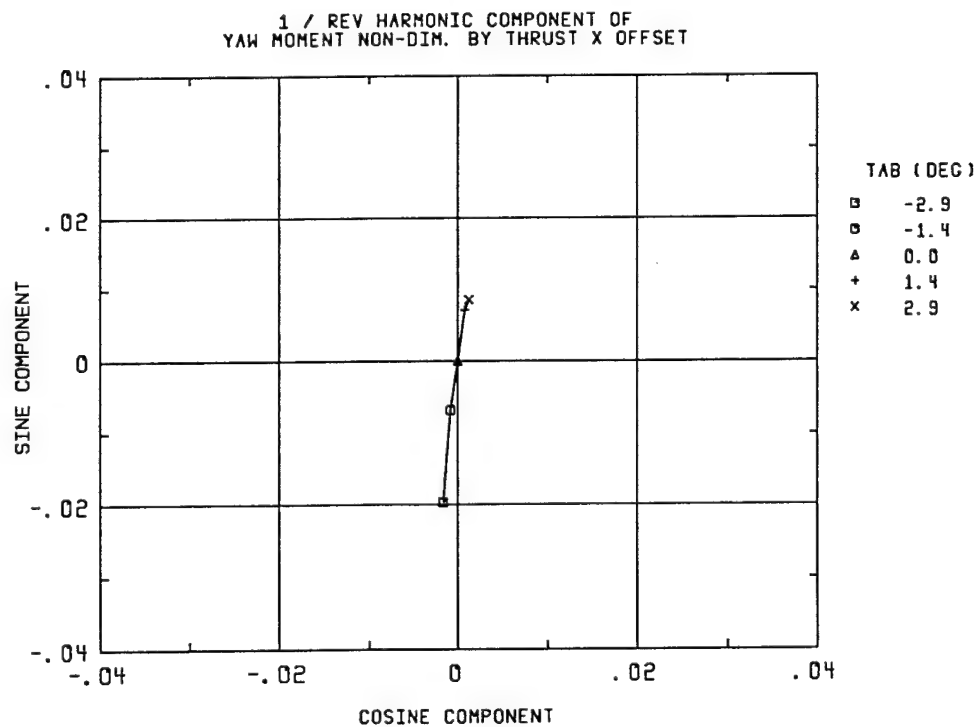
Figure 2-31. Vertical moment at 1P for various tab angles, mu=0.2

32
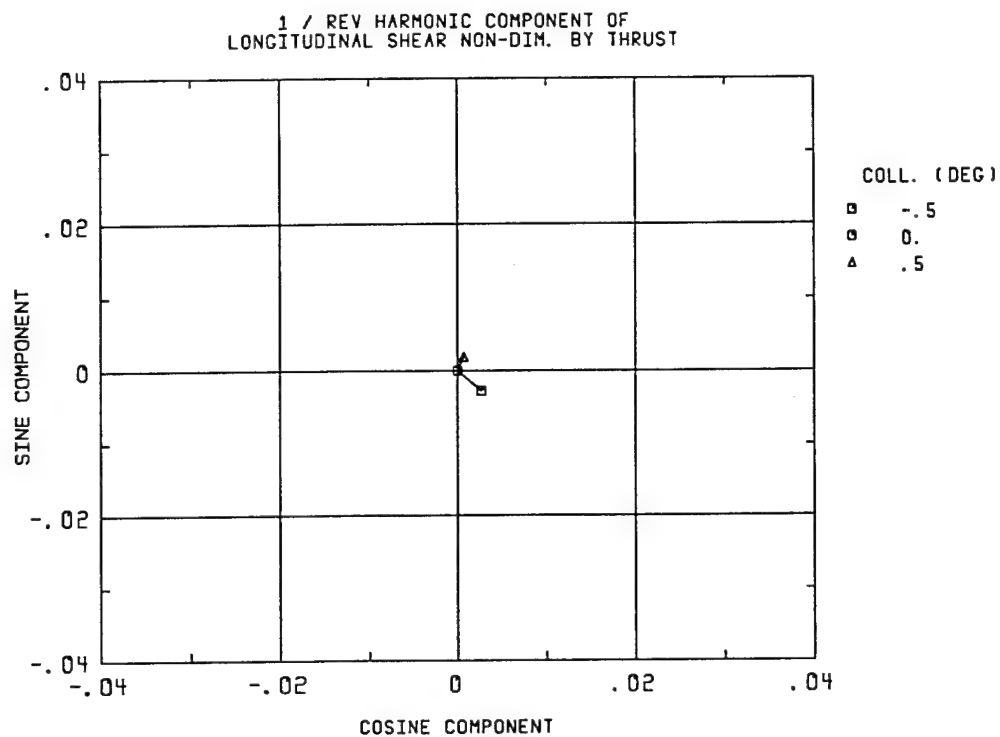
Figure 2-32. Longitudinal shear at 1P for various collective angles, mu=0.2
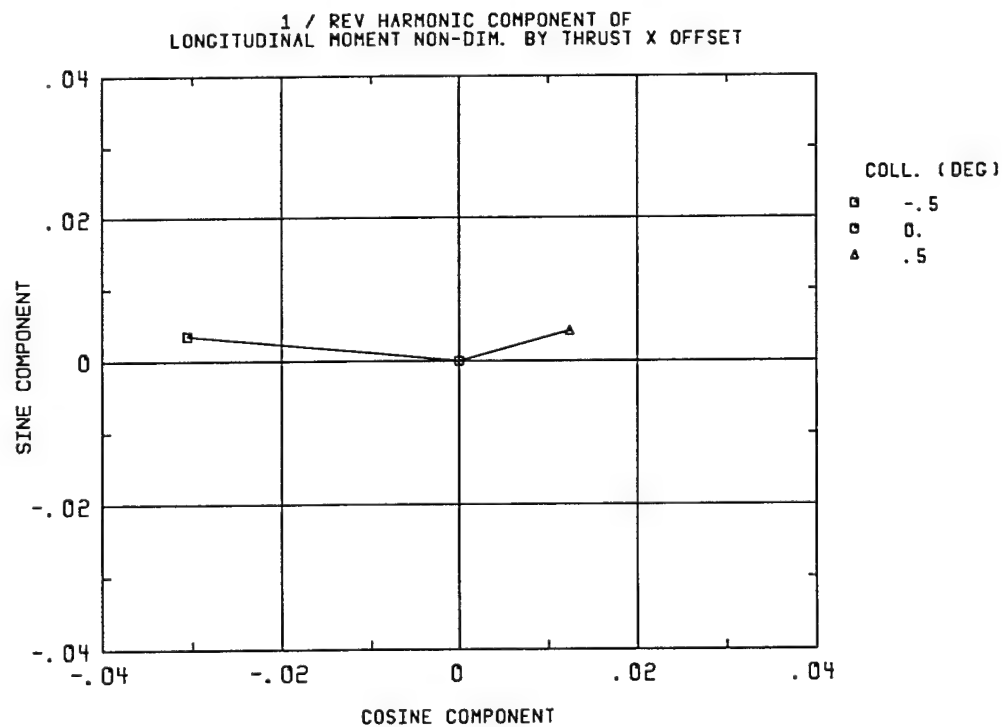
Figure 2-33. Longitudinal moment at 1P for various collective angles, mu=0.2

33

1 / REV HARMONIC COMPONENT OF
LATERAL SHEAR NON-DIM. BY THRUST
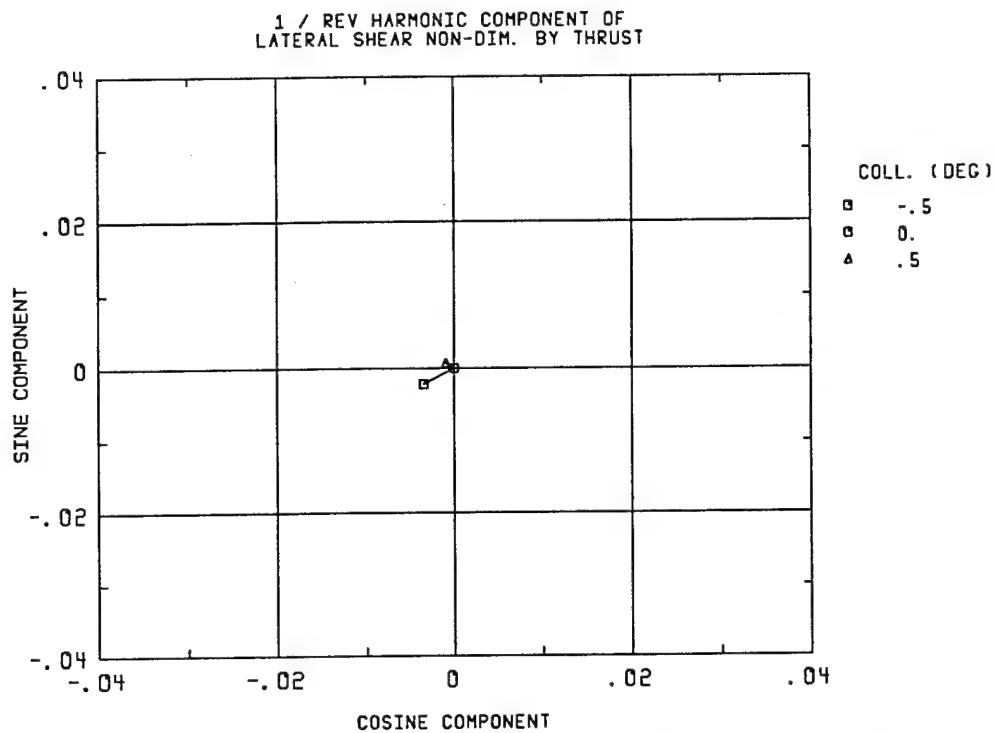
Figure 2-34. Lateral shear at 1P for various collective angles, mu=0.2

1 / REV HARMONIC COMPONENT OF
LATERAL MOMENT NON-DIM. BY THRUST X OFFSET
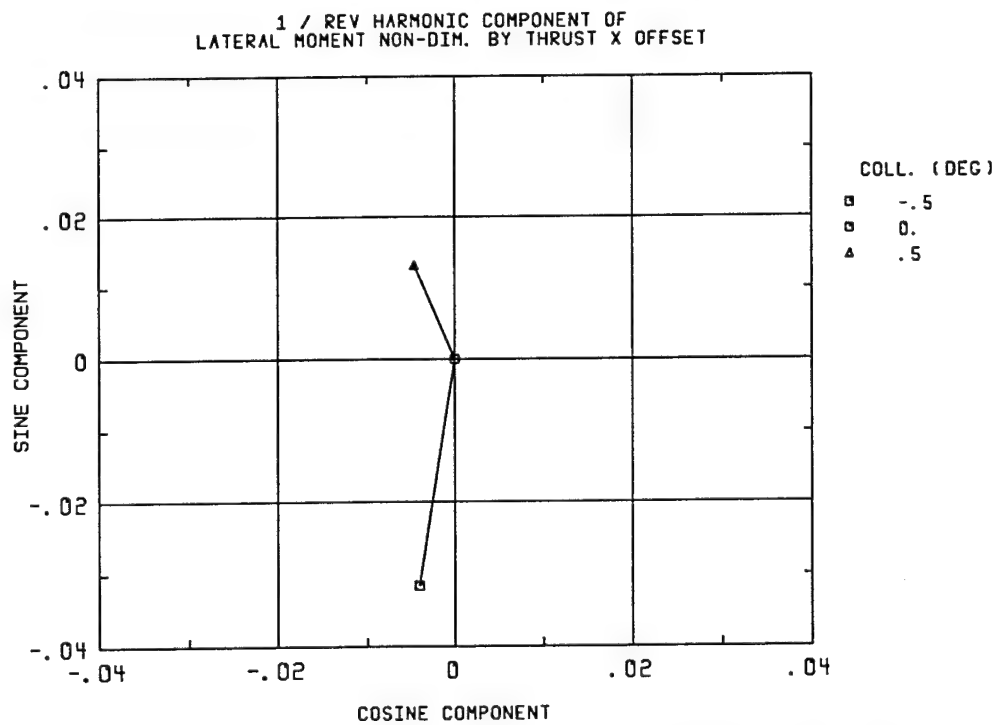
Figure 2-35. Lateral moment at 1P for various collective angles, mu=0.2

1 / REV HARMONIC COMPONENT OF
VERTICAL SHEAR NON-DIM. BY THRUST
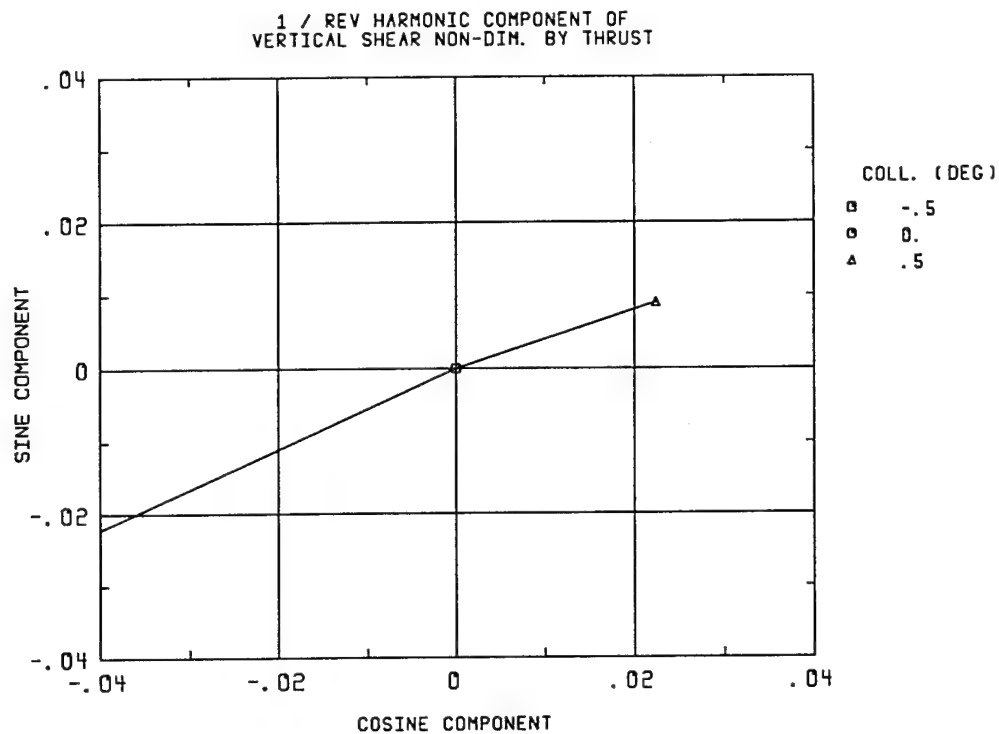
Figure 2-36. Vertical shear at 1P for various collective angles, mu=0.2

1 / REV HARMONIC COMPONENT OF
YAW MOMENT NON-DIM. BY THRUST X OFFSET
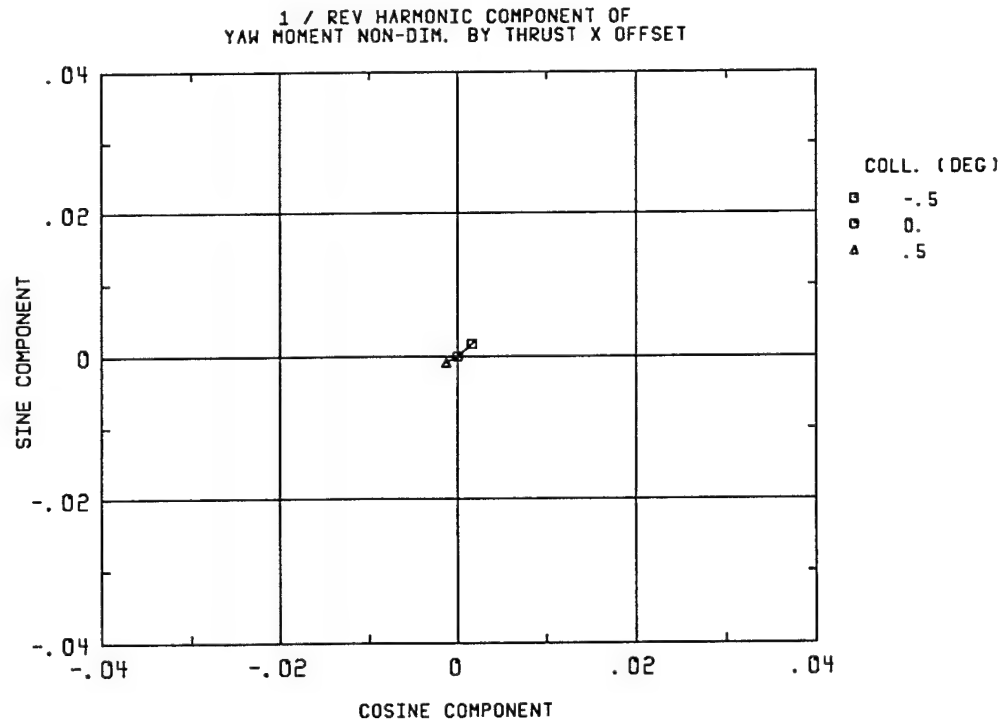
Figure 2-37. Vertical moment at 1P for various collective angles, mu=0.2

35

1 / REV HARMONIC COMPONENT OF
LONGITUDINAL SHEAR NON-DIM. BY THRUST

Figure 2-38. Longitudinal shear at 1P for various tip mass locations, mu=0.2

1 / REV HARMONIC COMPONENT OF
LONGITUDINAL MOMENT NON-DIM. BY THRUST X OFFSET

Figure 2-39. Longitudinal moment at 1P for various tip mass locations, mu=0.2

Figure 2-40. Lateral shear at 1P for various tip mass locations, mu=0.2

Figure 2-41. Lateral moment at 1P for various tip mass locations, mu=0.2

37

Figure 2-42. Vertical shear at 1P for various tip mass locations, mu=0.2
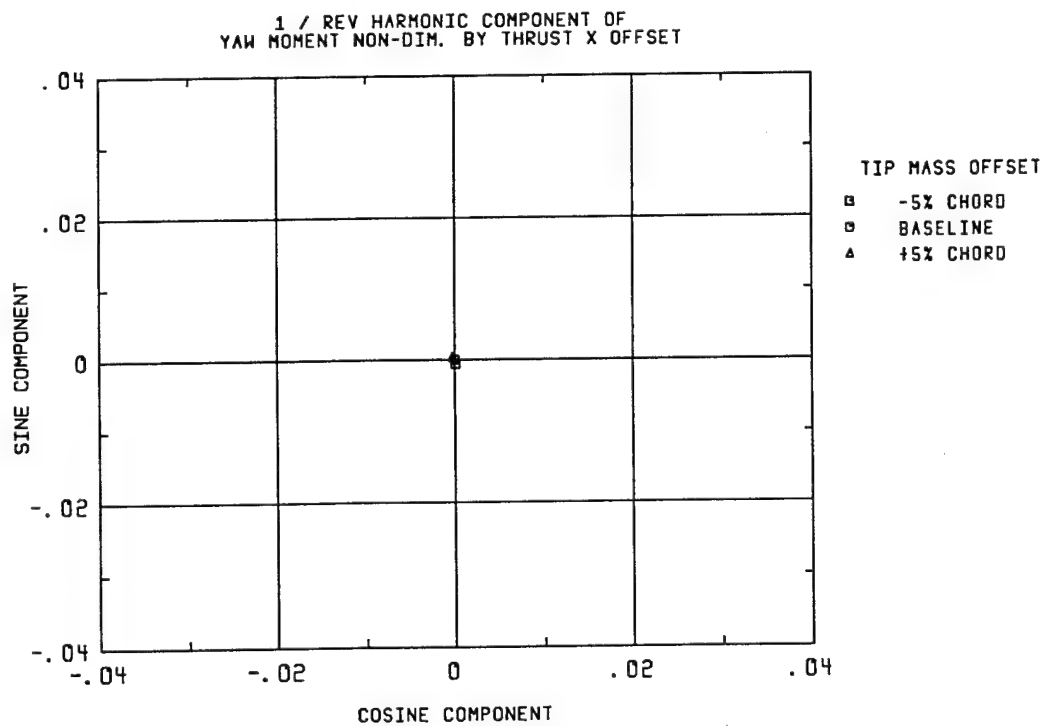
Figure 2-43. Vertical moment at 1P for various tip mass locations, mu=0.2
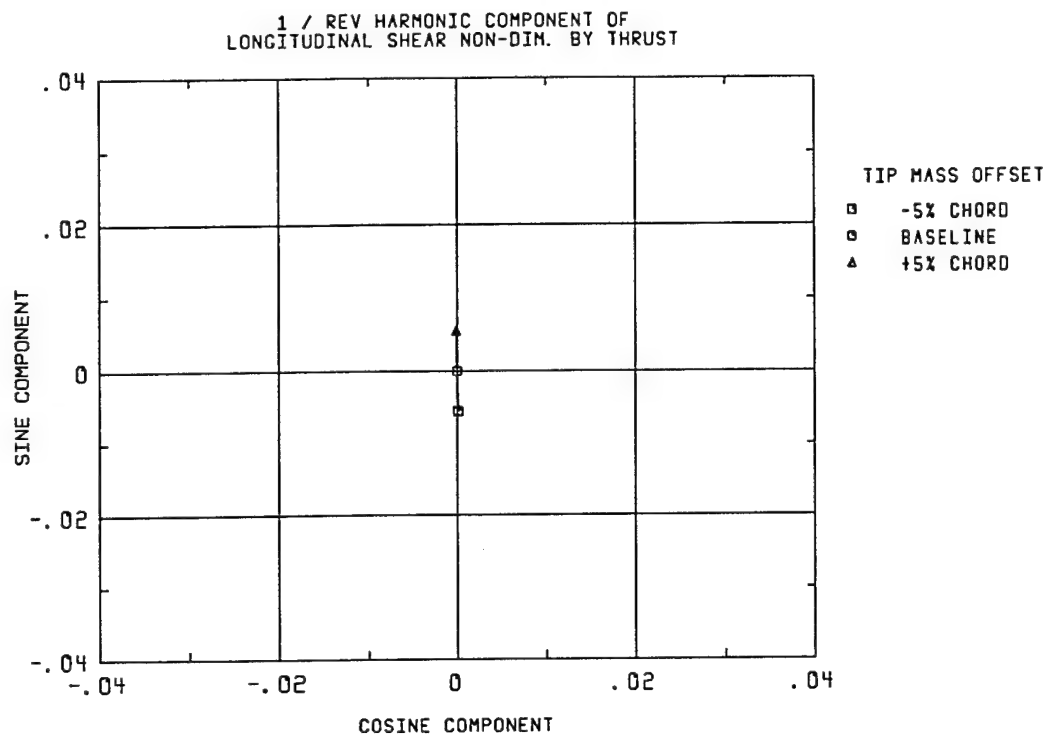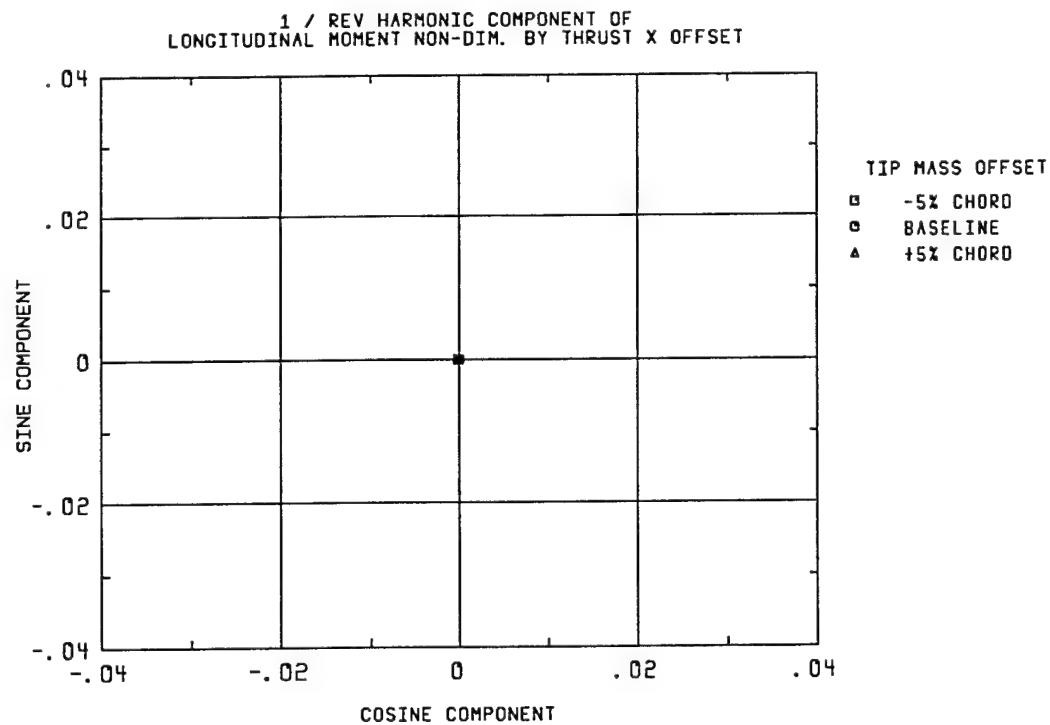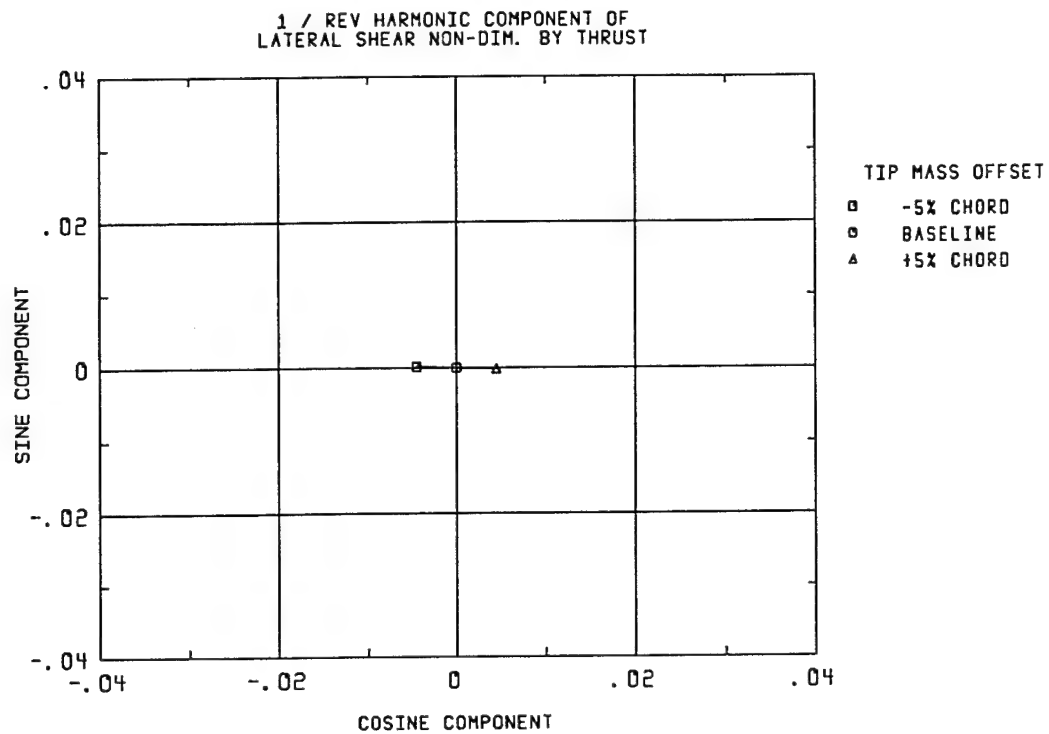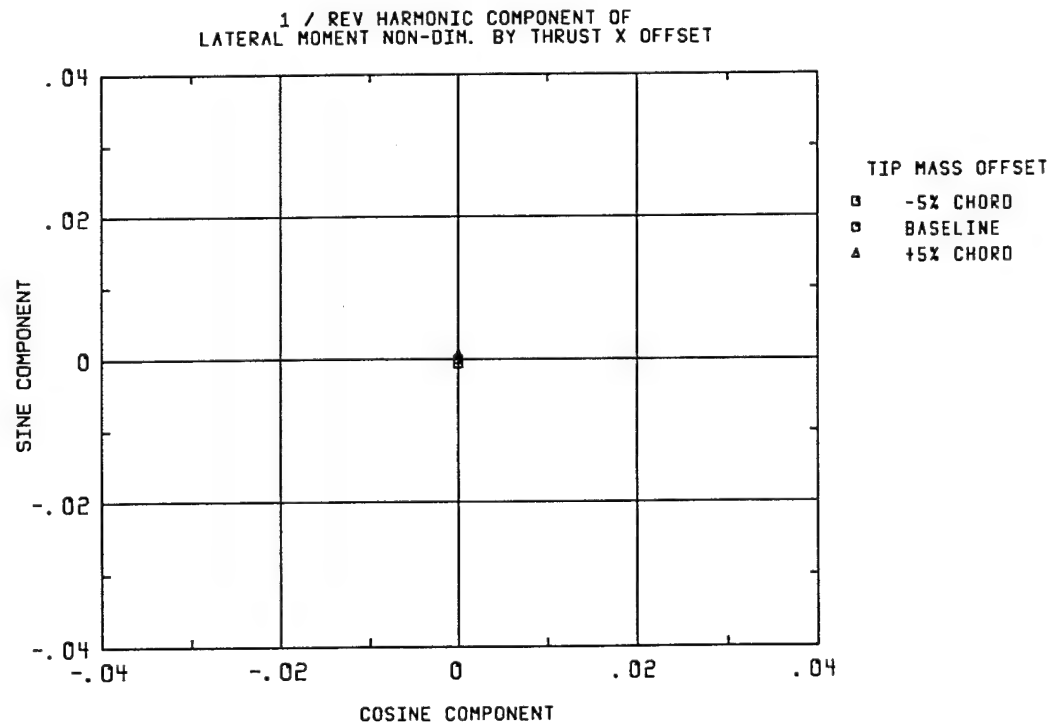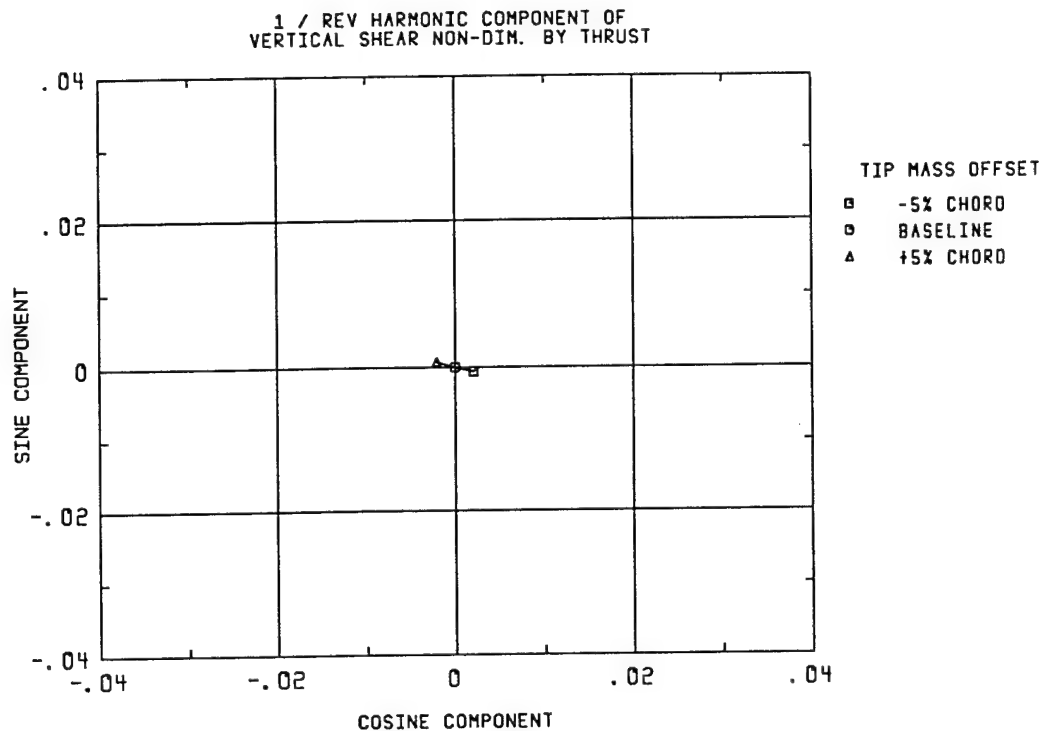
38

2.5 Potential 1/Rev Sensor Concepts

While it is certainly important to provide a means for controlling 1/rev vibration, if one is to perform this task <u>automatically</u>, then adequate measurement of the 1/rev vibrations and/or their consequences are required to exercise the proper control. Sensing of 1/rev vibrations in current T/B devices is done at various pre-specified locations on the helicopter airframe. While these locations are more convenient than on the rotor system itself, the T/B device must often make use of pre-measured relationships on that particular aircraft type to provide guidance on appropriate blade modifications to eliminate (or merely reduce) the measured vibration. Such an approach assumes that: (1) the response at the vibration measurement location is a linear function of the aircraft dynamics to changes in individual rotor blade properties, and (2) this response function is identical for all helicopters of this type. While similarities between aircraft in a commercial operator's fleet would be fairly common, military mission requirements may call for a widely varying assortment of armament, stores and gross weight conditions for the same aircraft, and thus the latter assumption may no longer be valid. Thus, a truly useful automatic IBC-based track and balance device would be "generic", in that <u>it could be incorporated on the entire fleet of Army helicopters without regard to aircraft type or particulars of airframe dynamics</u>.

Airframe-independent T/B sensing would only be possible for a system that sensed 1/rev vibrations at the <u>source</u>, via accelerometer measurements at the hub. Such an approach appears possible, in light of the successful previous applications of accelerometer-based instrumentation for rotor control feedback (McKillip, 1988a; McKillip, 1988b; Ham, 1987; Ham 1992). These studies used the predictive information content of blade-mounted accelerometers, coupled with a signal processing scheme called a Kinematic Observer, to generate estimates of blade rigid and elastic modal deflections in real time. This method allows measurements of blade deflections using simple processing of on-blade accelerometer measurements, without recourse to complicated instrumentation at the hub or optical recording of blade tip deflections.

This technique has very recently been further developed under a Navy-sponsored SBIR Phase I research program, and has produced a novel approach for on-blade vibration and modal response measurement (McKillip, 1995). By incorporating two accelerometers on the same device, one may use their combined signals in a differential and summation relationship to provide a unique and robust measurement of rotor blade flapping. As shown in Figure 2-44, if an accelerometer is located on the blade span with its sensitive axis oriented perpendicular to the rotor blade chord, then it will sense acceleration components both due to blade out-of-plane acceleration (flapping acceleration) *and* due to centrifugal acceleration, the latter component proportional to the local blade slope at the sensor location. For a rigid blade, this slope is essentially the flapping angle, and thus, the centrifugal component provides flapping <u>position</u> information, which may be separated from the flapping <u>acceleration</u> information if one uses two sensors, since one may then solve two equations for two unknowns.
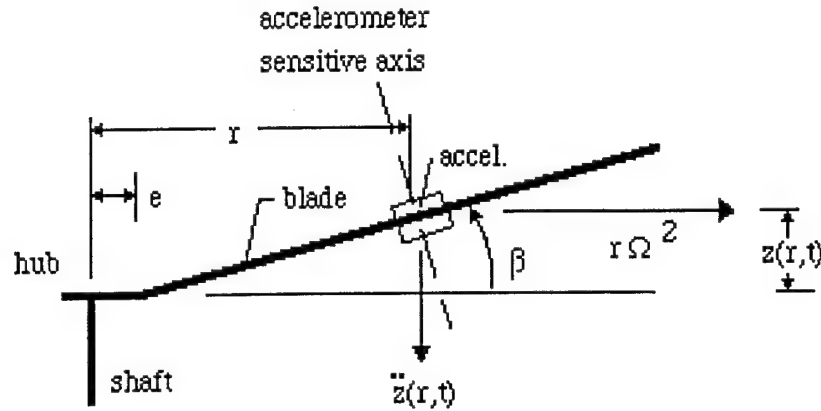
$$accel(r,t) = \ddot{z}(r,t) + r\Omega^2 \frac{\partial z(r,t)}{\partial r}$$

$$for \quad z(r,t) = \sum_i \eta_i(r)q_i(t),$$

$$accel(r,t) = \sum_i \left\{ \eta_i(r)\ddot{q}_i(t) + r\Omega^2 \frac{\partial \eta(r)}{\partial r} q_i(t) \right\}$$

Figure 2-44. Accelerometer signal content for flapwise mounted sensor.

If one incorporates these two accelerometers on the *same* device, then one may use the sum (average) and difference (derivative) of the two signals as a means of providing the required measurement components for resolving flap acceleration and position. Using the above equations, if an accelerometer is mounted at location r on a rotorblade having an offset hinge of distance e from the rotor hub, then its signal content for measurement of flapping mode response is:

$$accel(r,t) = (r-e)\ddot{\beta}(t) + r\Omega^2\beta(t) \tag{2-8}$$

If a second accelerometer is located adjacent to this one, but displaced radially, then the difference between the two sensors, when divided by this radial separation distance is:

$$\frac{\Delta accel(r,t)}{\Delta r} = \ddot{\beta}(t) + \Omega^2\beta(t) \tag{2-9}$$

If one now considers the flapping motion to be comprised of a coning and first harmonic component according to:

$$\beta(t) = \beta_0(t) + \beta_{1c}(t)\cos(\Omega t) + \beta_{1s}(t)\sin(\Omega t) \tag{2-10}$$

Then substitution of this expression into the differential acceleration expression of 2-9 above results in a cancellation of the first harmonic component of "steady" flapping, leaving:

$$\frac{\Delta accel(r,t)}{\Delta r} = \Omega^2\beta_0(t) + \ddot{\beta}_0(t) + \ddot{\beta}_{1c}\cos(\Omega t) + \ddot{\beta}_{1s}\sin(\Omega t)$$

$$-2\Omega(\dot{\beta}_{1c}\sin(\Omega t) + \dot{\beta}_{1s}\cos(\Omega t)) \tag{2-11}$$

Of particular interest is the fact that in steady forward flight, <u>all terms of the above expression except the first would be zero</u>. This would mean that the above differential acceleration measurement could be used to provide a *direct measurement of an individual blade's coning angle* , thus allowing for active control of rotor tracking.

This sensing scheme provides a number of advantages for the proposed active control system proposed here. First, by using spanwise-mounted accelerometers in this differential fashion, <u>hub-mounted instrumentation is not required to measure flapping response</u>. These sensors may be co-located at the blade radial station where the active tab is attached to the blade. Second, the differential sensor <u>is not sensitive to a particular spanwise placement</u>, thus providing freedom for active tab placement without regard to sensing requirements or restrictions. Third, by co-locating the sensor with the actuator, only a minimal number of signal paths are required for active tracking control. Tracking of the rotor system would require that all blades have the same coning angle, which could be communicated to the active tab device as a desired "reference" command for commanding the blade's response. Thus, only power and the reference signal need be supplied to the active tab device proposed here. And finally, the capability to incorporate accelerometer sensors in extremely small packages would make such a combined sensor-actuator system sufficiently compact to significantly reduce the aerodynamic drag penalty associated with mounting this combination on the rotorblade surface.

Of course, the sensing technique proposed above is not the only means of providing 1/rev vibration measurements to the on-blade actuation system. Sensing of 1/rev in the fuselage, by both discrete sensors and by the pilot, could be used in addition to this method. Such sensing would allow for additional tuning of the blade-mounted actuators for smoother operation over the complete flight envelope, but would require a compliment of logic equivalent to that currently used in electronic T/B systems fielded today. These are often a combination of known response transfer functions stored in the instrument, that are combined with a gradient searching strategy using test weights and control perturbations with an assumed linear dynamic response of the rotor system. Methodology for dynamic balancing in this manner is well established and available in the literature (e.g., Harris, 1988).

2.6 Control Law Development

The final component in an automatic rotor smoothing system would be the control law or algorithm used in processing the measurements and driving the blade-mounted actuators. Technology for providing this function, called Individual Blade Control (IBC) is reasonably well developed, albeit for alternate applications. IBC has been demonstrated for rotor blade stabilization, N/rev vibration suppression, lag damping augmentation, dynamic stall alleviation, and performance enhancement on model rotors (Ham, 1985; McKillip, 1985; Ham, 1983; Quackenbush, 1984; Kretz, 1976; Guinn, 1982), and has recently been tested on a limited basis in flight (Teves, 1992). While a majority of these applications have relied on blade root pitch control as the primary actuation mechanism, other approaches using spanwise servoflaps or variable camber devices are amenable to the same control design approach (Straub, 1993; Millott, 1993; Lemnios, 1990). Because Individual Blade Control provides sensing and feedback around each blade on an individual basis, non-harmonic as well as steady aerodynamic inputs may be applied to each blade. This is in direct opposition to Higher Harmonic Control (HHC), where blade pitch inputs are restricted to certain multiples of rotor rotation frequency. Steady, or "zero frequency" inputs for each <u>individual</u> blade (in the rotating frame) are what is required to track and balance a rotor, and hence IBC is ideally suited to provide an automated track and

balance capability. This feature could become particularly important in combat conditions, as on-board track and balance using IBC may provide a "fly home" capability not otherwise possible with a sufficiently battle-damaged rotor blade.

Many of these previous IBC applications were directed at "modal control", where feedback signals were used to modify the blade dynamic properties governing a particular mode of response, often to provide disturbance rejection and/or damping augmentation. Such applications require careful attention to the dynamic characteristics of the modes being controlled, and achieve enhanced performance through the use of high-gain feedback control structures. The system investigated here, due to its quasi-static nature, is essentially a static shape control system that would only be modified when 1/rev vibration exceeded a given threshold as determined by an automatic system or pilot wishes. Since the system would not need to remain active indefinitely (providing significant power savings), and since modification of the blade actuator tab is performed at very low frequencies relative to rotational speeds, the control law for such a system may completely neglect rotor dynamic modes. That is, the control law for static shape control could be made to provide for shape adjustment over a sufficiently long time period (several seconds) that the rotor dynamic response to these changes would appear to be instantaneous. A simple low-gain integral control loop around a command variable could be used, with the command variable representing a desired rotor coning angle, or a 1/rev vibration amplitude to be nulled.

An advantage of this type of "regulator" approach toward on-blade control is that the feedback signal could represent a measure of the desired performance of the rotor smoothing system, and thus inner loop control around the blade-mounted actuator *would not be necessary*. This implies that an absolute measurement of the tab deflection may not be required, if it is sufficiently limited in its control authority. Since the control actuation would be slow enough to directly monitor the consequence of the control action, regulation of a particular tab deflection angle would be both unwarranted and extraneous. Tab deflection commands for such a system could be essentially a "rate" command, where a signal is sent to the tab to increase or decrease its deflection until the rotor response at 1/rev is smoother or the tab has reached its maximum excursion in that direction.

While such a simple control concept would allow for relatively easy incorporation of an active tab system onto a current helicopter rotor, the actual interface of which tab to actuate, and how to set the pilot controls or thresholds for determining when the devices would operate, remains an open issue. This implementation issue associated with the "system management" of an active tab IBC system is to be addressed in the Phase II follow on work suggested below, and did not comprise part of the Phase I study documented here. Additional details on the potential implementation issues associated with such a "rate command" actuation scheme are addressed in Section 3 which follows.

3.0 ACTUATOR IMPLEMENTATION STUDIES

3.1 Scope of the Investigations

"Smart" materials, such as piezoelectric ceramics, magnetostrictive materials, and shape-memory alloys (SMA) all provide new capability to the designer of active components unavailable a decade ago. Relative motion of structural components becomes possible through direct application of electrical or magnetic energy, without the associated mechanical complexity of armatures and rotating shafts as in conventional electric motors. These materials are rapidly being incorporated into a wide assortment of uses, due to improvements in both material fatigue life and in the quality and consistency of their production.

Use of smart materials in rotorcraft has already been considered, but primarily for HHC and high bandwidth applications (Ormiston, 1991; Spangler, 1990; Fabunmi, 1991; Straub, 1993a, 1993b, 1995). Most of these studies have suffered from attempting to extract too much displacement at too high a frequency from the smart materials-based actuators. Unlike high frequency vibration control, 1/rev vibration reduction may be achieved from static adjustments of the inertial and aerodynamic properties of individual rotor blades, and hence required speed of response drops from milliseconds to several seconds. Also, since only a few degrees (at most) of trailing edge tab or a fractional degree of root pitch angle is required to sufficiently track a rotor blade, the actuator displacement requirements for this application are very modest. Thus, while high speed actuators constructed from smart materials may still be several years away, low-speed, high force actuators may now be constructed from materials incorporating smart materials, such as shape-memory alloys (Rogers, 1991).

Further comparison of the various "smart" materials is given by Crawley (1994), in Table 3-1 below. It is readily apparent that high-force, high-strain actuation is best achieved using SMA-based actuation, provided that the thermal time constants associated with material heating and cooling are acceptable to the application at hand. For the quasi-static 1/rev vibration control as envisioned for on-blade actuation, the low bandwidth of SMA-based actuators does not present a problem.

Table 3-1. Comparison of various "smart" material properties (from Crawley, 1994)

Material	PZT G-1195	PVDF	PMN	Terfenol DZ	Nitinol
Actuation mechanism	Piezoceramic	Piezo film	Electro-strictor	Magneto-strictor	Shape alloy
Λ_{max}, μstrain	1000	700	1000	2000	20,000
E, 10^6 psi	9	0.3	17	7	4(m);13(a)
Bandwidth	High	High	High	Moderate	Low

Note especially that these high-force, low displacement actuators need not be limited to just aerodynamic contour or pitch change mechanisms. Track and balance problems have a long history of being caused by defective in-plane blade dampers, and thus, the actual dampers are a potential candidate themselves for application of active control. This may involve active adjustments of orifice sizes for hydraulic dampers, or

changes to the operating characteristics of elastomeric dampers through smart material induced stresses to change their steady operating point. As will be discussed later, however, such applications tend to represent aircraft-specific applications, and thus were deemed of secondary interest in the development of the proposed approach for this Phase I study.

Previous work on SMA-based actuators performed under a Phase I SBIR grant investigating helicopter maneuver performance enhancement using on-blade flap control has been extended for this effort (Quackenbush, 1993). While a sufficiently detailed electromechanical model of SMA wire performance has been used to predict strain behavior of a single spring-biased SMA wire undergoing heating and cooling cycles, this model had not (until this Phase-I work) been demonstrated on other SMA-based actuation systems.

The goal of this portion of the current Phase I effort was to determine what (if any) practical limitations exist in the various possible implementations of SMA-based actuators for rotorcraft 1/rev vibration control, and to address them as necessary in order to design a system that would have the most beneficial effect on mitigating the vibration. This lead to a combination of preliminary assessment of available technologies, and benchtop tests to refine material mathematical models, culminating in the determination of a candidate actuation system for subsequent detail design and testing under follow-on Phase II work. The results from these investigations are presented in the paragraphs that follow. But first, in order to aid in appreciating how on-blade actuation may be used in control of 1/rev vibration, it is important to review how this vibration is currently controlled using conventional methods.

3.2 Current Practice for Rotor Track and Balance Adjustments

While current track and balance (T/B) procedures were generally described in the introductory paragraphs of this report, the details of actual T/B operations were omitted. Prior to detailed design assessment of various active approaches to 1/rev vibration suppression, discussion were held between the Principal Investigator and the maintenance personnel at the Army Air National Guard 1st Battalion, 150th Aviation, in Ewing, New Jersey. Issues of importance related to T/B operations were outlined, and a general discussion ensued on the most desirable modifications that might be made to various rotor components to improve T/B of rotor systems. This Guard unit operates and maintains UH-1, AH-1 and OH-6 helicopters, and provided C.D.I. with copies of appropriate sections of the maintenance manual on the rotor systems for the OH-6 and AH-1 aircraft.

The UH-1 and AH-1 aircraft, both manufactured by Bell Helicopter Textron, Inc., have semi-rigid (teetering) rotor systems (thus having no lag dampers), and the AH-1 aircraft of this Guard unit use a composite blade (K747) manufactured by Kaman Aerospace having no adjustable trailing edge tabs. The OH-6 rotor system is a four-bladed unit with flexstraps in place of conventional flap and pitch articulated joints, and incorporates frictional dampers to control lag motion about an outboard pin. Tracking operations for these two rotor systems are similar, in that initial track is performed using pitch link adjustments at reduced and then full rotor rpm during ramp run-up. Hover track is noted (but not adjusted), and then forward flight tracking is measured. Adjustments for forward-flight tracking use primarily tab bending for the OH-6, but only pitch link changes for the K747 blades. Earlier AH-1 blade sets (B-540) also used tabs, but the composite blades have been found not to need tabs for forward flight track adjustments. Once an acceptable track has been achieved, a dynamic balancer unit incorporating an accelerometer measurement on the fuselage is used to provide information on how much balance weight needs to be added to smooth the rotor system. Tape is used as a temporary means of

adding weight, until the proper mass has been determined, and then the tape is replaced with washers at the appropriate locations on the blade tip or root. Finally, rotor autorotation speed must be checked after these adjustments to ensure that the rotor may still be safely operated in the event of an aircraft powertrain failure.

Track and balance operations must typically be performed after any maintenance activity has been done on the rotor head, blades, or other rotating-frame dynamic components. This is particularly true if any of these items has been replaced, since the new unit may have different mass (or stiffness) properties from the original. Of particular interest is the difference in the troubleshooting procedures suggested for the semi-rigid rotor and the articulated rotor for the same symptoms. For the semi-rigid rotor, lateral 1/rev vibration in hover or forward flight may be caused by spanwise or chordwise out-of-balance conditions, the former correctable using tape/weights at the blade tip, and the latter through changes in blade "sweep" using length changes in the drag brace on the offending blade. For the articulated rotor, lateral 1/rev vibration is symptomatic of: (1) incorrect damper torque, (2) incorrect damper phasing, (3) main rotor imbalance, or (4) loose blade tip weights. This observation in the maintenance manual is confirmed by the Army personnel, in that damper overhauling and repair constituted the primary rotor head maintenance activity performed during rotor smoothing efforts. Vertical 1/rev vibrations for both types of rotor systems is primarily due to the blades flying out-of-track, although malfunctioning blade vibration absorbers and lag damper defects may generate 1/rev vertical vibrations for the articulated rotor as well.

Thus, some of the maintenance procedures involve aircraft-specific adjustments, such as the drag brace on the semi-rigid rotors and the damper phasing and torque changes for the articulated rotors, and some are consistent across platforms, such as adding or subtracting weights, or changing pitch link lengths. In order to design a system that would have the largest utility across aircraft types, automation of *aircraft-independent* components was addressed in this Phase I study, and thus concepts for alteration of blade damper units or drag links were abandoned. Note however, that even though the K747 blades described above did <u>not</u> used trailing edge tabs in their tracking adjustments, active tabs were still considered fairly generic across rotor systems to warrant their inclusion. This is particularly true for the case of using such a device in a <u>retro-fit</u> arrangement, where the tab would be added to a blade on a fielded aircraft. In this manner, the active device could be used in a *product improvement program*, versus only providing capability to new blade sets or a new production aircraft.

The potential SMA-based actuators considered in this Phase I study included: (1) active blade trailing edge tabs; (2) active pitch links having limited extensional or compressive capability; and (3) active balance weight adjustment (chordwise) at the blade tip. Each of these concepts was evaluated in terms of its effectiveness in Section 2 above for mitigating postulated 1/rev vibration sources, and the active tab and active pitch link were seen to provide sufficient capability to improve 1/rev vibration signatures. The active weight adjustment system was discarded upon examination of its limited effectiveness in the Section 2 simulation study, and since its actual installation in a blade tip cap would be difficult to achieve in a *generic* fashion due to the large variation in blade structural designs. Design details and engineering analyses for both the active tab and active pitch link device are given in separate sections that follow.

3.3 Active Rotor Blade Tab Device

An actively controlled trailing edge tab for rotor blade applications would be both a powerful and useful control for helping mitigate 1/rev vibrations. Providing active tab

positioning *in flight* would eliminate the requirement to shut down the rotor system to perform tracking adjustments in forward flight, and would also allow for selective tuning of the blades for steady cruise operation at any particular forward flight speed desired by the pilot. The proposed scheme for active tab control here is to replace the bending operation usually performed by the T/B mechanic with a mechansim incorporating SMA material actuation. Since tab adjustments may have the trailing edge bent upward or downward, similar ranges of actuation would be required from an SMA-based device. In addition, this bending operation is not restricted to particular quantized angles and thus the actuation scheme would need to provide continuous adjustments as required when actuated. Typical angular deflections are limited to +/-5°, and as was seen in the sensitivity analysis performed in Section 2 above, this is more than adequate for addressing most 1/rev vibration problems of interest.

Previous work at C.D.I. directed at helicopter maneuver enhancement using on-blade flap control (Quackenbush, 1993) considered the generation of trailing edge control (or, camber modifications) through the use of SMA wires acting in agonist-antagonist fashion to pull on flap control horns. In this effort, a validated thermo-mechanical model of SMA wire properties was used to predict flap response to actuation signals using computer simulation studies. While these simulations showed that the concept was feasible, detailed data on SMA behavior under actual agonist-antagonist conditions was lacking. Because this control technique appeared promising for providing trailing edge tab bending control, work continued on this actuation scheme under the present Phase I effort. This has led to the construction of two "iron bird" test articles at C.D.I. that were used for both SMA constitutive model validation work and control law development.

The first actuation scheme, shown schematically in Figure 3-1 below, consists of two opposing SMA wires controlling the rotary deflection (δ_{flap}) of a device (such as a tab or flap) through alternate heating and cooling of each individual wire. The wire "state" properties are defined by its stress (σ), temperature (T), and martensitic fraction (ξ). Pretensioning of the wires is possible through a sliding mechanical arrangement that can lock the assembly in place with a measured axial force on each wire; rotary motion is measured through a single turn potentiometer. Note that the only other force acting on the torsion rod for this actuator is bearing friction. Heating of the wire is accomplished using pulse-width modulation of a current source, since the associated control electronics are drastically simplified with this method. This actuation device was based upon similar work done by NASA (1992), where the use of a capstain provides significant rotary motion by allowing fairly long lengths of SMA wire to be wound around a grooved outer surface. In this manner, 2-3 percent contraction of the wire can be effectively multiplied mechanically to provide significant rotational motion of the capstain, which would then drive an attached flap or similar device.

A variation of this device, using a cantilevered tab in place of the rotary rod, was also constructed and tested. The tab had an inboard attachment for the wire actuators, with clearance holes in the mounting block to provide for free wire motion. Since the tab was constructed from shim stock material, the mounting block attached to the force gauge was replaced with an equivalent block made from plastic, in order to provide separate electrical stimulation of each SMA wire. Deflection of the tab was measured using an infra-red emitter and photodetector, that was coupled to an integrated circuit to provide pulse-width output proportional to the detector output voltage. This circuit was calibrated to determine tab angle as a function of pulse width output. Excitation of each SMA wire was similar to the previous actuator, in that pulse-width modulation was used to control a power MOSFET transistor that switched on wire current (thus providing resistive heating). A picture of both benchtop actuators may be seen in Figures 3-2 and 3-3.
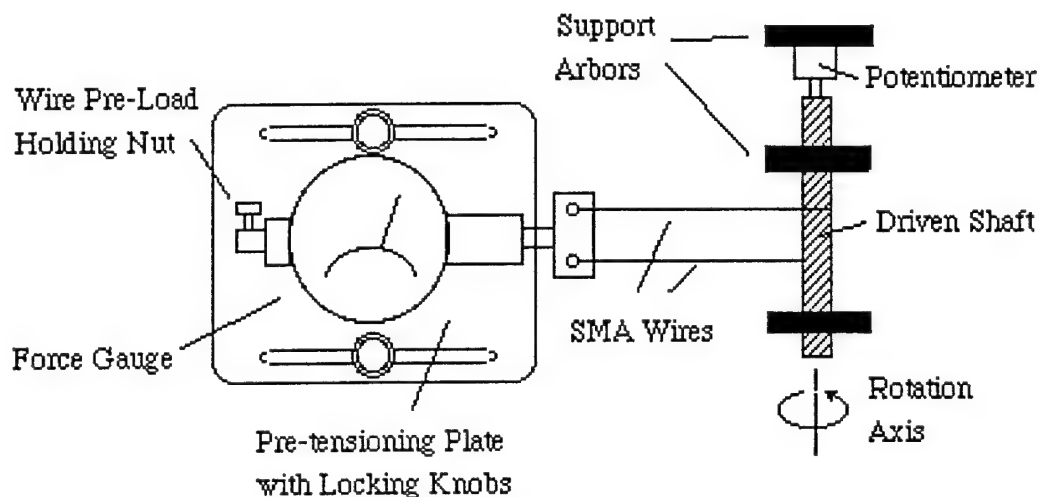
Figure 3-1. Schematic of benchtop agonist-antagonist rotary actuator test mechanism

This second tab actuator was coupled to a BASIC Stamp™ microcontroller (Parallax, 1993), in order to allow for closed-loop control of tab actuation. This remarkable device allows for the downloading of control logic, written as a BASIC program on an IBM-PC, into a serial EEPROM coupled to the microcontroller, which then begins to execute the instructions repeatedly as long as power is provided to the device. As will be shown in the following paragraphs, rather sophisticated control logic may be readily programmed and tested using this device, including the transmission of current system parameters back to the connected IBM-PC/AT for cataloging in an ASCII file.

Pretensioning of the SMA wires is important, since SMA-based actuators use temperature changes to alter the material modulus of elasticity; thus, the resultant deflection due to temperature changes is often only dependent upon the pre-load present on the material. If no load exists on the material, changes in the material "spring constant" will not affect the displacement of the actuator - provided it has not been previously deformed. One of the well-known properties of SMA materials, however, is their ability to be "trained" to a given geometric position, and some force-free recovery is possible if the material has been previously pseudoelastically deformed to a different shape while in the martensitic crystalline phase. Thus, an additional requirement for wire pretensioning in the benchtop actuation schemes tested is due to the fact that the crystalline lattice of SMA metals may change from austenitic to martensitic state through application of *stress alone*. Hence, full material model validation would only be realized through a series of stress and temperature ranges for each of the two actuation wires. Note also that pretensioning of the wires may be achieved through partial heating of the wires themselves, and hence part of the performance testing of the benchtop actuator addressed the control aspects of heating both actuator wires simultaneously, but at different rates.
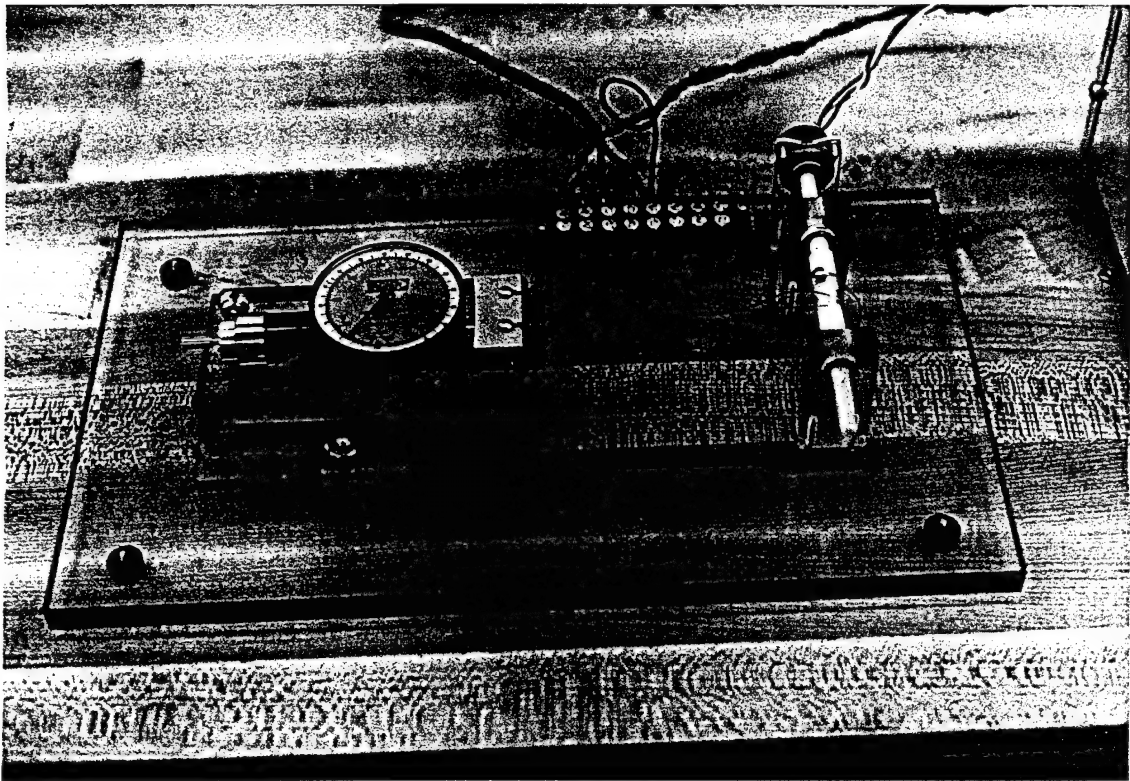
47

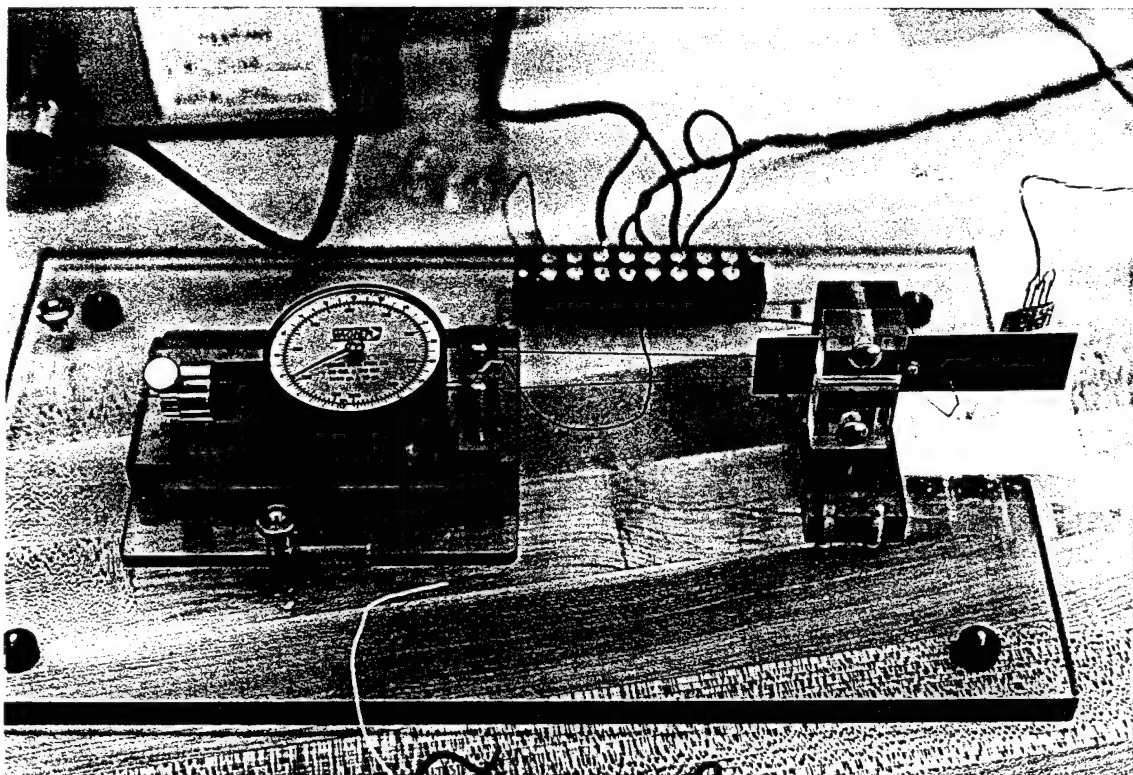Figure 3-2. Torsion rod actuator benchtop demonstration device.

Figure 3-3. Tab actuator benchtop demonstration device.

The tab actuator has two fundamental advantages over the torsion rod actuator tested here: first, it is mechanically simple, in that it has no "moving" parts (although it does plastically deform); and second, it does not require power to maintain its new shape. This is because the tab is made to deform plastically during SMA wire heating, and then the tab assumes its newly deflected shape when the moments induced by the wires are removed. While allowing an actuator to plastically deform would limits its fatigue life, actual trailing edge tabs are exposed to the same plastic bending under regular T/B adjustments, and thus, this is not considered to be a significant contstraint, since it would be expected that adjustment of a rotor blade tab would constitute a fairly infrequent event (a maximum of two times per flight).

As mentioned above, the goal of the investigation was to determine if any practical implementation issues existed in translating SMA-based actuation to a device designed for 1/rev vibration control. Thus, the ultimate purpose of these two benchtop test devices was to provide design data and practical experience to support the development of mathematical models used in the development of a prototype actuator concept. Despite the obvious advantages of a direct "tab-bending" device described above, validation of this actuation concept would require the inclusion of the buckling performance of the tab under applied wire actuator loads, further complicating the modeling for simulation purposes. Hence, the proper simulation of the first actuator, having simple torsion control of a rod, is a desirable first step in the validation process of the engineering design tools necessary for prototyping work. The basic mathematical model for the agonist-antagonist wire actuator is described below, and then simulation results are compared to open-loop test data for this first device. Then the model is extended to include tab buckling, and comparisons with open and closed loop performance tests are made in a following sub-section.

3.3.1 Agonist-Antagonist SMA Wire Actuator Modeling

The sketch shown in Figure 3-4 represents an engineering approximation of a device where two SMA wires are used in an agonist-antagonist fashion to change the position of a flap or tab attached to a hinge point. This representation has been used as an aid in understanding SMA wire performance and in improving the correlation of a simple constituitive law governing the behavior of SMA wires. This system also presents an interesting control problem due to its inherent hysterisis (from the SMA wire properties), and because two potential control inputs exist (individual wire temperature) to control one output (the flap/tab position).
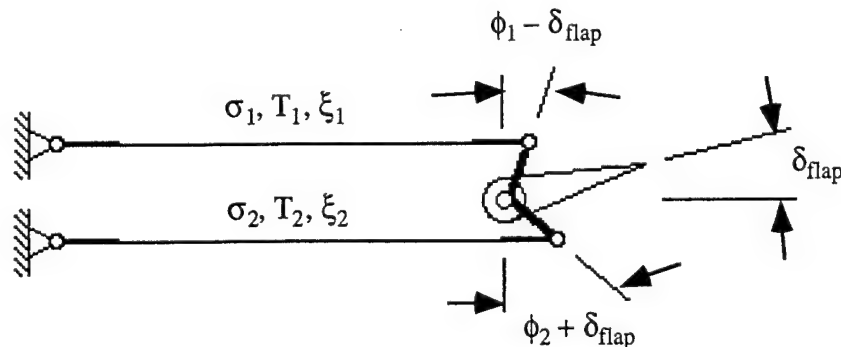

Figure 3-4. Schematic of Continuously-Variable SMA Actuation Scheme

Through the selection of various parametric relationships, this model may be made to represent either of the two benchtop actuators tested as part of this Phase I investigation.

For the torsion rod actuator, the angular offsets and radial arms for each wire actuator are equal, and for the tab actuator, the plastic bending at the effective hinge point may be modeled as a nonlinear spring, with the "break point" in the spring stiffness set to match the yield point of the tab material.

Four fundamental relationships are used to formulate the system equations for this actuator: (1) the constituitive law for each SMA wire; (2) the compatibility relationships regarding the perturbations in strain between the two wires; (3) the expression for the moment balance about the flap hinge point, and (4) a geometric relation between the wire strain and the flap deflection.

Wire Constituitive Law

The one-dimensional constituitive law governing the SMA wire behavior follows Liang and Rogers (1990) in that the perturbation in wire stress is modeled as a linear sum of constants multiplying perturbations in wire strain, temperature, and martensitic fraction (crystalline lattice structure). A differential model of SMA wire behavior is particularly convenient, as the material exhibits hysteresis in its variation of crystalline structure with temperature changes. As a consequence, an additional internal state, called the martensitic fraction of the material, is required to adequately capture this hysteretic behavior. The incremental constitutive law used to model the SMA wire material is thus:

$$\Delta\sigma = D\,\Delta\varepsilon + \Theta\,\Delta T + \Omega\,\Delta\xi \tag{3-1}$$

where $\Delta\sigma$ is the incremental stress in the wire, $\Delta\varepsilon$ is the incremental strain, ΔT is the change of wire temperature, $\Delta\xi$ is the change in martensitic fraction, D is Young's Modulus of the SMA wire material, Θ is the thermoelastic tensor, and Ω is the transformation tensor due to changes in material martensitic fraction. This simple linear constitutive law is complicated by the fact that variations in martensitic fraction show decidedly nonlinear variations due to both temperature changes and material stress levels. These nonlinear effects are a direct consequence of the hysteresis in material crystalline properties with temperature, and result in generating distinct variations of martensitic fraction between positive and negative changes in both temperature and material stress. In differential form this becomes:

$$\Delta\xi = \frac{\partial\xi}{\partial T^+}(\sigma, T)\,\Delta T^+ + \frac{\partial\xi}{\partial T^-}(\sigma, T)\,\Delta T^- \frac{\partial\xi}{\partial\sigma^+}(\sigma, T)\,\Delta\sigma^+ + \frac{\partial\xi}{\partial\sigma^-}(\sigma, T)\,\Delta\sigma^- \tag{3-2}$$

One or the other of the single-sided derivatives with temperature or stress will be zero, depending upon the current stress and temperature of the SMA wire. Such a formulation typically requires computing solutions for both positive and negative stress variations, and then keeping the perturbation that is consistent with the assumed sign of the variational quantity.

Strain Compatibility Expressions

From Fig. 3-4 above, each SMA wire is shown to have a bellcrank-like attachment to the flap at an angle ϕ_1 and ϕ_2, and if we assume each has a respective radius r_1 and r_2 about the flap hinge point, then a change in strain of the first wire $\Delta\varepsilon_1$ produces a change in strain of the second wire such that the angular rotation of each bellcrank is the same; that is:

$$\frac{\Delta\varepsilon_1 l_1}{r_1 \cos(\phi_1 - \delta_{flap})} = -\frac{\Delta\varepsilon_2 l_2}{r_2 \cos(\phi_2 + \delta_{flap})} \qquad (3\text{-}3)$$

Moment Balance About Flap Hinge

A simple moment balance about the flap hinge adds the moment due to each wire, and may include any disturbance torque or inertial load as well, according to:

$$\sigma_1 A_1 r_1 \cos(\phi_1 - \delta_{flap}) - \sigma_2 A_2 r_2 \cos(\phi_2 + \delta_{flap}) + \tau_{dist.} - I\ddot{\delta}_{flap} = 0 \qquad (3\text{-}4)$$

where A_1 and A_2 are the cross-sectional areas of each wire, τ_{dist} is a disturbance torque, and I is the inertia about the flap hinge.

Flap Angle Geometry

The flap angle may be related to the strain in the first wire according to:

$$\Delta\delta_{flap} r_1 \cos(\phi_1 - \delta_{flap}) = \Delta\varepsilon_1 l_1 \qquad (3\text{-}5)$$

Equation Solution Procedure

To solve these equations, one first substitutes equation (3-2) into equation (3-1) for each actuator wire, thereby producing a perturbation equation for each wire in terms of stress, strain, and applied temperature. Temperature of each wire is controlled through electric resistive heating, and thus is an input to the model; applied torque is also treated as an external input (for now), with inertial effects ignored. The wire perturbation equations are combined with equations (3-3), (3-4) and (3-5) in a matrix-vector solution scheme that incorporates the unknown variables $\Delta\varepsilon_1$, $\Delta\sigma_1$, $\Delta\varepsilon_2$, $\Delta\sigma_2$, and $\Delta\delta_{flap}$:

$$
\left[
\begin{array}{cccc}
(1 - \Omega\frac{\partial\xi}{\partial\sigma_1^*}) & -D & 0 & 0 \\
0 & 0 & (1 - \Omega\frac{\partial\xi}{\partial\sigma_2^*}) & -D \\
A_1 r_1 \cos(\phi_1 - \delta_{flap}) & 0 & -A_2 r_2 \cos(\phi_2 + \delta_{flap}) & 0 \\
0 & l_1 r_2 \cos(\phi_2 + \delta_{flap}) & 0 & l_2 r_1 \cos(\phi_1 - \delta_{flap}) \\
0 & l_1 & 0 & -r_1 \cos(\phi_1 - \delta_{flap})
\end{array}
\right. \cdots
$$

$$
\cdots \left.
\begin{array}{c}
0 \\
0 \\
[\sigma_1 A_1 r_1 \cos(\phi_1 - \delta_{flap}) + \sigma_2 A_2 r_2 \cos(\phi_2 + \delta_{flap})] \\
0 \\
0
\end{array}
\right]
\times
\begin{bmatrix}
\Delta\sigma_1 \\
\Delta\varepsilon_1 \\
\Delta\sigma_2 \\
\Delta\varepsilon_2 \\
\Delta\delta_{flap}
\end{bmatrix}
=
\begin{bmatrix}
(\Theta + \Omega\frac{\partial\xi}{\partial T})\Delta T_1 \\
(\Theta + \Omega\frac{\partial\xi}{\partial T})\Delta T_2 \\
-\Delta\tau_{dist} \\
0 \\
0
\end{bmatrix}
$$

$$(3\text{-}6)$$

Because of the hysteresis present in the crystalline lattice transformation with temperature, the stress perturbations and their influence on the above equations will be

sign-dependent. Thus, these equations will need to be solved <u>four</u> times, for all combinations of each sign posibility for the two wire stress pertubations. The appropriate solution, then, would be the values of $\Delta\sigma_1$ and $\Delta\sigma_2$ that are consistent with the assumed sign used to generate the perturbation sensitivities above.

3.3.2 Active Tab Testing and Simulation Correlation

This model of agonist-antagonist wire performance was applied to the geometry of the torsion rod actuator shown previously. Test data was also taken on this configuration, in open-loop fashion, whereby each wire was independently excited in order to generate a deflection of the rod. No direct feedback of rod position was used in the testing of this first actuation concept. Figure 3-5 shows a typical result from open-loop testing of this device, and Figure 3-6 shows a comparable result using the above simulation model. Although the simulation model includes a smooth time lag for the wire heating transient, the algebraic solution procedure outlined above results in the rod angle showing some kinks due to the inherent hysterisis of the SMA material.

The above mathematical model was further refined to include a nonlinear spring model that approximately represents the buckling behavior of the tab when a significantly high stress is applied to cause plastic deformation. Further validation of this model was performed using the results from open-loop tests on the tab (shown in Figure 3-7), where different initial temperatures were used for approximately the same pulse width of wire excitation. This updated model was then used to design a simple closed-loop controller, that used a potentiometer as a command reference for controlling tab deflection. Loop closure was performed using a simple BASIC program loaded into the Stamp™ microcontroller that selectively turned on and off the wires necessary to drive the tab position to the commanded value. Results from closed-loop testing are shown in Figure 3-8, with the command angle from the potentiometer offset from the tab output for clarity of presentation. Despite the simplicity of this simple control law, the tab manages to track the desired position quite well. It may be noted, however, that as the closed-loop test progressed beyond approximately 45 seconds, both wires had elevated temperatures, and thus, the stress levels in each were alternating between increasing values. This explains the apparent oscillation seen in the tab position trace toward the end of the test in this Figure. The conclusion from the simulation comparisons and the successful design of a closed-loop tab controller is that the model developed under this Phase I effort is sufficiently accurate for preliminary design work and actuator performance estimation. Thus, *the goal of developing design tools for SMA wire tab actuator prototyping was achieved.*

3.4 Active Pitch Link Device

The second actuation concept considered for application to 1/rev vibration control was the use of SMA materials for active control of rotor blade pitch link length. This is currently performed manually, through selective adjustment of threaded rod ends, of opposite thread direction, on each end of the pitch link rod body. Some links include additional threaded attachments that allow adjustments of both coarse and fine threads, however, the basic procedure is the same: through rotation of the pitch link housing, the rod ends move toward or away from each other, thereby decreasing or increasing the root pitch of the rotor blade to which they are attached.

Pitch links are one of the most crucial dynamic components on a helicopter, in that they are subject to the integrated spanwise torsional moments induced on the rotor blade as it spins about the shaft. These torsion loads can become excessive in high speed flight, both from transonic aerodynamic effects on the advancing side of the rotor disk that induce
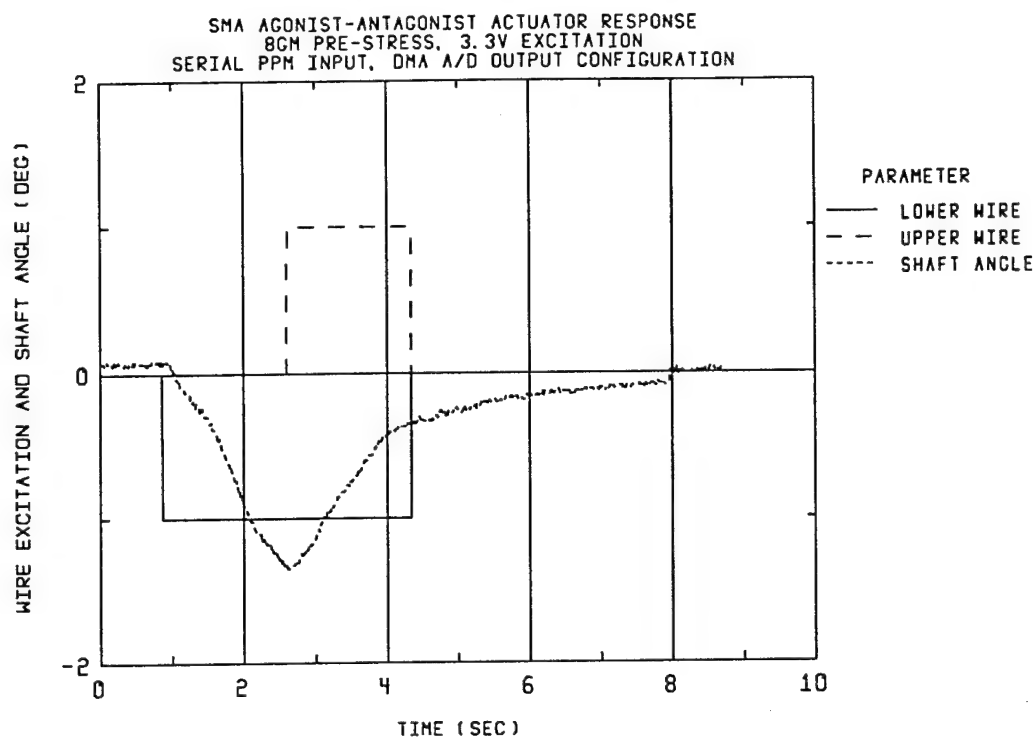
Figure 3-5. Torsion rod benchtop actuator open-loop response.
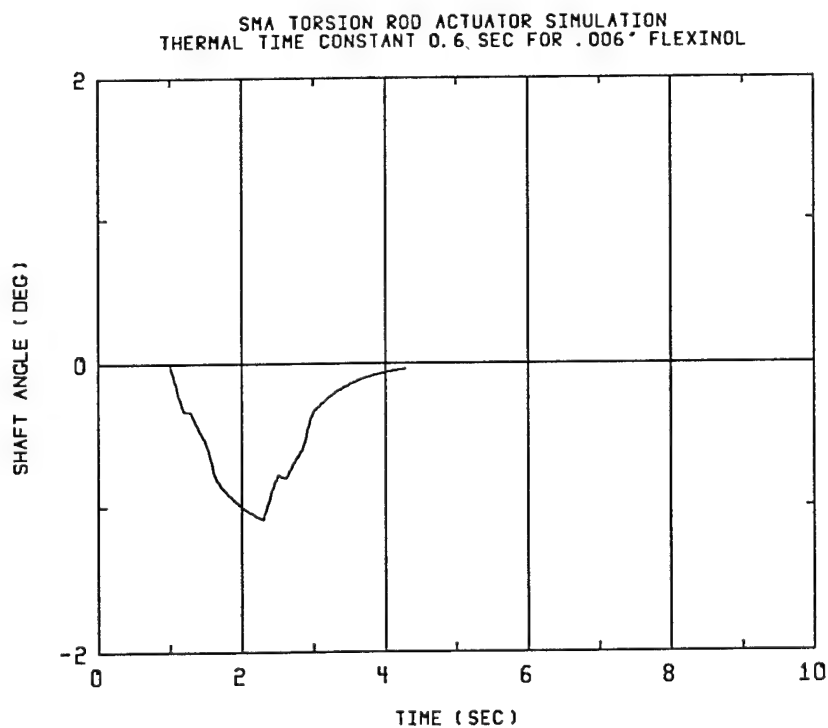

Figure 3-6. SMA Agonist-antagonist torsion rod simulation response.
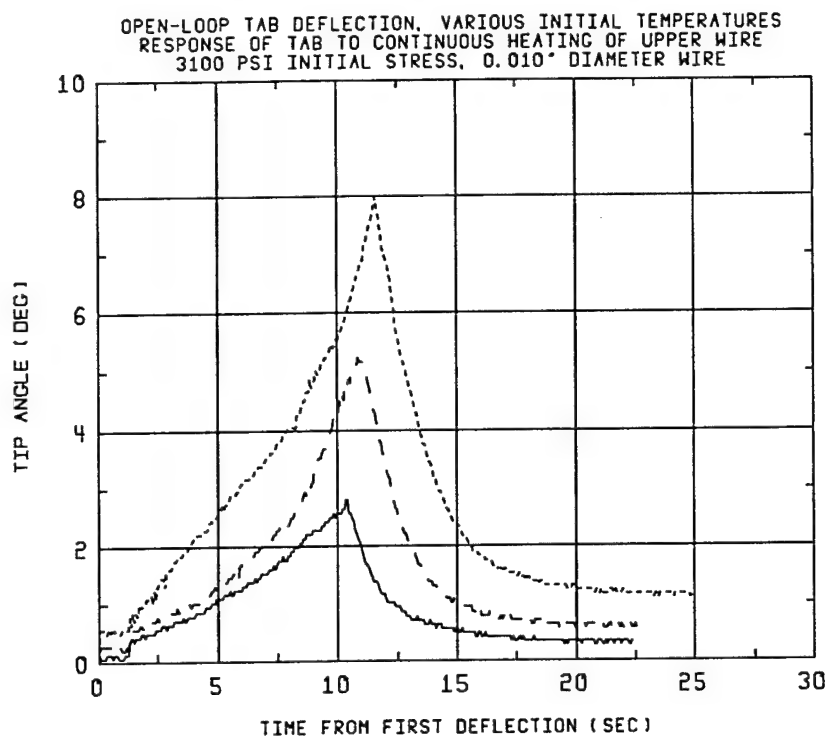
53

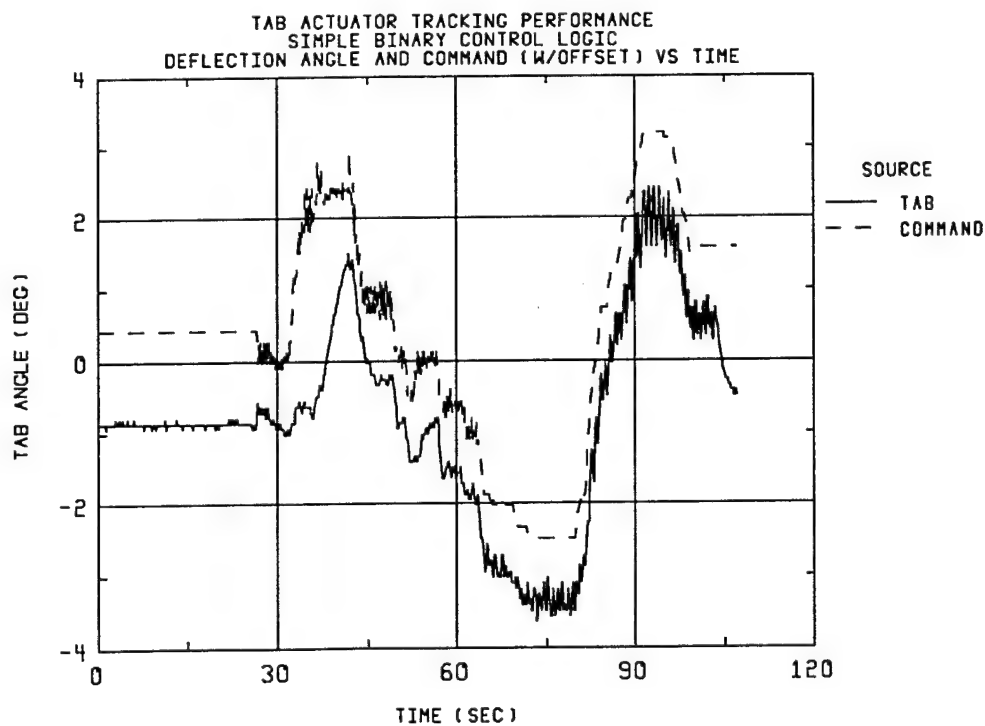Figure 3-7. Open-loop tab deflection for pulse input, various initial temps.

Figure 3-8. Closed-loop tab actuation response using on/off control logic.

54

significant torsional blade response, and from stall-induced separation and flow reattachment on the retreating side, which generates significant torsional loading of its own. Some aircraft are actually limited in forward flight speed due to vibratory response, and not installed power, or due to fatigue and endurance limits imposed on the pitch links themselves. As a consequence, pitch links are often designed to handle severe load amplitudes at high frequencies.

Any adjustment mechanism for pitch link lengths would require that the full load being transmitted through the link be carried in the adjustment mechanism, during periods of relative motion of the mechanism. This is true even if considerable mechanical advantage were employed to provide for this relative motion. Thus, any SMA-based actuator that provided for relative motion of the rod ends would have be designed to transmit these same static forces. While SMA materials are capable of handling large stressed, continuous operation to hold these forces would constitute a serious power drain.

One potential remedy to the power demand of the above actuation scheme is to provide an actuator that only has a finite number of allowable positions. Such an actuation concept might provides a ratchet-type mechanism for holding the actuator in a particular position, with the application of the SMA material for control of ratchet engage/release operation and direction. This approach would constitute a fundamental change in the application of SMA materials, from that of direct force generation for deflection to that of a state change device. The SMA wire (or possibly spring) could provide the motive force to change the ratchet mechanism to a new mechanical position, with the externally applied loads reacted by mechanical stiffness of the ratchet mechanism and linkages, and not continuously by the thermally-controlled stiffness of the SMA material. Such a usage would only incur power losses during a *change* of position, and would have no power required to maintain a particular discrete actuator displacement. Position sensing requirements would be limited to merely providing a switch to sense current actuator pawl position, as opposed to a sensor that must detect a continuous range of displacements.

A common example of this type of mechanical approach can be found in a common retractable ball-point pen. Shown schematically in Figure 3-9, the spring-biased ratchet assembly has two discrete locking positions that change state as the tip button is squeezed by the user. The squeezing action rotates the inner pawl along the curved outer race, and the spring forces the pawl to latch into a new position. If one were to load the pen axially, pushing the button would require a force to overcome the bias spring plus whatever static force was applied at the ball-point tip. Thus, even though continuous power is not expended to change state, the state change forces must react whatever additional load is applied to the device.
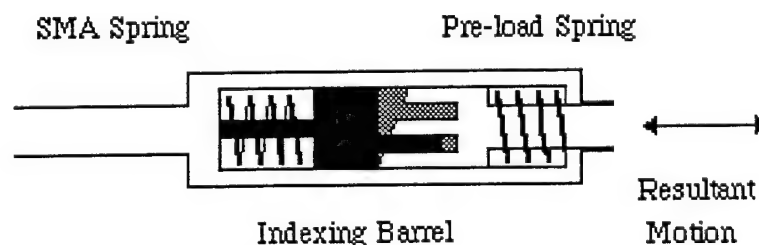

Figure 3-9. Schematic of two-position SMA-based ratchet mechanism.

Despite these attractive features, this concept still has several disadvantages. The power reduction comes as the expense of added mechanical complexity, since the actuator contains at least one moving part. This may be difficult to justify for such a highly dynamically loaded component as a pitch link. Second, since continuous motion is not possible, a sufficient number of ratchet locations would have to be added to allow for an appropriate range of possible adjustment positions. And finally, if more than two ratchet locations are available, some form of directional selection may be required, so that the device does not have to cycle through all its possible indexing values in one direction. Inclusion of direction control would add even more complexity.

While these drawbacks are not insurmountable, attempts to rectify them appeared to be unwarranted, based upon the successful mechanization of the active trailing edge tab device investigated in the benchtop tests described above. For a slight increase in angular deflection, the tab is an equally effective means of controlling 1/rev vibration at a <u>fraction</u> of the complexity, required power, or sophistication of an active pitch link. Thus, further consideration of the active pitch link system was eliminated.

3.5 Notional Actuator Installation, Power Requirements, and Control

Based upon the successful efforts performed under this Phase I work at designing and controlling an active rotor blade tab device, some consideration must be given as to the remaining technical challenges involved in realizing this device as a prototype for installation onto a helicopter rotor system. Clearly, construction of a device that contains discrete SMA wires suspended over a moment arm above the tab surface would incur such a severe drag penalty and be so prone to damage that the actuator would be useless. If active tabs are to be installed on a rotor blade, they must be of sufficiently small dimension that the drag associated with their installation is no more than a passive tab would be at the same location.

This is not a difficult task to achieve, if one considers the operating restrictions on SMA wire actuators as defined in the literature (Waram, 1992). SMA wires may be operated over millions of cycles if their strain is limited to 3% of the wire length. Considering the geometry of Figure 3-10, if a wire that bridges an equivalent hinge joint shrinks to 97% of its original length, the deflection of an attached tab would be a full 28°! Thus, to accommodate a 5° deflection for a similar arrangement, the wire would only have to contract 0.1% of its length. Of course, this idealization cannot be realized due to finite thicknesses in both the tab and the actuator wires, but suggests that use of SMA wires for hinge bending does <u>not</u> require large lengths of Nitinol stretched across the rotorblade chord. This implies that the tab could be designed such that its primary impact on blade drag would come from the physical dimensions of the tab only and would not be related to the actuator wires at all.

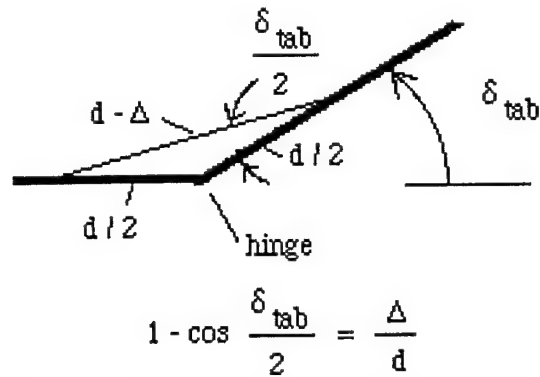$$1 - \cos \frac{\delta_{tab}}{2} = \frac{\Delta}{d}$$

Figure 3-10. Schematic of actuator wire contraction across a hinge joint.

While the actuator used in the benchtop testing was not optimized for reduced power consumption, it provides a reasonable design basis for judging the required power during tab actuation. The tab length used in the testing was only 1" wide, and if one assumes that two wires of .010" diameter would be used for each inch of tab length, the UH-60A would require a total of 13 wires per blade. Since each wire required a maximum of .58 amps of current to change temperature to the austenitic crystalline state, the power required during actuation was 1.5W per 1" tab, which translates to 20W during actuation of the full tab length on the rotor blade. While this would most likely <u>not</u> be used at once, since only partial tab bending is used in forward flight tracking operations, in order to control this complete tab deflection over, say, four minutes per two hour flight, one would need electrical storage of 1.33 Watt-hours for one flight. If one then assumes a nominal battery energy density of 10 W-hr/kg (NiCad batteries are typically 20), then the battery weight would be approximately 140g, or a little less than 2.5 oz/flight hour. This is a very reasonable weight penalty, given the added advantage of not requiring multiple flights (takeoffs and landings) in order to achieve proper rotor tracking.

Finally, while it was shown that blade flap position could be sensed using co-located accelerometers with the active tab device, some form of communication would be necessary *between* blades if a completely active system were to be realized. This could be as simple as providing a reference command for desired blade coning position, or as complicated as using all rotor blades to provide the optimal mixture of 1/rev loads and phasing to smooth the entire rotor system. Communication with the active tab could be performed using either direct electrical connections from the rotor hub to the tab device, with possibly the control signal superimposed on the power lines running to the tab, or optical link using serial digital links of modest bandwidth, since actuation is required over <u>seconds</u> and thus rapid data transfer is not required. This limited bandwidth requirement would allow for the possible use of infra-red communication links, since these have sufficient capability over these distances (approximately 30 to 50 feet) to accommodate data rates up to 9600 baud. This is actually well below the evolving standard being adopted for the newer IRDA devices used in computer to computer communications in an office environment (Hewlett-Packard, 1994). This topic was not addressed during this Phase I work, but is an obvious next step that would be required under a Phase II continuation program.

4.0 CONCLUSIONS

The work addressed under this Phase I effort was directed at determining the viability of the use of Individual Blade Control for 1/rev vibration reduction on helicopter rotors. The combination of a novel measurement scheme using blade-mounted accelerometer sensors, coupled with the use of Shape Memory Alloy-based active trailing edge tab devices, appears to provide the desired 1/rev shears and moments necessary to mitigate a wide range of potential sources of helicopter 1/rev vibration. Benchtop tests of notional device subsystems were used to expand and validate a mathematical model of the SMA-based actuator performance, so that this engineering model may be subsequently used in the prototype design of an actuator under a Phase II program. The power required for the device, and the installation issues associated with mounting the actuator in the rotor blade aerodynamic environment, do not appear to pose undue difficulties that would diminish the utility of the proposed control scheme.

Control of the active tab was shown to be straightforward, since the response time of the actuator is sufficiently below any rotor dynamic modes so as to make the system function in a quasi-static fashion. It is anticipated that its use would be limited to a small fraction of the total helicopter flight time, and as such, it may even be operated under battery power. The use of integral sensors, battery power, and possibly optical interfacing for data transmission and device control would make the unit an attractive *product improvement* system for both Army and civilian helicopter systems.

5.0 PHASE I OPTION TASKS

While the Phase I work was able to validate an engineering design model for actual device prototype development use, tests to date have only been performed on representative subsystems of the active tab that did not conform to the notional device geometry that would be anticipated for the prototype unit. It is proposed that any Phase I Option task elements address the construction of a tab having a geometry with SMA wire actuators in close proximity to the effective tab hinge, with subsequent benchtop testing and evaluation. Construction of this device would aid the selection of appropriate adhesives, insulating materials, and thermal modeling that would be required to properly design a device that would have minimal aerodynamic impact upon installation. It is anticipated that the construction of such a device, and testing both on the bench and possibly in a wind tunnel environment, would encompass two additional months of effort.

6.0 SUGGESTED PHASE-II CONTINUATION TASKS

Phase II development of the proposed active tab device would naturally lead to the design and construction of a working prototype actuator. While a full description of a complete Phase II program is best left to a formal Phase II proposal, a brief outline of tasks that would be appropriate milestones leading to the prototype realization are given in what follows.

Task 1: Notional actuator construction and wind tunnel testing -

Assuming that a notional geometry for the active tab device and SMA wires was constructed under a Phase I option task above, this effort would involve the formal testing of the actuator in a wind tunnel environment, in order to present the tab with aerodynamic loads that would represent possible reaction forces to be expected during tab actuation in flight. While wind tunnel tests of 2D sections could not duplicate the full range of dynamic pressures and Mach numbers associated with rotor blade flows, the interaction with the flow would provide additional design data for improvement and extension of the engineering models for the active tab performance.

Task 2: Validation of the accelerometer-based tab sensing scheme -

While the differential accelerometer sensing scheme described here appears promising for use with this tab device, selection of the accelerometers and actual on-blade testing has yet to be performed. This task would use a Froude-scaled model rotor to experimentally determine the viability of this technique for rotor flapping sensing, using similar hardware to that from previous blade-mounted accelerometer sensing tests performed by the Principal Investigator. These test data would provide valuable information in the design of appropriate signal processing schemes for tab control and interaction across the complete rotor system.

Task 3: Design of a 1/rev vibration suppression scheme -

While the sensitivity studies performed here showed that the active tab could mitigate many sources of 1/rev vibration, a complete system design was not attempted that would coordinate the various tabs on an individual rotor blade with those on other blades. While this may not be a terribly difficult task to complete, the best means for identification of the magnitude and "direction" of the 1/rev vibration in the nonrotating frame would have to be determined in order to provide an appropriate interface to the on-blade tab controllers. This design and analysis work would first be performed using extensions to the RotorCRAFT code used in the sensitivity analysis, followed by actual model rotor testing that would comprise the follow-on task.

Task 4: Model rotor tests using active tabs -

This portion of the Phase II effort would provide validation of the approach for active tab control for 1/rev vibration reduction, through a series of tunnel tests whereby various 1/rev vibration "events" were generated that the active system would attempt to alleviate. Such tests would help "wring out" the control logic associated with the intercommunication of the tab elements, thus aiding the eventual migration of the system to a full-size helicopter test aircraft.

Task 5: Electronic system integration -

Final system integration using the rotor controller, active tabs, power supplies and communication hardware would be performed in a "hot bench" setup, that would allow for a complete electronic simulation of the 1/rev vibration control system. This environment would be used in "simulated" flight testing to confirm that the various components were operating in harmony, and provide substantiation for any pre-flight qualification review of the prototype system.

Final testing of the prototype units would be performed under a Phase III commercialization program, in concert with appropriate Army personnel, most likely using an Army test aircraft. This testing could be performed as an adjunct to a previously planned flight test program in order to help defray Phase III program costs. The ultimate objective resulting from the Phase III flight tests would have a tested prototype active tab system with a proven performance record, suitable for commercialization and distribution to both Army and commercial helicopter operators.

7.0 REFERENCES

Anthoine, M., Beroul, F., Otho, A., and Vincenti, J., "Influence of Dissimilar Blades on Vibrations," Proc. 19th European Rotorcraft Forum, Como, Italy, September 1993.

Augustin, M. J. and Middleton, G. D., "A Review of the V-22 Health Monitoring System," Proc. 45th AHS Annual Forum, Boston, MA, May 1989.

Bauchau, O. A. and Lee, M., "Helicopter Blade Design for Vibration Minimization by Optimal Placement of Adjustable Masses," Proc. AHS Specialists Meeting on Rotorcraft Multidisciplinary Design Optimization, Atlanta, GA, April 1993.

Bielawa, R. Rotary Wing Structural Dynamics and Aeroelasticity. AIAA Education Series, Washington, D.C., 1992.

Bliss, D., Dadone, L, and Wachspress, D., "Rotor Wake Modeling for High Speed Applications," Proc. 43rd AHS Annual Forum, May 1987.

Brooks, T., and Booth, E., "Rotor Blade/Vortex Interation Noise Reduction and Vibration Using Higher Harmonic Control, Proc. 16th European Rotorcraft Forum, Sept. 1990.

Chadwick Helmuth, Model 8500C Balance Analyzer Manual, El Monte, California, 1992.

Clay, D. and Chadwick, J., "Helicopter Vibration and Analysis," Proc. 44th AHS Annual Forum, Washington, D.C., June 1988.

Crews, S. T. and Berger, V. C., "Smoothing the CH-47D with the OBSERVE, an On Board Vibration Analyzer, Tracker, and Balancer," Proc. 49th AHS Annual Forum, St. Louis, MO, May 1993.

Crews, S. T., Personnal Communication, June 1993.

Crews, S. T., "Rotorcraft Vibration Criteria: A New Perspective," Proc. 43rd AHS Annual Forum, St. Louis, Missouri, May 1987.

Duerig, T., Melton, K., Stockel, D., and Wayman, C., eds. Engineering Aspects of Shape Memory Alloys. London: Butterworth-Heinemann, 1990.

Fabunmi, J. A., "Control of Helicopter Rotorblade Aerodynamics," NASA CR-4350, July 1991.

Fries, J., "The Effect of Structural Variations on the Dynamic Characteristics of Helicopter Rotor Blades," Proc. 31st AIAA Structures, Structural Dynamics and Materials Converence, AIAA Paper 90-1161, 1990.

Gelb, A., ed. Applied Optimal Estimation. M.I.T. Press, Cambridge, MA, 1974.

Guinn, K., "Advanced Rotor Actuation Concepts," USAAVRADCOM TR-82-D-21, December 1982.

Harris, C., ed. Shock and Vibration Handbook, Third Edition. New York: McGraw-Hill, 1988.

Ham, N. D., and McKillip, R. M., Jr., "Research on Measurement and Control of Helicopter Rotor Response Using Blade-Mounted Accleerometers: 1991-1992," Proc. 18th European Rotorcraft Forum, September 1992.

Ham, N. D., Balough, D. L., and Talbot, P. D., "The Measurement and Control of Helicopter Blade Modal Response Using Blade-Mounted Accelerometers," Proc. 13th European Rotorcraft Forum, September 1987.

Ham, N. D., Behal, B. L., and McKillip, R. M., Jr., "Helicopter Lag Damping Augmentation Through Individual Blade Control," Vertica, Vol. 7, no. 4, pp. 361-371, 1983.

Ham, N. D., "Individual Blade Control and Its Applications," Proc. 41st AHS Annual Forum, Fort Worth, TX, May 1985.

Hamade, K., and Kufeld, R., "Modal Analysis of UH-60 Instrumented Rotor Blades," NASA TM-4239, 1990.

Hammond, C., "An Application of Floquet Theory to Prediction of Mechanical Instability," Journal of the American Helicopter Society, Vol. 19, no. 4, Oct. 1974.

Hewlett-Packard, IrDA Transciever Module, Hewlett-Packard Company, Santa Clara, California, 1994.

Hodges, D. and Ormiston, R., "Nonlinear Equations for Bending of Rotating Beams with Application to Linear Flap-Lag Stability of Hingeless Rotors," NASA TM X-2770, November 1972.

Houbolt, J. and Brooks, G., "Differential Equations of Motion for Combined Flapwise Bending, Chordwise Bending, and Torsion of Twisted Nonuniform Rotor Blades", NACA Report 1346, 1958.

Johnson, W. Helicopter Theory. Princeton University Press, Princeton, New Jersey, 1980.

Kloppel, V., and Marsch, G., "Aspects of See-Saw Tail Rotor Balancing," Proc. 10th European Rotorcraft Forum, The Hague, The Netherlands, August 1984.

Kretz, M., "Research in Multicyclic and Active Control of Rotary Wings," Vertica, Vol. 1, 1976.

Lemnios, A. Z., and Jones, R., "The Servo Flap - An Advanced Rotor Control System," Proc. AHS Design Specialist's Meeting on Vertical Lift Aircraft Design, San Francisco, CA, January 1990.

Liang, C., and Rogers, C. A., "One-Dimensional Thermomechanical Constitutive Relations for Shape Memory Materials," AIAA Paper 90-1027 CP, 1990.

Loewy, R. G., "Helicopter Vibrations: A Technical Perspective," Journal of the American Helicopter Society, Vol. 29, no. 4, October 1984, pp. 4-30.

Lorber, P., "Blade-Vortex Interaction Data Obtained from a Pressure-instrumented Model UH-60A Rotor at the DNW," Journal of the AHS, Vol. 38, n. 3, July 1993.

Lorber, P., "Pressure-Instrumented Model UH-60A Blackhawk Rotor Test at DNW, Vol. 1: Description of Experiment," United Technologies Research Center Report R91-153577-1, Feb. 1991.

McDonnell-Douglas Helicopter Company, Inc., OH-6 Helicopter Maintenance Manual, TM 55-1520-214-23, 1990 revision.

McKillip, R. M., Jr., "A Novel Instrumentation System for Measurement of Helicopter Rotor Motions and Loads Data," Continuum Dynamics, Inc. Rept. 95-03, April 1995.

McKillip, R. M., Jr., "Experimental Studies in System Identification of Helicopter Rotor Dyanmics," Vertica, Vol. 12, no. 4, 1988b.

McKillip, R. M., Jr., "Kinematic Observers for Active Control of Helicopter Rotor Vibration," Vertica, Vol. 12, no. 1/2, pp. 1-11, 1988a.

McKillip, R. M., Jr., "Periodic Control of the Individual Blade Control Helicopter Rotor," Vertica, Vol. 9, no. 2, pp. 199-225, 1985.

McNulty, M. J., "Effects of Blade-to-Blade Dissimilarities on Rotor-Body Lead-Lag Dynamics," Journal of the American Helicopter Society, January 1988, pp. 17-28.

Millott, T. A., and Friedmann, P. P., "The Practical Implementation of an Actively Controlled Flap to Reduce Vibrations in Helicopter Rotors," Proc. 49th AHS Annual Forum, St. Louis, MO, May 1993.

NASA Tech Briefs, "Shape-Memory Wires Switch Rotary Actuators," MFS-28581, Marshall Space Flight Center, Alabama, 1992.

Ormiston, R., "Can Smart Materials Make Helicopters Better?", Presentation at Univ. of Maryland ARO Workshop on Dynamics and Aeroelastic Stability Modeling of Rotorcraft Systems, November 1991.

Parallax, Inc. BASIC Stamp™ User's Manual, Parallax, Inc., Rocklin, CA, 1993.

Quackenbush, T. R., and McKillip, R. M., Jr., "Design and Control Strategies Using Smart Structures Technology for Rotorcraft Performance Enhancement,"

Continuum Dynamics, Inc. Report 93-14, Princeton, New Jersey, 1993 (Also, AIAA Paper no. 94-4283-CP).

Quackenbush, T. R., Bliss, D. B., Wachspress, D. A., and Boschitsch, A. H., "Analysis of Rotor Vibratory Loads Using Higher Harmonic Pitch Control," NASA CR-189591, April 1992.

Quackenbush, T. R., "Testing of a Stall Flutter Suppression System Using Individual Blade Control," Journal of the American Helicopter Society, Vol. 29, no. 3, July 1984.

Quackenbush, T. R., Wachspress, D. A., and Boschitsch, A. H., "Computation of Rotor Unsteady Airloads with a Constant Vorticity Contour Free Wake Model," AIAA Paper 91-3229, Sept. 1991.

Quackenbush, T., Bliss, D., Wachspress, D., Boschitsch, A., and Chua, K., "Computation of Rotor Aerodynamic Loads in Forward Flight Using a Full-Span Free Wake Analysis," NASA CR-177611, Oct. 1990.

Quackenbush, T., Lam, C.-M., Wachspress, D., and Bliss, D., "Analysis of High Resolution Unsteady Airloads for Helicopter Rotor Blades," Proc. AHS Annual Forum, Washington, D.C., May 1994.

Reichert, G., "Helicopter Vibration Control - A Survey," Vertica, Vol. 5, no. 1, 1981.

Rogers, C. A., Liang, C., and Jia, J., "Structural Modification of Simply-Supported Laminated Plates Using Embedded Shape Memory Alloy Fibers," Computers and Structures, Vol. 38, no. 5/6, 1991.

Scheiman, J., "A Tabulation of Helicopter Rotor-Blade Differential Pressures, Stresses, and Motions Measured in Flight," NASA TM-X 952, March 1964.

Scientific Atlanta, RADS-AT Rotor Analysis and Diagnostic System, 1993.

Smith, E., et. al., "Formulation and Validation of a Finite Element Model for Elastomaric Lag Dampers," Proc. 51st AHS Annual Forum, Ft. Worth, TX, May 1995.

Spangler, R. L., Jr., and Hall, S. R., "Piezoelectric Actuators for Helicopter Rotor Control," 31st AIAA Structures, Structural Dynamics and Materials Conference, May 1990.

Straub, F. K., "A Feasibility Study of Using Smart Materials for Rotor Control," Proc. 49th AHS Annual Forum, St. Louis, MO, May 1993a.

Straub, F. K., and Robinson, L. H., "Dynamics of a Rotor with Nonharmonic Control," Proc. 49th AHS Annual Forum, St. Louis, MO, May 1993b.

Straub, F. K., and Merkley, D. J., "Design of a Smart Material Actuator for Rotor Control," Proc. SPIE Smart Structures and Materials 1995 Meeting, Vol. 2443, San Diego, CA, 1995.

Teves, D., Kloppel, V., and Richter, P., "Development of Active Control Technology in the Rotating System, Flight Testing and Theoretical Investigations," Proc. 18th European Rotorcraft Forum, Avignon, France, September 1992.

Torok, M., and Berezin, C., "Aerodynamic and Wake Mdthodology Evaluation Using the Model UH-60A Wind Tunnel Experimental Data," Proc. 48th AHS Forum, May 1992.

TRENDS UH-60A Phase-II Airloads Data Base, Flight Annotations for Flights 46-80, February 1990 - April 1993.

Trigg, N., "Helicopter Vibration Flight Testing: The Rotortuner Approach," Paper no. 106, Proc. 10th European Rotorcraft Forum, The Hague, The Netherlands, August 1984.

U.S. Army Aeronautical Design Standard (ADS-27), "Requirements for Rotorcraft Vibration specifications, Modeling and Testing," U.S. Army Aviation Systems Command, St. Louis, Missouri, validated 1993.

Viswanathan, S. P., Meyers, A. W., and McLarty, T. T., "An Analytical Model for Describing the Response of an Unsymmetrical Rotor," Proc. 33rd AHS Annual Forum, May 1977.

Wang, J. M. and Chopra, I., "Dynamics of Helicopters with Dissimilar Blades," Proc. 47th AHS Annual Forum, Phoenix, AZ, May 1991.

Waram, T. Actuator Design Using Shape Memory Alloys. Published by the author, Hamilton, Ontario, Canada, 1992.

Wellman, B., "Advanced Technology Blade Testing on the XV-15 Tilt Rotor Research Aircraft," Proc. 48th AHS Annual Forum, Washington, D.C., June 1992.

Wilson, W. F., "Technical Aspects of 1/Rev Vibration," Rotorcraft Dynamics, NASA SP-352, 1974.

Young, D., and Tarzanin, F., "Structural Optimization and Mach Scale Test Validation of a Low Vibration Rotor," Proc. 47th AHS Annual Forum, Pheonix, Arizona, May 1991.